Peroxiredoxin III: A candidate for drug resistance to chemotherapy

A thesis presented in partial fulfillment of the requirements for the degree of Master of Science in Biochemistry at Massey University, Palmerston North, New Zealand.

Miranda Aalderink

2008

Acknowledgements

I would like to express my thanks to Dr. Kathryn Stowell, who was an exceptional supervisor. Thanks for always making time to talk to me, always being approachable and always encouraging me. Thanks also for allowing me to make my own mistakes without letting me get too far off track. Thanks also to Dr. Richard Isaacs for your help in organizing patients to take part in this study.

Words can not express how grateful I am for the support of my family and friends. Thank you to my Mum and Dad for the encouragement, support, and patience, and for always taking the time to listen to me, even when you didn't understand what I was talking about. Thank you to Jeroen for being the best brother and friend a girl could have. Thank you to Kelly Gilchrist for always being there, always believing in me, and always convincing me to believe in myself whenever things got difficult.

Thank you to everyone in the Twilite Zone for making being in the lab so much fun. Special thanks to Natisha Magan, for all the help, encouragement and entertainment over the past two years, and to Rebecca Hole, Hilbert Grievink, Lili Rhodes and Robyn Marston for always being available to give advice or provide entertaining conversation.

Thank you to the amazing women who took part in this study during an incredibly trying time. Thank you also to Massey University for the financial support.

To my Mo – this one's for you.

Abstract

The development of drug resistance to chemotherapeutic drugs is a serious obstacle in the successful treatment of cancer. New cancer drugs are continually being developed with the goal of increasing the effectiveness of chemotherapy. However, new mechanisms of drug resistance are also continually being identified. Understanding the mechanisms of drug resistance is a vital step in identifying new drug targets which may prevent or reduce the development of drug resistance. A recent unpublished study identified peroxiredoxin III (prx III) as being up-regulated in breast cancer cells in culture following exposure to the commonly used anti-cancer drug doxorubicin.

Doxorubicin and the almost identical drug epirubicin have multiple mechanisms of activity. One function of these drugs is to increase intracellular hydrogen peroxide (H_2O_2) concentrations to induce cell death. As prx III is a mitochondrial protein which reduces H_2O_2, it has been suggested that increased expression of prx III may contribute to the development of drug resistance to doxorubicin or epirubicin. However, before such a role for prx III in the development of drug resistance can be further investigated, prx III expression needs to be examined in patients undergoing chemotherapy.

The aim of this study was to examine prx III expression in the white blood cells of patients undergoing chemotherapy with epirubicin, and in healthy control subjects. Additionally, as the activity of a number of peroxiredoxins has been shown to be modulated through the formation of complexes and over-oxidation, complex formation and over-oxidation in response to treatment with doxorubicin or epirubicin was also examined. The results of this study could identify a new target for preventing or reducing the development of drug resistance. While the sample sizes were too small to draw conclusions, some patients showed a change in the expression of peroxiredoxin III following chemotherapy with epirubicin, suggesting that further investigation into the expression of peroxiredoxin III following chemotherapy would be worthwhile.

Abbreviations

2-cys	2-cysteine
2DE	Two-dimensional electrophoresis
ABC	ATP-binding cassette transporter
APS	Ammonium persulfate
ARE	Antioxidant response element
ATP	Adenosine triphosphate
bp	Base pairs (DNA)
BSA	Bovine serum albumin
cDNA	Complimentary DNA
c-Myc	Proto-oncogene
CS	Citrate synthase
C_T	Threshold cycle
DCF	Dichlorofluorescein
DCFH-DA	2',7'-dichlorofluorescin diacetate
DEPC	Diethylpyrocarbonate
DMSO	Dimethyl sulfoxide
DNA	Deoxyribose nucleic acid
dNTP	Deoxynucleoside triphosphate (dATP, dTTP, dGTP, dCTP)
Dox	Doxorubicin
DTT	Dithiothreitol
EDTA	Ethylene diamine tetra-acetic acid
EGF	Epidermal growth factor
EMSA	Electrophoretic mobility shift assay
Epi	Epirubicin
ER	Estrogen receptor
ERRα	Estrogen-related receptor α
FBS	Fetal bovine serum
G1	Gap 1

HeLa	Human cervical carinoma cells
Hi95	Human sestrin
HRP	Horseradish peroxidase
IEF	Isoelectric focusing
IPG	Immobilised pH gradient
K562	Human leukemia cell line
kDa	Kilodaltons
MCF10A	Normal human breast epithelial cell line
MCF7	Human breast carcinoma cell line
MEM	Minimum essential medium
mRNA	Messenger RNA
NADPH	Nicotinamide adenine dinucleotide phosphate
NFκB	Nuclear factor kappa B
$O_2^{\cdot-}$	Superoxide anion
p53	Tumour suppressor protein
PA26	Human sestrin
PAGE	Polyacrylamide gel electrophoresis
PBS	Phosphate buffered saline
PCR	Polymerase chain reaction
PDGF	Platelet derived growth factor
Pen-Strep	Penicillin-streptomycin
PGC-1α	Peroxisome proliferator-activated receptor γ coactivator-1α
P-gp	P-glycoprotein
pI	Isoelectric point
Prx	Peroxiredoxin
Prx III	Peroxiredoxin III
prxs	Peroxiredoxins
PVDF	Polyvinylidine fluoride
RBC	Red blood cell
RIPA	Radio-immuno precipitation
RNA	Ribonucleic acid

RNase	Ribonuclease
ROS	Reactive oxygen species
rpm	revolutions per minute
rRNA	Ribosomal RNA
RT	Reverse transcription
SDS	Sodium dodecyl sulfate
Srx1	Sulfiredoxin
TAE	Tris acetate EDTA buffer
TBST	Tris-buffered saline-TWEEN 20
TEMED	N,N,N',N'-Tetramethylethylenediamine
TEN	Tris-EDTA-Sodium chloride buffer
Thr	Threonine
TNF-α	Tumour necrosis factor α
tRNA	Transfer RNA
TrypLE	Express stable trypsin-like enzyme plus phenol red
UV	Ultraviolet
WBC	White blood cell

List of Figures

		Page number
Figure 1.1:	Mechanism of H_2O_2 reduction by 2-cys peroxiredoxins	7
Figure 3.1:	Outline of the principles of real time PCR	40
Figure 3.2:	Primer sequences	42
Figure 3.3:	β-actin and peroxiredoxin III PCR products	44
Figure 3.4	Digestion of peroxiredoxin III product with *Sph*I	45
Figure 3.5:	Alignment of PCR product sequence and prx III mRNA sequence	46
Figure 3.6:	Low primer concentration results in a shift in amplification curves	48
Figure 3.7:	Western blot results for all control samples	56
Figure 3.8:	Western blot results for all patient samples	57
Figure 3.9:	Longer exposures results showed higher molecular weight bands were detected by the β-actin antibody	58
Figure 4.1:	Native PAGE and western blotting of MCF7 extracts	64
Figure 4.2:	Representative western blot results for patient samples	67
Figure 4.3:	Representative western blot results for control samples	68
Figure 5.1:	Outline of two-dimensional electrophoresis experiments	71
Figure 5.2:	Over-oxidation of peroxiredoxin III	73
Figure 5.3:	Exposure of MCF7 cells to doxorubicin did not result in peroxiredoxin III over-oxidation	75
Figure 6.1:	Overview of a possible explanation of prx III complex formation	83

List of Tables

		Page number
Table 2.1:	Resolving and stacking gel solutions for SDS-PAGE	23
Table 2.2:	Resolving and stacking gel solutions for native PAGE	29
Table 2.3:	Real time PCR components required for one reaction	35
Table 2.4:	The LightCycler 480 cycle programme	35
Table 3.1:	Efficiency values determined from ten individual standard curves	50
Table 3.2:	Peroxiredoxin III fold changes calculated for patients	52
Table 3.3:	Peroxiredoxin III fold changes calculated for all control samples	53

Table of Contents

Acknowledgements ..... **ii**

Abstract ..... **iii**

Abbreviations ..... **iv**

List of Figures ..... **vii**

List of Tables ..... **viii**

Table of Contents ..... **ix**

Chapter 1: Introduction **1**

1.1 Cancer *1*

1.2 Mechanisms of drug resistance *3*

1.3 Searching for new mechanisms of resistance *4*

1.4 Peroxiredoxins *5*

1.5 Peroxiredoxins and Reactive Oxygen Species *7*

1.6 Peroxiredoxins as molecular chaperones *9*

1.7 Regeneration of active peroxiredoxin *11*

1.8 Peroxiredoxins and disease *11*

1.9 Peroxiredoxin III *12*

1.10 Research aims *15*

Chapter 2: Materials and methods **17**

2.1 Materials *17*

2.2 Mammalian cell culture *19*

2.2.1 Media *19*

2.2.2 Starting cells from frozen stocks *19*

2.2.3 Passage of cells *19*

2.2.4 Freezing of cells *20*

2.2.5 Exposure of cells to doxorubicin *20*

2.2.6 Exposure of cells to oxidative stress *20*

2.3 Isolation of white blood cells *20*

2.4 Protein extraction and quantification *21*

2.4.1 Preparation of cells grown in monolayer for protein extraction 21
2.4.2 Extraction of total cellular protein 21
2.4.3 Quantification of protein extracts 22
2.5 Sodium dodecyl sulfate-polyacrylamide gel electrophoresis (SDS-PAGE) 22
2.5.1 Casting of 10% SDS-PAGE gels 23
2.5.2 SDS-PAGE 24
2.5.3 Coomassie staining of polyacrylamide gels 24
2.6 Immunoblotting 24
2.6.1 Transfer of proteins to PVDF membrane 25
2.6.2 Immunoblotting 25
2.6.3 Stripping of PVDF membranes 26
2.7 Two-dimensional electrophoresis 26
2.7.1 Preparation of protein sample for 2DE 26
2.7.2 Isoelectric focusing 27
2.7.3 Polyacrylamide gel casting for 2DE 27
2.7.4 Second dimension: SDS-PAGE 28
2.7.5 Immunoblotting of 2DE gel 28
2.8 Native polyacrylamide gel electrophoresis 28
2.8.1 Casting of native PAGE gels 28
2.8.2 Native PAGE 29
2.9 Extraction of RNA 30
2.9.1 Diethylpyrocarbonate treatment of tubes, tips and water 30
2.9.2 Extraction of RNA 30
2.10 Complimentary DNA synthesis 31
2.11 Polymerase chain reaction (PCR) 32
2.11.1 Reaction set up 32
2.11.2 Agarose gel electrophoresis 33
2.11.3 Purification of PCR product for sequencing 33
2.11.4 DNA sequence analysis 34
2.11.5 Restriction endonuclease digests 34
2.12 Real time PCR 34
2.12.1 Setting up the basic reaction 34
2.12.2 Determination of optimal primer concentrations 36

2.12.4 Determination of primer efficiency 36
2.12.5 Calculation of relative expression levels 37
2.13 Statistical Analysis 37
2.14 Ethics Approval 37

Chapter 3: Expression of peroxiredoxin III *in vivo* **38**
3.1 Introduction 38
3.2 Expression of peroxiredoxin III mRNA 41
3.3 Specificity of prx III primers 42
3.4 Determination of optimal primer concentrations 47
3.5 Determination of average primer efficiency 49
3.6 Fold change in prx III mRNA 51
3.7 Expression of prx III protein 54
3.8 Chapter summary 60

Chapter Four: Formation of complexes **62**
4.1 Introduction 62
4.2 Detection of higher molecular weight complexes in MCF7 cells 62
4.3 Detection of higher molecular weight complexes in white blood cells 65
4.4 Chapter summary 69

Chapter 5: Inactivation of peroxiredoxin III **70**
5.1 Introduction 70
5.2 Oxidative stress and peroxiredoxin III over-oxidation 72
5.3 Over-oxidation of peroxiredoxin III in response to doxorubicin exposure 74
5.4 Chapter summary 76
6.1 Overview 77
6.2 Summary of results 78
6.3 Future research 84
6.4 Conclusion 87

References **89**

Appendix One: Bradford Protein Quantification Assay **95**

Appendix Two: One-sample, two-sided *t*-test **96**

Appendix Three: Sample of data used to generate standard curves **97**

Appendix Four: Example of Coomassie-stained SDS-PAGE gel **98**

Appendix Five: α-tubulin antibody **99**

Appendix Six: Sample of data used to calculate fold change **100**

Appendix Seven: Identification of β-actin band **101**

Appendix Eight: Example of agarose gel electrophoresis results obtained during real time RT-PCR optimisation **102**

Appendix Nine: Example amplification curves obtained during real time RT-PCR experiments **103**

Appendix Ten: Example of results obtained during real time RT-PCR experiments **104**

Appendix Eleven: Coomassie stained 2DE gel to confirm successful isoelectric focusing **105**

Appendix Twelve: Chromatogram from peroxiredoxin III DNA sequencing **106**

Chapter 1: Introduction

1.1 Cancer

Cancer is a leading cause of death and disease in many (Ministry of Health, 2007). Cancer, or the development of tumours, appears to be the result of a number of genetic changes in a cell. Hanahan and Weinberg (2000) outlined six "hallmarks" of cancer – changes that are seen in most, if not all, tumours.

The first is the ability of cells to mimic normal growth signals. Normal cells require signals from their environment to grow. Without these signals, normal cells do not proliferate. Cancer cells develop the ability to grow without these signals, through a number of mechanisms. Some cells appear to develop the ability to synthesise their own growth factors, while other cells over-express growth factor receptors allowing stronger responses to background levels of growth factor, or express mutant receptors which are constitutively active, mimicking constant stimulation with growth factor (Faivre and Lange, 2007).

Cells must also develop insensitivity to the anti-growth signals received from their environment. Similarly to growth factors, anti-growth signals are received by cell-surface receptors. If these cell-surface receptors are lost or mutated, cells become unresponsive to anti-growth signals. This in turn allows cells to grow when they otherwise would not.

As well as being able to proliferate inappropriately, it appears that cells also need to be able to avoid programmed cell death (apoptosis) if a tumour is to develop. Sensors continually monitor both the intracellular and extracellular status for any signs of abnormality, such as DNA damage or hypoxia. Signals suggesting an abnormality or a lack of signals indicating the normal situation trigger apoptosis. For example, a major protein involved in sensing DNA damage and triggering apoptosis is p53. Loss of p53 is seen in a large percentage of cancers and appears to represent an important mechanism for avoiding apoptosis (Harris, 1996).

Normal cells in culture appear to be able to double only 60 to 70 times, while tumour cells are able to double indefinitely (Hayflick, 1965). The ends of the chromosomes, called telomeres, appear to be responsible for this limit in the number of doublings a normal cell can undergo. Telomeres consist of many copies of a short repeat sequence. Due to the inability of the replication machinery to reach the ends of the chromosomes, 50-100 base pairs (bp) are lost from the end of the telomeres at each cycle of replication. Eventually the telomeres become too short, chromosomes become unstable and cell death occurs (Counter *et al.*, 1992). Cancer cells however are able to prevent telomere shortening by up-regulating expression of telomerase, the telomere maintenance enzyme (Shay and Bacchetti, 1997).

A large network of capillaries supplies oxygen and essential nutrients to all cells of the body; without this blood supply cells die. The same is true for cancer cells. Therefore if tumours are to continue to grow, new blood vessels are required. Not surprisingly, many tumours develop the ability to induce angiogenesis (the growth of new blood vessels). A number of changes in gene expression appear to be involved in the ability to induce angiogenesis however, these are not yet fully understood (Bouck *et al.*, 1996).

Finally, many tumours eventually develop the ability to invade surrounding tissue and form tumours at new sites, a process known as metastasis. This is responsible for approximately 90% of cancer deaths (Sporn, 1996). Once tumours metastasise, often the only practical treatment available is chemotherapy (Sauna *et al.*, 2007), a treatment which presents its own problems as will be discussed later in this chapter.

The development of cancer is clearly a complicated process, involving numerous alterations of the genome and gene expression patterns. Not surprisingly, the treatment of cancer is also complicated. Currently a combination of surgery, chemotherapy, and in some cases radiotherapy is used to target cancer cells. There are numerous anti-cancer drugs available for use, and new drugs are continually being developed. Two drugs routinely used to treat a variety of tumours are doxorubicin (adriamycin), and the almost identical drug epirubicin. Doxorubicin (dox) and epirubicin (epi) differ only in the orientation of one hydroxyl group, which appears to be responsible for the slightly decreased cardiotoxicity of epirubicin

(Salvatorelli *et al.*, 2006). Dox binds DNA by intercalating between base pairs, inhibiting both RNA synthesis and DNA replication. This prevents production of proteins and replication of cells (Blum and Carter, 1974). Dox also associates with the topoisomerase II-DNA complex, inhibiting DNA re-ligation which results in the accumulation of double-stranded DNA breaks (Lothstein *et al.*, 2001). Finally, doxorubicin has been associated with an increase in the generation of reactive oxygen species (ROS) such as hydrogen peroxide (H_2O_2), which in turn have been linked to the induction of apoptosis (Lothstein *et al.*, 2001). Epirubicin functions through the same mechanisms as doxorubicin (Salvatorelli *et al.*, 2006).

Chemotherapy is usually administered in three week cycles, giving patients time to recover between doses. Optimal doses of anti-cancer drugs are designed to produce maximal death of cancer cells, without being toxic to the patient. However, the side-effects associated with anti-cancer drugs often prevent use of the optimal dose, or prevent patients from receiving all doses of chemotherapy, which reduces the effectiveness of the treatment. Individual variations in the rate of absorption, metabolism and excretion of anti-cancer drugs can also influence the efficacy of treatment (Ralph *et al.*, 2003). However, the ability of cells to develop resistance to anti-cancer drugs poses the biggest challenge to chemotherapy and the treatment of cancer.

1.2 Mechanisms of drug resistance

A number of mechanisms of drug resistance have been characterized. These mechanisms may be present before treatment, or develop as a response to chemotherapy, and usually involve up-regulation of resistance mechanisms or down-regulation of drug targets (Di Nicolantonio *et al.*, 2005). One of the most extensively studied mechanisms of drug resistance involves up-regulation of P-glycoprotein (P-gp). P-gp is expressed in several cell lines which are resistant to a number of different chemotherapeutic agents. P-gp is an ATP-binding cassette (ABC) transporter protein found in the plasma membrane, and is capable of pumping drugs such as doxorubicin and epirubicin out of cells. P-gp expression has been shown to quickly increase in some patients in response to a variety of chemotherapeutic

drugs (Di Nicolantonio *et al.*, 2005). Increased expression of P-gp leads to increased efflux of drugs from the cells, reducing their ability to induce cell death.

Changes that result in a decrease in the uptake of certain drugs may also play a role in the development of drug resistance. For example in the case of methotrexate, a toxic folate analog, resistance occurs through the mutation of one or both of the folate transporters (Gottesman, 2002). Reduced uptake decreases the effectiveness of a drug in mediating cell death and preventing cellular proliferation.

Expression of topoisomerase II (topo II) appears to be down-regulated in response to a number of topo II-targeting drugs, including doxorubicin and epirubicin (Gottesman, 2002; Allen *et al.*, 2004). Down-regulation of topo II results in decreased accumulation of double-stranded DNA breaks. This allows DNA replication and transcription to occur, and prevents activation of cell death pathways usually activated in response to extensive DNA damage. Increased DNA repair has also been associated with the development of drug resistance, as increased repair of DNA damage allows cells to continue to proliferate (Gottesman, 2002).

As with the development of cancer, the development of drug resistance appears to involve changes in the expression of multiple genes. While many mechanisms involved in drug resistance have been partially characterized, new mechanisms are continually being identified. Understanding the mechanisms involved in drug resistance is a vital step in the development of new and more effective treatments for cancer.

1.3 Searching for new mechanisms of resistance

As drug resistance plays such an important role in decreasing the effectiveness of anti-cancer drugs, a great deal of work is being carried out to identify new target proteins involved in its development. Recent developments in both microarray technology and two-dimensional electrophoresis have provided researchers with new ways to compare gene expression in drug-sensitive and drug-resistant cells. For example, complimentary DNA (cDNA) microarrays have been used to examine camptothecin resistance in glioblastoma cell lines (Morandi *et al.*, 2006), and two-dimensional electrophoresis has been used to

examine doxorubicin resistance in MCF7 breast cancer cells (Liu *et al.*, 2006). An unpublished study which used cDNA microarrays to examine changes in the expression patterns of cells in culture following doxorubicin exposure identified peroxiredoxin III (prx III) as one protein which is up-regulated in response to treatment with doxorubicin (Williams *et al.*, unpublished). In this study, MDAMB231, MCF12A and MCF7 cells were exposed to 3 μM doxorubicin for 2 hours, 24 hours or 48 hours before RNA was extracted, first strand cDNA was synthesized and microarray experiments were performed. Expression of peroxiredoxin III was found to be highest 24 hours after exposure to doxorubicin. MDAMB231, MCF12A and MCF7 cells showed 4-fold, 2.5-fold and 2-fold increases in peroxiredoxin III expression respectively, 24 hours following treatment with doxorubicin. Prx III may therefore play a role in the development of resistance to doxorubicin, or epirubicin.

1.4 Peroxiredoxins

The peroxiredoxins (prxs) are a family of small, ubiquitously expressed peroxidases, which are highly conserved in both prokaryotes and eukaryotes (Kim *et al.*, 2005). There are six known human isoforms, which localize to different regions of the cell. Prx I and II are found in the cytoplasm and nucleus, and prx III localizes to mitochondria, while prx IV is found in the endoplasmic reticulum and extracellular space. Prx V exists in two forms, long and short. The long form localizes to mitochondria while the short form is found in peroxisomes (Kinnula *et al.*, 2002). Prx VI is found in the cytosol, mitochondria and peroxisomes (Knoops *et al.*, 1999). Based on the number of conserved cysteine residues present and the mechanism of activity, the peroxiredoxins have been divided into three separate classes – 2-cys (2-cysteine), atypical 2-cys and 1-cys (1-cysteine) peroxiredoxins. Peroxiredoxins I to IV are 2-cys proteins as they contain two conserved cysteine residues and form a homodimer during catalysis (Jeong *et al.*, 2006). Prx V is an atypical 2-cys peroxiredoxin as it forms an intramolecular rather than an intermolecular disulfide bond during catalysis (Jang *et al.*, 2006). Prx VI only contains one of the conserved cysteine residues, and is classed as a 1-cys peroxiredoxin, however other cysteine residues may play a role in catalysis (Kinnula *et al.*, 2002).

The mechanism of the 2-cys peroxiredoxins has been the most extensively examined, and an outline is presented in figure 1.1. H_2O_2 oxidises the conserved amino-terminal cysteine residue to produce an unstable cysteine-sulfinic acid intermediate. This unstable residue forms an intermolecular disulfide bond with the carboxyl terminal cysteine residue of a second prx molecule, to produce a head-to-tail homodimer. Thioredoxin then reduces the disulfide bond, to restore prx to an active state. Thioredoxin reductase then reduces thioredoxin at the expense of a molecule of nicotinamide adenine dinucleotide phosphate (NADPH) (Seo *et al.*, 2000; Chang *et al.*, 2004). In the case of prx III, thioredoxin-2 the mitochondrial thioredoxin, is the electron donor, and thioredoxin reductase-2 restores active thioredoxin-2 (Chang *et al.*, 2004).

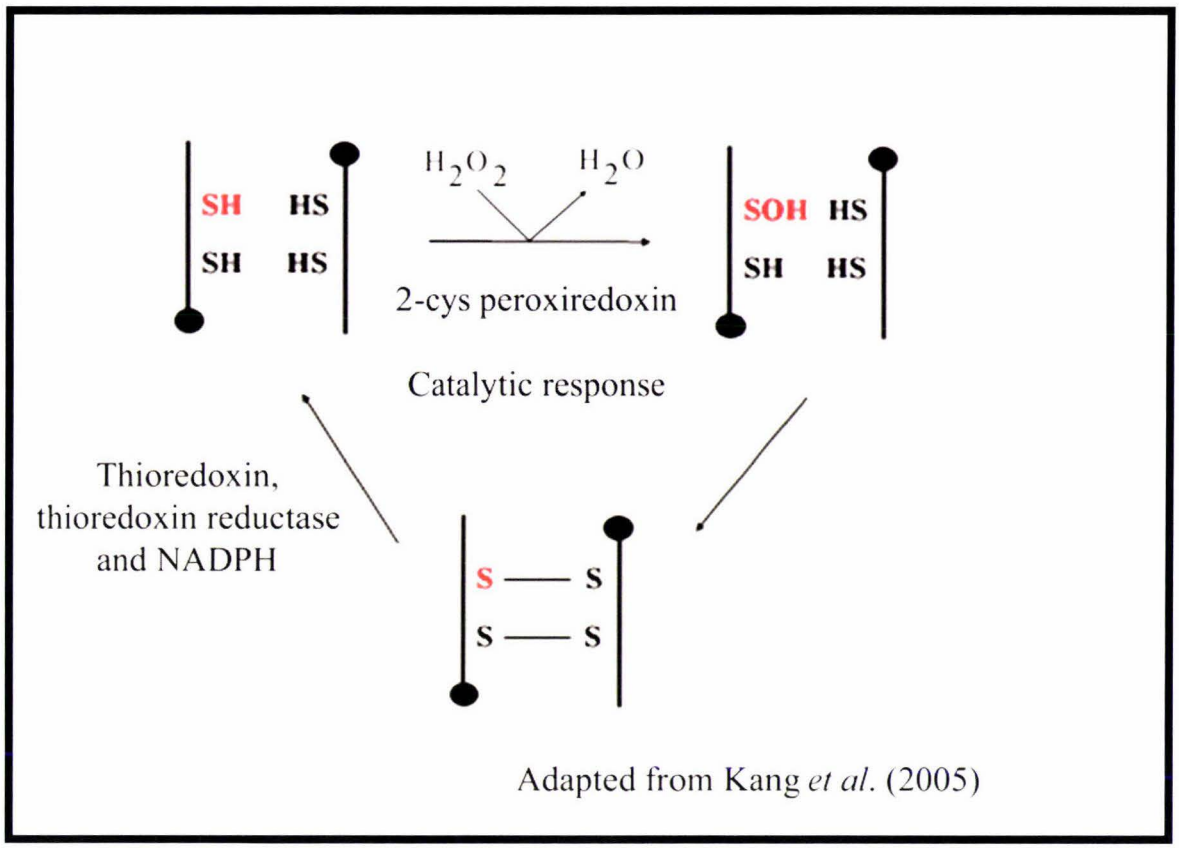

Figure 1.1 Mechanism of H_2O_2 reduction by 2-cys peroxiredoxins

H_2O_2 oxidises the conserved amino-terminal cysteine residue to produce an unstable cysteine-sulfinic acid intermediate (SOH). This unstable residue forms an intramolecular disulfide bond with the carboxyl terminal cysteine residue of a second prx molecule, to produce a head-to-tail homodimer. Thioredoxin reduces the disulfide bond, to restore prx to an active state and thioredoxin reductase reduces thioredoxin at the expense of a molecule of nicotinamide adenine dinucleotide phosphate (NADPH).

1.5 Peroxiredoxins and Reactive Oxygen Species

Reactive oxygen species such as H_2O_2 and the superoxide anion ($O_2^{\cdot-}$) are generated through the activity of the electron transport chain within mitochondria, and through cellular processes such as inflammation, the immune response and removal of foreign compounds (Apel and Hirt, 2004). The superoxide anion can be converted to H_2O_2 spontaneously, or through the activity of a number of superoxide dismutases. H_2O_2 is removed from cells through the activity of a number of enzymes, including the

peroxiredoxins, catalase and glutathione peroxidases (Rhee *et al.*, 2003). It is generally accepted that reactive oxygen species (ROS) such as H_2O_2 play an important role in oxidative damage and apoptosis. ROS are associated with damage to molecules such as DNA, proteins, carbohydrates and lipids (Rhee *et al.*, 2003). Furthermore, generation of H_2O_2 in response to apoptotic signals, such as those received in response to serious DNA damage, appears to lead to the release of cytochrome *c* into the cytoplasm, which in turn triggers the activation of caspases and eventually leads to cell death (Ragu *et al.*, 2007; Tsang *et al.*, 2003).

A number of studies have shown that the peroxiredoxins are able to remove H_2O_2 from cells, and protect cells from H_2O_2-induced apoptosis when over-expressed. Bae *et al.* (2007) found that the normal breast cell line (MCF10A) transfected with prx I and II allowed cells to resist H_2O_2-induced cell death, when non-transfected cells could not. Depletion of prx III sensitized HeLa cells, a human cervical carcinoma cell line, to staurosporine- and TNF-α (tumour necrosis factor α)-induced apoptosis, and also resulted in increased intracellular H_2O_2 levels (Chang *et al.*, 2004).

ROS have also been implicated in a number of non-apoptotic signaling pathways. Signals from both platelet derived growth factor (PDGF) and epidermal growth factor (EGF) result in transient increases in intracellular H_2O_2 concentration. Inhibition of the increase in H_2O_2 prevents protein tyrosine phosphorylation normally seen in response to PDGF or EGF (Sundaresan *et al.*, 1995; Bae *et al.*, 1997). Stimulation of these cells with PDGF or EGF results in an increase in intracellular H_2O_2. Over-expression of prx I or II prevented this increase in H_2O_2 in a number of different cell lines (Kang *et al.*, 1998). Furthermore, extracellular H_2O_2 activates the transcription factor NFκB, which is then able to bind to NFκB binding sites to modulate expression of a number of genes. Over-expression of prx II in HeLa cells reduced NFκB binding to NFκB binding sites and reduced expression from a reporter construct under the control of NFκB binding sites (Kang *et al.*, 1998). Over-expression of prx III has also been shown to result in decreased cell proliferation, providing further evidence in support of a role for peroxiredoxins in regulating or terminating signals from growth factors (Nonn *et al.*, 2003). Therefore, ROS appear to be important in a

number of cellular signaling pathways, and peroxiredoxins are capable of terminating the signals generated by these pathways.

1.6 Peroxiredoxins as molecular chaperones

In 2002, Rabilloud *et al.* (2002) used two-dimensional electrophoresis and tandem mass spectrometry to examine the cellular response to oxidative stress. Their results showed that under oxidative stress a second, more acidic, form of several of the peroxiredoxins was present in cells. This more acidic form was most prominent for peroxiredoxin II, possibly because it is one of the most abundant peroxiredoxins in the Jurkat cells used in the study. These more acidic forms were not seen in response to other types of stress, therefore it is unlikely that this acidic form is associated solely with cell death. The more acidic form of prx appears to be caused by over-oxidation of the acidic site cysteine residue. The authors also report that cell death correlated with a decrease in the levels of normal prx under oxidative stress, suggesting that without functional peroxiredoxins a cell is more susceptible to oxidative stress-induced cell death.

Moon *et al.* (2005) examined prx II structural changes in response to oxidative stress, and found that over-oxidised prx II forms much higher molecular weight complexes than the dimer formed by active prx II. To test whether the higher molecular weight complexes showed chaperone activity, the aggregation of several proteins in the presence and absence of prx II was measured. The first protein to be examined was citrate synthase (CS), a protein known to aggregate at high temperatures. In the presence of prx II, thermal aggregation was inhibited. The insulin β chain was also found to be protected from dithiothreitol-induced precipitation in the presence of prx II. Finally α-synuclein aggregation in response to oxidative stress was found to be inhibited by the presence of prx II. These higher molecular weight complexes were found to possess little peroxidase activity. In contrast, prx II dimers showed high levels of peroxidase activity, and did not exhibit any molecular chaperone activity. These results suggest that prx II is able to prevent aggregation and unfolding of a wide variety of proteins, rather than a small sub-set of proteins. Therefore, prx II may function as a peroxidase in dimer form and as a molecular chaperone, preventing protein unfolding and aggregation, when over-oxidised. In contrast

to the results presented by Rabilloud *et al.* (2002), Moon *et al.* (2005) report that the over-oxidised forms of prx may increase resistance to H_2O_2-induced cell death. Kang *et al.*, (2005) suggest that when H_2O_2 concentrations increase to higher than normal levels as a result of a "death signal" the prxs are over-oxidised to prevent termination of this signal. The prxs then take on the role of molecular chaperone, protecting proteins present in the cell. If the cell survives, the prxs may be reduced and return to functioning as peroxidases.

Prx I also appears to act as a molecular chaperone after inactivation of its peroxidase activity. Jang *et al.* (2006) report that inactivation of prx I can occur through the phosphorylation of a threonine residue (Thr^{90}). Prx I phosphorylated at Thr^{90}, or mutated to aspartate at this residue to mimic phosphorylation, forms higher molecular weight complexes which exhibit negligible levels of peroxidase activity. Instead these complexes were found to possess chaperone activity, inhibiting thermal aggregation of malate dehydrogenase. Phosphorylation of Thr^{90} was found to be mediated by several cyclin-dependent kinases *in vitro*. *In vivo*, prx I phosphorylation levels cycled in parallel with cyclin-dependent kinase 2 (cdc2), suggesting that cdc2 is likely to play the most important role in prx I phosphorylation *in vivo* (Chang *et al.*, 2002). The authors suggest that phosphorylation of prx I is likely to occur after disintegration of the nuclear envelope, and that the subsequent increase in H_2O_2 levels may play an important role in cell cycle progression.

While there is evidence of molecular chaperone activity in higher molecular weight forms of prx I and II, formed following over-oxidation of the active cysteine residues, similar studies do not appear to have been carried out with other peroxiredoxins despite evidence for similar over-oxidation of these proteins.

Recently Cao *et al.* (2007) examined the structures of oxidised and reduced prx III *in vitro*. The results suggest that reduced prx III spontaneously forms into a decameric ring structure, while oxidised prx III forms homodimers. Oxidised prx III was only found to form decameric rings at high protein concentrations (10 mg/mL), which may not be physiologically relevant. Whether these complexes also acted as molecular chaperones was

not examined. However, if the results obtained with the high molecular weight complexes formed by prx I and II apply to the structures formed by prx III these results suggest that prx III may have dual functions within the cell and that adopting the role of molecular chaperone may not be dependent on enzyme inactivation. Further work on the higher molecular weight structures formed by the 2-cys prxs clearly need to be carried out to determine the exact role these structures play within the normal cellular environment.

1.7 Regeneration of active peroxiredoxin

As peroxiredoxins appear to play an important role in signal transduction through the removal of H_2O_2 from cells, it was necessary to determine whether over-oxidised peroxiredoxin could be returned to its active form. Woo *et al.* (2003) used extracts from cells incubated with $^{[35]}$S-labelled amino acids, followed by washing and incubation with un-labelled amino acids, to examine whether re-generation of active prx I was due to *de novo* synthesis or reduction of the over-oxidised form. The results indicate that the active form of prx I can be regenerated through reduction of the over-oxidised form. Regeneration of other prx isoforms has since been shown. Sulfiredoxin (Srx1), is a *Saccharomyces cerevisiae* protein encoded by a gene induced by high H_2O_2 levels. Biteau *et al.* (2003) discovered this protein was able to reduce the over-oxidised form of peroxiredoxins in yeast (a previously unknown role for Srx1). Following this discovery, the human sestrins Hi95 and PA26 were also found to reduce over-oxidised peroxiredoxins. Over-expression of Hi95 or PA26 was found to significantly increase the regeneration rate of active prx I (Budanov *et al.*, 2004) however further work is required to determine the mechanism of prx regeneration, and to identify proteins involved in regeneration of other prxs.

1.8 Peroxiredoxins and disease

Altered expression of sub-sets of the six peroxiredoxin isoforms has been linked to several diseases. Prx I expression appears to be enhanced in thyroid cancer (Yanagawa *et al.*, 1999), and lung cancer (Chang *et al.*, 2001). Prxs I, II and III appear to be over-expressed in breast cancer (Noh *et al.*, 2001). Prxs I, II, III, V and VI show increased expression compared to normal tissue in malignant mesothelioma (Kinnula *et al.*, 2002). Furthermore, prxs I and II have been found to be over-expressed, and prx III down-regulated in both

Alzheimer's disease and Down's syndrome (Kim *et al.*, 2001; Sanchez-Font *et al.*, 2003). Prxs III to VI have been shown to be down-regulated in failing human myocardium (Brixius *et al.*, 2007), while prx V appears to be up-regulated in cells of the central nervous system in multiple sclerosis patients (Holley *et al.*, 2007). This list is far from exhaustive as changes in prx expression patterns are continually being associated with new diseases.

Cancer cells are generally dividing rapidly, and as a result of constant stimulation by growth factors may have higher than normal intracellular H_2O_2 levels. The increased expression of peroxiredoxins in cancer cells may therefore be an attempt by cells to adapt to increased oxidative stress (Park *et al.*, 2006). The expression of different peroxiredoxins in different disease states suggests that while they all remove H_2O_2, the peroxiredoxins have distinct functions within the cell.

1.9 Peroxiredoxin III

Recent unpublished work suggested that peroxiredoxin III (AOP-1, MER5, PRDX3) may be up-regulated in cells exposed to doxorubicin. The exact role of prx III within the cell remains to be elucidated, however experimental results suggest that prx III plays a role in the regulation of H_2O_2 levels. Depletion of prx III from HeLa cells results in increased intracellular levels of H_2O_2, and sensitizes cells to induction of apoptosis by TNF-α (Chang *et al.*, 2004). These cells showed increased rates of mitochondrial membrane potential collapse, cytochrome *c* release and caspase activation, which suggests that prx III plays a role in mitochondria-mediated apoptosis by regulating intracellular H_2O_2 levels. Furthermore, prx III (MER5) knockout mice showed increased susceptibility to lipopolysaccharide-induced oxidative stress, and 1.5 to 2.0 fold higher intracellular H_2O_2 levels in macrophages compared to normal mice (Li *et al.*, 2007). Lee *et al.* (2007) examined prx III expression in cultured human lens epithelial cells, and cultured whole lenses and found that prx III mRNA transcript levels significantly increased following exposure to H_2O_2 concentrations as low as 2 μM. These results further support the suggestion that prx III plays an important role in the removal of H_2O_2 *in vivo*.

There is some evidence that prx III plays a role in a number of signaling pathways within the cell. Nonn *et al.* (2003) reported reduced cell proliferation in cells over-expressing prx III, which may be due to increased removal of H_2O_2 produced during growth factor signaling. Yang *et al.* (2007) also report a role for prx III in proerythrocyte differentiation. Prx III expression was found to fluctuate in human leukemia K562 cells following chemical induction of differentiation into erythrocytes. Furthermore, a K562 cell line over-expressing prx III was found to arrest in the G1 phase of the cell cycle. These results suggest that prx III plays an important role in proerythrocyte differentiation, possibly by regulating intracellular H_2O_2.

As both doxorubicin and epirubicin function to increase intracellular H_2O_2 levels (Lothstein *et al.*, 2001; Tsang *et al.*, 2003) this suggests a possible role for prx III in the development of drug resistance. Increased expression of prx III following chemotherapy with dox or epi may make cells more tolerant to the increases in H_2O_2 caused by these drugs, increasing cell survival and reducing the effectiveness of chemotherapy. Such a role for prx III is supported by the observation that prx III over-expression in WEHI7.2 mouse thymoma cells protected cells against apoptosis induced by the anti-cancer drug imexon, which also functions to increase intracellular H_2O_2 (Nonn *et al.*, 2003).

As increased or reduced peroxiredoxin expression has been shown to have consequences for a number of cellular processes and signaling pathways, it is likely that the expression of prx III and other peroxiredoxins is carefully regulated. Currently little is known about the regulation of prx III expression however recent work has identified some possible mechanisms of prx III regulation. Baker *et al.* (2007) found that prx III mRNA transcripts are up-regulated in the peripheral blood mononuclear cells (PBMC) of some patients treated with imexon. This up-regulation was seen within three hours of treatment; however sample sizes were very small. The authors also identified a putative antioxidant response element (ARE) in the prx III promoter which may play a role in this up-regulation. Specific binding of transcription factors to the ARE in the prx III promoter was not examined.

Prx III expression also appears to be partly regulated by c-Myc, and is required for Myc-mediated transformation. Wonsey *et al.* (2002) examined prx III expression using a cell system where c-Myc was fused to the hormone binding domain of the estrogen receptor. This retains c-Myc in the cytoplasm until tamoxifen, an estrogen analog, is added. Cyclohexamide was used to inhibit protein synthesis. Prx III expression was found to increase following treatment with tamoxifen and cyclohexamide, which provides indirect support for a link to c-Myc. Chromatin immunoprecipitation experiments coupled with real time PCR identified a number of regions within the prx III gene which are bound by c-Myc following the addition of serum to serum-starved cells (Haggerty *et al.*, 2003). Together, these results suggest that c-Myc directly regulates prx III expression. Logarithmically growing c-*myc*-null fibroblasts showed a reduction, but not a complete loss, in prx III expression (Wonsey *et al.*, 2002), suggesting that while c-Myc plays a role in regulating expression of prx III, other factors are likely to be involved.

Rangwala *et al.* (2007) report a further mechanism of regulation of prx III in mouse embryonic fibroblasts. Peroxisome proliferator-activated receptor γ coactivator-1α (PGC-1α) appears to induce prx III expression in an estrogen-related receptor α (ERRα)-dependent manner. ERRα regulates transcription of a number of genes by binding to estrogen response elements, however it does not bind estrogens. Prx III mRNA expression also appears to be up-regulated in mouse uterine cells in response to estradiol. This up-regulation appears to be dependent on the presence of the estrogen receptor (ER) (Deroo *et al.*, 2004), a ligand-activated transcription factor. Therefore, while prx III expression appears to be ubiquitous, there may be tissue-specific differences in the levels of prx III expression.

The regulation of prx III expression appears to be a complicated process, and remains to be fully elucidated. However, a number of studies suggest that regulation of prx III expression may be further complicated by regulation of the process of protein synthesis, or degradation. A number of studies have reported that prx III mRNA transcripts do not increase significantly, with increases above three-fold rarely being reported (Lehtonen *et al.*, 2005; Baker *et al.*, 2007; Williams *et al.*, unpublished) . Instead, larger changes are seen

in protein expression. Therefore, examining both prx III mRNA and protein levels is important when studying and drug-induced changes in prx III expression.

1.10 Research aims

Prx III was identified as being up-regulated in response to doxorubicin treatment in cultured cells, which has led to the suggestion that prx III may play a role in the development of resistance to doxorubicin and epirubicin. However, before such a role can be investigated further, the expression of prx III needs to be examined in patients undergoing chemotherapy with doxorubicin or epirubicin. White blood cells were collected from patients immediately before and three weeks after their first dose of chemotherapy with epirubicin. Samples were also collected from control subjects at three week intervals. Real time reverse transcription PCR was used to examine prx III mRNA expression, while sodium dodecylsulfate polyacrylamide gel electrophoresis (SDS-PAGE) coupled with western blotting was used to examine prx III protein levels. Furthermore, as prx III has been shown to form higher molecular weight structures, native polyacrylamide gel electrophoresis (PAGE) coupled with western blotting was used to examine complex formation by prx III in cultured MCF7 cells and white blood cells. Finally, prx III is known to be inactivated by over-oxidation of the active cysteine residue. Therefore two-dimensional electrophoresis was used to examine over-oxidation of prx III in MCF7 cells following exposure to doxorubicin.

The specific objectives of this work were:

- To examine peroxiredoxin III mRNA and protein expression in patients undergoing chemotherapy with epirubicin using real time RT-PCR and SDS-PAGE coupled with western blotting.
- To examine peroxiredoxin III mRNA and protein expression in control subjects using real time RT-PCR and SDS-PAGE coupled with western blotting.

- To examine prx III complex formation in MCF7 cells in response to doxorubicin exposure, and the white blood cells of patients and control subjects using native-PAGE coupled with western blotting.
- To examine over-oxidation of prx III in MCF7 cells following exposure to doxorubicin using two-dimensional electrophoresis coupled with western blotting.

Chapter 2: Materials and methods

2.1 Materials

Tissue culture

All sterile tissue culture flasks and cell scrapers were obtained from Nunc Inc, Naperville, IL, USA. Tissue culture plates were obtained from Greiner Bio-One, Germany. Opti-minimum essential medium (Opti-MEM®), foetal bovine serum (FBS), trypsin and penicillin-streptomycin (5,000 units/mL) were purchased from Invitrogen Corporation, Auckland, New Zealand. Acrocap Filter Unit (0.2 μm) filters were obtained from Pall Corporation, MI, USA. Dimethyl sulfoxide (DMSO) was obtained from Sigma Chemical Company, St Louis, MO, USA. Human insulin was purchased from Roche, Mount Wellington, New Zealand.

Protein manipulations

Complete™ Mini EDTA-free protease inhibitor cocktail tablets were purchased from Roche Molecular Biochemicals, IN, USA. Bradford protein assay dye concentrate and Dual Colour Precision Plus protein markers were purchased from BioRad Laboratories, CA, USA. Purified bovine serum albumin (BSA) was purchased from New England BioLabs. PlusOne™ DryStrip Coverfluid, isoelectric focusing strips, and immobilised pH gradient (IPG) buffer were purchased from GE Healthcare. N,N,N',N'-Tetramethylethylenediamine (TEMED) was obtained from Sigma Chemical Company, St Louis, MO, USA. Polyacrylamide-bis (29.1:0.9) ready-to-use solution (40%) was purchased from Merck. Monoclonal mouse antibody to peroxiredoxin III (12B) and polyclonal goat antibody to peroxiredoxin III (14-C) were purchased from Santa Cruz Biotechnology, CA, USA. Mouse monoclonal antibody to β-actin (AC-74) and rabbit anti-mouse secondary antibody conjugated to horseradish peroxidase were purchased from Sigma-Aldrich, St Louis, MO, USA. Polyvinylidine fluoride (PVDF) membrane was acquired from Pall Corporation, MI, USA. BM chemiluminescence blotting substrate A and B were purchased from Roche, Mount Wellington, New Zealand.

RNA purification and manipulation

TRIzol® was obtained from Invitrogen Corporation. Diethylpyrocarbonate (DEPC) was purchased from BDH Laboratory Supplies, Poole, England. RNaseZap™ was purchased from Ambion. First strand complimentary DNA (cDNA) synthesis kit components were obtained from Invitrogen Corporation, Auckland, New Zealand.

DNA manipulation

*Sph*I restriction endonuclease and buffer, were obtained from New England BioLabs. *Taq* polymerase was purchased from Roche, Mount Wellington, New Zealand. Agarose was purchased from BioLine Pty Ltd, New South Wales, Australia. PureLink™ PCR purification kit and 1 kb plus DNA ladder were obtained from Invitrogen Corporation. GE Healthcare supplied the dNTPs.

Real time PCR

ABsolute SYBR Capillary mix was purchased from Thermo Scientific. 96-well LightCycler 480 plates and cover sheets were purchased from Roche, Mount Wellington, New Zealand. LightCycler 480 software release 1.3.0.0705 was obtained from Roche. Primers were synthesized by Sigma Genosys Australia Pty Ltd, NSW, Australia.

General laboratory supplies

1.5 mL micro-centrifuge tubes and all pipette tips were purchased from Axygen. Ammonium persulfate (APS), KCl, NaCl, NaOH, sodium dodecyl sulfate (SDS) and urea were purchased from Merck. 15 mL and 50 mL tubes were purchased from Nunc Inc, Naperville, IL, USA. Iodoacetamide, and dithiothreitol (DTT) were acquired from Sigma Chemical Company, St Louis, MO, USA.

All other chemicals and reagents used were of an analytical grade or better.

2.2 Mammalian cell culture

All manipulations of mammalian calls, with the exception of protein and RNA extraction, were performed in a class II biohazard cabinet. Cells were grown at 37°C under humid conditions, with 5% CO_2. Media on slow growing cells was changed every 2-3 days.

2.2.1 Media

Opti-minimum essential medium (Opti-MEM®) I reduced serum medium (Invitrogen) was prepared as directed by the manufacturer. Powdered medium was dissolved in MilliQ water and 2.4 grams of tissue culture grade sodium bicarbonate was added per litre of medium. Following adjustment of the pH to 6.8, medium was filtered using a 0.2 μm AcroCap™ filter (Pall Corporation). Medium was stored in sterile glass bottles at 4°C and required supplements were added before use. Medium for MCF7 cells was supplemented with 1% penicillin-streptomycin (pen-strep), 2% fetal bovine serum (FBS), 0.1 mg/mL recombinant human insulin. Medium was warmed to room temperature immediately before use.

2.2.2 Starting cells from frozen stocks

Cell lines were stored in the gaseous phase of liquid nitrogen. When required, cells were removed from storage, thawed quickly and transferred to sterile 15 mL tubes containing 5 mL of the appropriate complete medium. Cells were pelleted by centrifugation at 1000 rpm in an Eppendorf Centrifuge 5702 and a 5702/R rotor for five minutes. Cells were re-suspended in 2 mL complete medium and 1 mL was dispensed into a Nunc T75 flask containing 12 mL of complete medium. Cells were left to grow for 2-3 days before passaging, depending on confluence.

2.2.3 Passage of cells

Cells grown to at least 80% confluence were passaged into fresh Nunc T75 flasks. Medium was removed and cells were incubated with 1.5 mL express stable trypsin-like enzyme plus phenol red (TrypLE™) for approximately two minutes. The TrypLE™ reagent was then removed and the sides of the flask were tapped sharply to aid in cell detachment.

Detachment of the cells was confirmed by examination under an inverted microscope. Cells were re-suspended in 5 mL complete medium and 2.5 mL was dispensed into new flasks containing 10 mL of complete medium. If protein was to be extracted, cells were dispersed into 150 mm tissue culture plates containing complete media.

2.2.4 Freezing of cells

Cells for storage were treated as outlined in 2.2.3 and re-suspended in 2 mL 10% DMSO in FBS and transferred to cryovials. The cryovials were wrapped in laboratory tissue and stored at -80°C overnight to slow the freezing process. The cryovials were then transferred to the gaseous phase of a liquid nitrogen store for long term storage.

2.2.5 Exposure of cells to doxorubicin

Cells were grown to approximately 70-80% confluence in 150 mm tissue culture plates or Nunc T75 flasks. Medium was removed from plates of cells to be exposed to doxorubicin. 3 mM doxorubicin-HCl (Delta West Pty Ltd) was prepared in the appropriate complete medium and carefully added to the cells. Cells were then returned to the incubator for the appropriate length of time, either 2 hours or 24 hours, before RNA or protein was extracted as outlined in sections 2.9 and 2.4 respectively.

2.2.6 Exposure of cells to oxidative stress

Cells were grown to at least 80% confluence in 150 mm tissue culture plates. Medium was removed from plates of cells to be exposed to oxidative stress. 100 μM hydrogen peroxide (H_2O_2) was prepared in the appropriate complete medium and carefully pipetted into the plate. The plate was then returned to the incubator for one hour before protein was extracted as outlined in section 2.4.

2.3 Isolation of white blood cells

Blood was collected in heparinised or EDTA-coated vacutainers at Palmerston North Hospital and transported to Massey University on ice. Three parts red blood cell (RBC) lysis solution (155 mM NH_4Cl, 10 mM $KHCO_3$, 0.1 mM EDTA) were added to one part

whole blood in sterile 15 mL or 50 mL Nunc tubes. The tubes were inverted gently to mix and incubated at room temperature for 10 minutes with shaking. RBC lysis solution is a hypotonic solution which causes lysis of RBCs but does not lyse the more robust white blood cells (WBCs). It is therefore useful for removing RBCs from a blood sample. After incubation at room temperature, the sample was centrifuged at 1300 rpm in a Sorvall RT7 centrifuge with an RTH750 rotor for 10 minutes to pellet WBCs and any remaining intact RBCs. The pellet was resuspended in RBC lysis solution and again centrifuged at 1300 rpm for 10 minutes. The WBC pellet was then washed with ice-cold phosphate-buffered saline (PBS: 0.14 M NaCl, 2.7 mM KCl, 10 mM Na_2HPO_4, 1.8 mM KH_2PO_4, pH 7.2 to 7.4) and pelleted by centrifugation for 10 minutes at 1300 rpm. This wash step was repeated to ensure that any remaining contaminants were removed. The cell pellet was then used immediately for RNA or protein extraction.

2.4 Protein extraction and quantification

2.4.1 Preparation of cells grown in monolayer for protein extraction

Cells were grown to at least 80% confluence in 150 mm tissue culture plates, with the appropriate medium. Medium was removed and cells were carefully washed twice with 5 mL PBS. Cells were then harvested in 1 mL Tris-EDTA-NaCl (TEN) buffer (40 mM Tris-Cl, pH 7.4, 1 mM EDTA, 0.15 M NaCl) using a cell scraper. Cells were transferred to a 1.5 mL micro-centrifuge tube and pelleted by centrifugation at 10,000 x g for 5 minutes at 4°C. The supernatant was discarded and the pellet was used immediately for extraction of total protein.

2.4.2 Extraction of total cellular protein

An appropriate volume of radio-immuno precipitation (RIPA) buffer (10 mM Tris-Cl, pH 8.0, 1 mM EDTA, 0.5 mM EGTA, 1% Triton X-100, 0.1% sodium deoxycholate, 0.1% SDS, 140 mM NaCl) was added to the cell pellet in a 1.5 mL micro-centrifuge tube. The mixture was passed through the pipette tip a number of times to aid with cell lysis. The sample was then incubated at 4°C for 30 minutes, with shaking. To remove unwanted cell

debris, the sample was centrifuged at approximately 13,000 x g for 30 minutes, at 4°C. The supernatant was dispensed into 20 µL, 50 µL and 100 µL aliquots in fresh micro-centrifuge tubes and stored at -80°C until required.

2.4.3 Quantification of protein extracts

The protein concentration of prepared total cellular extracts, and acetone precipitated samples in incomplete rehydration buffer (7 M urea, 2% CHAPS) was determined using a method that is based on the assay described by Bradford (1976). This method utilises the shift in the absorbance of Coomassie Brilliant Blue G-250 from 465 nm to 595 nm upon binding to protein. The increase in absorbance at 595 nm can be measured and used to calculate the concentration of protein in an unknown sample. Protein samples were diluted appropriately in MilliQ water and 5 µL was dispensed in triplicate into wells of a 96-well microplate. A 10 mg/mL stock solution of BSA (New England BioLabs) was diluted 50-fold in MilliQ water and used to produce a series of standards containing between 0 µg and 2.0 µg of protein. The standards were also prepared in triplicate. Protein Assay dye reagent concentrate (Bio-Rad) was diluted 5-fold in MilliQ water and 200 µL was added to each well. The plate was left to stand at room temperature for 10 minutes to allow the colour to develop. Absorbance at 595 nm was determined using an Anthos LabTec HT2 plate reader. A standard curve was constructed using the absorbance values for the standard samples and concentration of the unknown samples was calculated using the standard curve. An example of such a calculation is shown in appendix one.

2.5 Sodium dodecyl sulfate-polyacrylamide gel electrophoresis (SDS-PAGE)

Sodium dodecyl sulfate-polyacrylamide gel electrophoresis (SDS-PAGE) is a technique that is used to separate proteins according to their relative molecular weights. Sodium dodecyl sulfate (SDS) is an anionic detergent which binds to proteins, disrupting their secondary structure and affording each protein a negative charge that is proportional to its mass. A current is then passed through the gel, separating proteins according to their relative negative charges.

2.5.1 Casting of 10% SDS-PAGE gels

Glass spacer and short plates (Bio-Rad) were carefully cleaned with isopropanol, using lint-free wipes, and placed in the casting frame and stand. The resolving and stacking gel solutions (per 0.75 mm gel) were prepared according to the manufacturer's instructions, as outlined in table 2.1.

Component	Resolving gel	Stacking gel
1.5 M Tris-Cl, pH 8.8	1.875 mL	-
0.5 M Tris-Cl, pH 6.8	-	1.25 mL
Acrylamide-bis ready-to-use solution, 40% (Merck)	1.25 mL	838 µL
MilliQ water	1.875 mL	2.86 mL
10% SDS (w/v)	100 µL	50 µL
13% APS*	75 µL	25 µL
TEMED*	7.5 µL	5 µL

Table 2.1 Resolving and stacking gel solutions for SDS-PAGE

* APS and TEMED were added immediately before casting the gel.

Immediately before casting, APS and TEMED were added to the resolving gel solution to initiate polymerization. The solution was carefully swirled to mix and approximately 3.6 mL was poured between the glass plates using a pipette. Approximately 1.5 cm was left at the top for addition of the stacking gel. The resolving gel was over-laid with water-saturated butanol to limit access of air to the gel and ensure formation of a smooth top surface. The resolving gel was left to set for at least 30 minutes at room temperature before the butanol was washed away with MilliQ water. Blotting paper was used to remove all water from the top of the gel. APS and TEMED were then added to the stacking gel solution which was swirled to mix and approximately 1 mL was poured over the resolving

gel using a pipette. A well-forming comb was placed into the top of the gel and the gel was left to set for approximately ten minutes. To ensure complete polymerization, the gel was wrapped in a damp paper towel and plastic film and stored at 4°C overnight.

2.5.2 SDS-PAGE

SDS-PAGE was performed using a Mini-Protean 3 cell (Bio-Rad). Gels were removed from the casting frame and placed into the cells according to the manufacturers instructions. The inner chamber was filled with electrode buffer (25 mM Tris, 192 mM glycine, 0.5% SDS, pH 8.3) and the assembly was left for several minutes to check for leaks. Approximately one third of the outer tank was then filled with electrode buffer. Samples to be separated by SDS-PAGE were treated to denature all proteins. Five x treatment buffer (60 mM Tris-Cl, pH 6.8, 25% glycerol (v/v), 2% SDS, 0.1% bromophenol blue, 14.1 mM β-mercaptoethanol) was diluted 5-fold in sample. The sample was then placed in a boiling water bath for five minutes. After boiling, the sample was left to cool at room temperature. Samples were then carefully loaded into individual wells. 5 µL of Precision Plus Protein™ Dual Color Standards (Bio-Rad) were loaded into an adjacent well. Electrophoresis was performed at 120 V until the dye front was just off the bottom of the gel.

2.5.3 Coomassie staining of polyacrylamide gels

Polyacrylamide gels could be stained to detect protein. Gels were stained for 15 minutes at room temperature, with shaking, using Coomassie R-250 stain (50% methanol, 10% glacial acetic acid, 0.25% Coomassie Brilliant Blue R-250). Excess stain was then removed, the gel was rinsed with de-stain (15% methanol, 8% acetic acid), then left shaking at room temperature in fresh de-stain for several hours, or overnight.

2.6 Immunoblotting

Following separation of proteins by SDS-PAGE, the proteins could be transferred to a membrane and antibodies used to detect specific proteins. After detection, the antibodies used to detect one protein could be stripped off the membrane, allowing detection of other proteins on the membrane.

2.6.1 Transfer of proteins to PVDF membrane

The Mini-Protean 3 cell was also used for transfer of proteins from a polyacrylamide gel to a PVDF membrane for immunoblotting. A sponge soaked in transfer buffer (25 mM Tris, 192 mM glycine, pH 8.3) was placed onto the transfer cassette. Two pieces of 3 mm Whatmann® paper soaked in transfer buffer were placed on top of the sponge. The gel was equilibrated in transfer buffer for several minutes before being placed on top of the Whatmann® paper. Before use, PVDF was 'activated' in methanol for five minutes and rinsed in MilliQ water. The membrane was then equilibrated in transfer buffer and carefully placed on top of the gel to avoid trapping air bubbles. Two more pieces of 3 mm Whatmann® paper and another sponge were soaked in transfer buffer and placed on top of the membrane. The transfer cassette was closed and inserted into the transfer apparatus. An ice block was inserted into the tank to keep the system cold. Proteins were transferred at 475 mA for 1.5 hours.

2.6.2 Immunoblotting

After transfer, the membrane was blocked for one hour at room temperature with shaking, in 1% non-fat skim milk powder in Tris-buffered saline-Tween 20 (TBST: 50 mM Tris, 150 mM NaCl, 0.1% Tween-20). The membrane was then incubated overnight at 4°C, with shaking, in 0.5% blocking solution (0.5% non-fat skim milk powder in TBST) containing the primary antibody at the correct dilution. After overnight incubation with primary antibody, the membrane was washed with TBST for 10 minutes at room temperature, with shaking. This step was repeated three times. The membrane was then incubated with the appropriate horseradish peroxidase-conjugated secondary antibody in 0.5% blocking solution for one hour at room temperature. Finally, the membrane was washed for 15 minutes at room temperature with shaking. This wash step was repeated three times.

Enhanced chemiluminescence was used to detect the horseradish peroxidase-conjugated secondary antibody. BM chemiluminescence blotting substrate A (Roche) and BM chemiluminescence blotting substrate B (Roche) were mixed at a ratio of 100:1. The membrane was incubated in the blotting substrate for three minutes. The membrane was then removed from the blotting substrate and left for five minutes to allow the reaction to

develop. Light produced by the reaction was detected in a dark room using X-ray film (Kodak). X-ray films were developed using a 100Plus™ Automatic X-ray film developer.

2.6.3 Stripping of PVDF membranes

Where more than one protein was to be detected on a single membrane, the antibodies were stripped off the membrane before the membrane was exposed to further primary antibodies. Antibodies were stripped off the membrane using a 0.1 M glycine, pH 3.0 solution. Membranes were incubated in this stripping solution for 24 hours at room temperature, with shaking. The membrane was then washed several times in TBST to remove any excess stripping solution. At this point the membrane was ready for further immunoblotting.

2.7 Two-dimensional electrophoresis

Two-dimensional electrophoresis (2DE) is a technique which uses two steps to separate proteins by two different properties. In the first dimension, proteins are separated by their isoelectric point (pI) using an immobilised pH gradient (IPG). In the second dimension proteins are separated by their molecular weight using SDS-PAGE.

2.7.1 Preparation of protein sample for 2DE

Protein samples to be used for 2DE were first acetone precipitated to remove impurities and allow re-suspension in rehydration buffer. Four volumes of ice-cold acetone were added to the sample and vortexed to mix well. The sample was stored overnight at -20°C before the white, 'fluffy' protein precipitate was collected by centrifugation at approximately 8,000 x g for 15 minutes at 4°C. The supernatant was removed and the pellet was allowed to dry at room temperature for 15 minutes. Care was taken not to over-dry the pellet as this would make re-suspension difficult. Incomplete rehydration buffer (7 M urea, 2% CHAPS) plus 1 x EDTA-free protease inhibitor cocktail (Roche) was added to the protein pellet and the sample was incubated at room temperature for one hour. The sample was vortexed every 10 minutes to aid with re-suspension. Incomplete rehydration buffer was used for resuspension as some components of the complete rehydration buffer can interfere with protein

quantification. An aliquot of the sample was removed for protein quantification and the remaining sample was used for 2DE immediately or stored at -80°C until required.

2.7.2 Isoelectric focusing

An appropriate amount of total protein in incomplete rehydration buffer, typically 200 to 300 µg, was added to sufficient incomplete rehydration buffer to give a total volume of 127.4 µL. To this, 2.6 µL of IPG buffer, 0.001 g DTT and a trace of bromophenol blue were added to complete the rehydration buffer (7 M urea, 2% CHAPS, 2% IPG buffer, bromophenol blue). A 125 µL aliquot of the sample was carefully transferred into a ceramic 7 cm strip holder. The protective plastic backing strip was removed from a 7 cm Immobiline IPG DryStrip. The strip was carefully lowered into the tray, gel side down, to avoid trapping air bubbles under the strip. PlusOne Immobiline DryStrip Coverfluid (Amersham Biosciences) was used to cover the entire strip, to prevent sample evaporation. A cover slip was placed over the coverfluid. Isoelectric focusing was performed using the Ettan IPGphor II IEF system (Amersham Biosciences) and the following run parameters:

30 Volts	13 hours	Active rehydration	390 Volt hours
300 Volts	30 minutes	Step and hold	150 Volt hours
1000 Volts	30 minutes	Gradient	385 Volt hours
5000 Volts	1 hour 20 minutes	Gradient	2500 Volt hours
5000 Volts	30 minutes	Step and hold	4000 Volt hours

If the required voltage was not reached for example due to impurities in the sample, the Ettan IPGphor II IEF system used volt-hour values to ensure focusing was complete.

2.7.3 Polyacrylamide gel casting for 2DE

The resolving gel was cast as outlined in section 2.5.1, however only 0.5 cm was left at the top of the gel before water-saturated butanol was added. Once the resolving gel had set, the butanol was washed away with MilliQ water, and a few drops of MilliQ water were added to the top of the gel to prevent dehydration. The gel was wrapped in a damp paper towel and plastic film and left overnight at 4°C to ensure compete polymerization.

2.7.4 Second dimension: SDS-PAGE

After IEF the strip was washed three times in electrode buffer (25 mM Tris, 192 mM glycine, 0.5% SDS (w/v)) to remove the coverfluid. The strip was then transferred to SDS equilibration buffer (50 mM Tris-Cl, pH 8.8, 6 M urea, 30% glycerol (v/v), 2% SDS (w/v), bromophenol blue) plus 10 mg/mL DTT for 20 minutes to reduce disulfide bonds. The strip was then incubated in SDS equilibration buffer plus 25 mg/mL iodoacetamide for 20 minutes. Iodoacetamide alkylates thiol groups, preventing re-formation of disulfide bonds. Following equilibration, the strip was rinsed in running buffer then placed onto the top of the gel with the plastic backing against the glass. Care was taken to avoid trapping air bubbles between the strip and the top of the gel. 5 µL of Precision Plus Protein™ Dual Color Standards (Bio-Rad) were mixed with hot 0.5% agarose and carefully pipetted onto the gel, at the end of the IPG strip. The IPG strip was then covered with 0.5% agarose containing a trace of bromophenol blue, to prevent movement of the strip and aid in movement of proteins from the strip to the gel. SDS-PAGE was performed at 120 V until the dye front reached the bottom of the gel.

2.7.5 Immunoblotting of 2DE gel

Transfer of proteins from the gel to PVDF membrane and subsequent immunoblotting was performed as outlined in section 2.6.

2.8 Native polyacrylamide gel electrophoresis

Native polyacrylamide gel electrophoresis (PAGE) separates proteins in their native state. Unlike SDS-PAGE, where proteins are separated by their relative molecular mass, native PAGE separates proteins on the basis of both charge and mass. This makes it possible to examine the formation of protein complexes.

2.8.1 Casting of native PAGE gels

Glass spacer and short plates (Bio-Rad) were carefully cleaned with isopropanol, using lint-free wipes, and placed in the casting frame and stand. The resolving and gel solutions were made up as outlined in table 2.2.

Component	Resolving gel	Stacking gel
1.5 M Tris-Cl, pH 8.8	1.875 mL	-
0.5 M Tris-Cl, pH 6.8	-	2.5 mL
Acrylamide-bis ready-to-use solution, 40% (Merck)	0.765 mL	0.375 mL
MilliQ water	2.46 mL	2.125 mL
13 % APS*	75 µL	25 µL
TEMED*	7.5 µL	5 µL

Table 2.2 Resolving and stacking gel solutions for native PAGE

* APS and TEMED were added immediately before casting the gel.

Native PAGE gels were poured as outlined in section 2.5.1.

2.8.2 Native PAGE

Native PAGE was performed as described in section 2.5.2, without the addition of SDS. Samples were not denatured. Instead samples were mixed with loading dye (25% glycerol (v/v), bromophenol blue) to ensure samples would sink into the wells. Electrophoresis was performed at 120 V until the dye front was just off the bottom of the gel.

The proteins were then transferred from the gel to a PVDF membrane and immunoblotted, as outlined in section 2.6.

2.9 Extraction of RNA

2.9.1 Diethylpyrocarbonate treatment of tubes, tips and water

As RNA is sensitive to degradation by RNases, all pipette tips, tubes and water used during RNA extraction and cDNA synthesis were first treated with DEPC. DEPC is an alkylating agent which modifies residues in the active site of RNase A-type enzymes, inactivating them. Tips and tubes to be treated were placed in glass beakers and submerged in MilliQ water containing 0.1% DEPC. Where DEPC-treated water was required, MilliQ water containing 0.1% DEPC was placed in small glass bottles, and lids were placed loosely over the bottle opening. Beakers containing tips and tubes were covered and left overnight. The following day excess water was removed and all tips, tubes and bottles of water were autoclaved three times to inactivate any remaining DEPC.

2.9.2 Extraction of RNA

Total RNA was extracted from cells using TRIzol® (Invitrogen), following the manufacturer's instructions. All manipulations involving RNA were performed using DEPC-treated pipette tips and micro-centrifuge tubes. Benches, pipettes and gloves were cleaned with RNaseZap® (Ambion).

An appropriate volume of TRIzol® was added to the WBC pellet or, in the case of cells grown in monolayer, directly to the flask after removal of medium. TRIzol® is a monophasic solution containing phenol and guanidine thiocyanate which inhibit RNases. The cell lysate was passed through a pipette tip several times before being left at room temperature for five minutes to allow complete dissociation of nucleoprotein complexes. Cells grown in a monolayer were then scraped off the flask using a cell scraper and transferred to a 1.5 mL micro-centrifuge tube. WBCs were also transferred to a 1.5 mL micro-centrifuge tube. For every 750 µL of TRI reagent® initially added, 200 µL of chloroform was added to the sample. The lid was capped tightly and the sample was shaken vigorously for 15 seconds. The sample was then stored at room temperature for approximately 10 minutes before being centrifuged at no more than 12,000 x g for 15 minutes at 4°C. Centrifugation produced three layers; a lower phenol-chloroform layer, an

interphase, and an upper aqueous phase containing RNA. The aqueous phase was transferred to a fresh tube and RNA was precipitated by addition of isopropanol. Samples were inverted several times then left at room temperature for 10 minutes. RNA was collected by centrifugation at no more than 12,000 x g for 10 minutes at 4°C. The supernatant was removed and the RNA pellet was washed with 75% ethanol in DEPC-treated water. If RNA was not required immediately, it was stored at -80°C at this point. If RNA was to be used immediately it was pelleted by centrifugation at 7500 x g for 5 minutes at 4°C. The ethanol was carefully removed and the pellet was air-dried at room temperature. RNA was redissolved in DEPC-treated water. To ensure RNA was completely redissolved the sample was incubated at 55 to 60°C for 10 minutes. RNA concentration was determined by ultraviolet (UV) spectrophotometry using 1 µL of sample in the Nanodrop® ND-1000 spectrophotometer (Nanodrop). As the Nanodrop® instrument can accurately and reproducibly measure nucleic acid samples up to 3700 ng/µL, dilution of samples was generally not necessary for quantification. The absorbance of a sample at 260 nm (A_{260}) can be used to calculate RNA concentration using the following formula:

$$\text{Concentration} = A_{260} \times 40 \text{ mg/mL}$$

RNA at a concentration of 40 mg/mL gives an A_{260} of 1.0. The ratio of absorbance at 260 nm compared to 280 nm (A_{260}/A_{280}) was used as a guide to RNA purity and also to identify partially re-dissolved samples. Partially re-dissolved RNA has an A_{260}/A_{280} of less than 1.6. RNA samples with an A_{260}/A_{280} of 1.8 or greater were used for cDNA synthesis.

2.10 Complimentary DNA synthesis

Complimentary DNA (cDNA) was synthesised using the Super-Script first-strand system for RT-PCR (Invitrogen) and oligo$(dT)_{12\text{-}18}$ primers. Total RNA preparations, such as those prepared with TRIzol™, contain a complex mix of RNA molecules of which only 1-3% is messenger RNA (mRNA). To reduce the complexity of the final cDNA preparation oligo(dT) primers, rather than random hexamers, were chosen for cDNA synthesis. Olido(dT) primers bind to the poly(A) tail found on the majority of eukaryotic mRNA molecules and can then be extended by reverse transcriptase. Transfer RNA (tRNA) and

ribosomal RNA (rRNA) molecules make up a large proportion of total RNA preparations. As tRNA and rRNA do not contain poly(A) tails, these molecules are not reverse transcribed when oligo(dT) primers are used. Random hexamers are short primers of random sequences which bind to complimentary regions of RNA and are extended by reverse transcriptase. As the random hexamers can anneal to complimentary sequences within any RNA molecule, the resulting cDNA sample is much more complex. A more complex sample of cDNA may interfere with real time RT-PCR experiments, particularly if the transcript of interest is of low abundance. Therefore oligo(dT) primers were chosen for cDNA synthesis.

1 µg of RNA was added to 0.5 µL oligo$(dT)_{12-18}$ (0.5 µg/µL) and 1 µL of 10 mM dNTP mix. Sufficient DEPC-treated water was added to give a total volume of 13 µL. Oligo(dT) primers were annealed by incubation of the sample at 65°C for five minutes. Samples were then placed on ice for one minute. cDNA synthesis mix containing 4 µL 5X first strand buffer (250 mM Tris-HCl, pH8.3, 375 mM KCl, 15 mM $MgCl_2$), 1 µL 0.1 M DTT, 1 µL RNaseOUT™ Ribonuclease Inhibitor (40 U/µL) and 1 µL SuperScript™ III Reverse Transcriptase (200 U/µL) was then added to the sample. Incubation of the sample for 45 minutes at 55°C allowed cDNA synthesis to occur. The reaction was stopped by incubation at 70°C for 15 minutes. Before the newly synthesised cDNA could be used for RT-PCR, the remaining RNA was removed. This was achieved by addition of 1 µL of RNase H (2 U/µL) and incubation at 37°C for 20 minutes. cDNA was used for RT-PCR immediately or stored at -20°C until required.

2.11 Polymerase chain reaction (PCR)

The polymerase chain reaction (PCR) is a method which allows logarithmic amplification of short, specific sequences of DNA using a pair of primers and *Taq* DNA polymerase, a thermo-stable DNA polymerase isolated from *Thermophilus aquaticus*.

2.11.1 Reaction set up

PCR reactions were set up in 0.2 ml thin-walled PCR tubes (Eppendorf) in a total reaction volume of 50µL. 25.5 µL of sterile water, 5 µL 10 x PCR buffer plus $MgCl_2$ (100 mM Tris-

HCl, 15 mM $MgCl_2$, 500 nM KCl, pH 8.3)(Roche), 5 µL of 3 mM dNTP mix, 5 µL of the forward and reverse primer each at concentration of 50 ng/µL, 2 µL of template cDNA and 2.5 µL of *Taq* polymerase (1 U/µL) were added to the PCR tube. The tube was vortexed to mix and centrifuged briefly to collect the contents at the bottom of the tube. PCR was carried out on the GeneAmp® PCR system 2700 using the program outlined below.

94°C	3 minutes	Initial denaturation
94°C	20 seconds	Amplification 30-40 cycles
55°C	30 seconds	
72°C	45 seconds	
72°C	5 minutes	Final extension

2.11.2 Agarose gel electrophoresis

Following PCR, 1/5 (10 µL) of each reaction was examined by agarose gel electrophoresis. 50 X Tris-Acetate EDTA (TAE: 2 M Tris, 2 M acetic acid, 50 mM EDTA, pH 8.5) was diluted 50-fold in MilliQ water to give 1 X TAE. 0.7% agarose was produced by melting 0.42 g agarose in 60 ml 1 X TAE, and poured into the electrophoresis apparatus. 1 µL of ethidium bromide (10 µg/µL) was added to the gel. A comb was placed into the gel and the gel was allowed to set for 30 to 60 minutes. The gel was then covered with 1 X TAE, and 2 µL of ethidium bromide (10 µg/µL) was added to the buffer. DNA samples were mixed with loading dye (40% sucrose (w/v) 0.25% bromophenol blue) and loaded into the wells of the gel. Electrophoresis was carried out at 100 V until the dye front was approximately 2/3 of the way down the gel. DNA was visualized using a Gel Doc™ (BioRad).

2.11.3 Purification of PCR product for sequencing

Prior to DNA sequence analysis the PCR product was purified using the PureLink™ PCR Purification kit (Invitrogen) according to the manufacturer's instructions. Briefly, DNA is precipitated and bound by PureLink™ Binding buffer. Centrifugation removes impurities in the sample, while the DNA remains trapped in the spin column. The DNA can then be eluted in sterile water.

2.11.4 DNA sequence analysis

Sequencing was performed by Ms Lorraine Berry at the Allan Wilson Centre Genome sequencing service (Massey University). 2 ng per 100 bp of PCR product and 3.2 pmol of the appropriate primer were supplied in 15 µL of sterile water. Sequencing was performed using an ABI3730 Genetic Analyzer (Applied Biosystems Inc.) and the BigDye™ Terminator Version 3.1 Ready Reaction cycle sequencing kit (Applied Biosystems Inc.).

2.11.5 Restriction endonuclease digests

15 µL of the PCR reaction was added to 1 µL *Sph*I, 5 µL 10 x Buffer 2 (0.5 M NaCl, 0.1 M Tris-HCl, 0.1 M $MgCl_2$, 10 mM DTT, pH 7.9)(New England BioLabs) and 29 µL of sterile water. The solution was vortexed to mix and incubated at 37°C for one hour. The solution was then incubated at 70°C for 20 minutes to stop the reaction.

2.12 Real time PCR

Real time PCR is a rapid PCR method which allows quantification of the amount of DNA present in the reaction after each round of amplification using a fluorescent dye or probe. As a result, amplification can be seen in real time, rather than only at the end of 30 or 40 cycles. Therefore real time PCR is more reliable for quantification studies.

2.12.1 Setting up the basic reaction

Real time RT-PCR reactions were set up in 96-well plates that were designed specifically for use with the LightCycler™ 480 (Roche). Reactions were prepared in 20 µL volumes. A master mix was created and 15 µL of this was carefully pipetted into each required well. The amount of each component required for one reaction is shown in table 2.3. When x number of reactions were to be prepared, a master mix was created for $(x + 1)$ reactions to ensure there was sufficient master mix for all reactions.

Absolute QPCR SYBR Green mix 2x concentration (ABgene)	10 µL
Forward primer	2 µL
Reverse primer	2 µL
Sterile water	1 µL
Total	15 µL

Table 2.3 Real time PCR reaction components required for one reaction

After addition of the master mix, 5 µL of DNA template was added to each well. Negative controls containing 5 µL of sterile water instead of template DNA were included with each real time PCR run. The LightCycler™ 480 was programmed to cycle as outlined in table 2.4.

Step	Cycles	Temp. (°C)	Hold	Ramp Rate (°C/s)	Acquisition mode	Analysis mode
Preincubation	1	95	15 min	4.4	None	None
		95	10s	4.4	None	
Amplification	30*	60	10s	2.2	None	Quantification
		72	25s	4.4	None	
		85	5s	4.4	Single	
	1	95	5s	4.4	None	Melting curves
Melting		65	1 min	2.2	None	
curve		97	-	-	Continuous	5 acquisitions/°C
Cooling	1	40	10s	1.5	None	None

Table 2.4 The LightCycler 480 cycle programme.

* The number of cycles was adjusted to 35 or 40 when required.

To reduce the influence of primer dimers formed by the peroxiredoxin III (prx III) primers, an additional step based on the method reported by Ball *et al.* (2003) was included in the program. Immediately before fluorescence was determined by the LightCycler™ 480, the sample temperatures were increased to 85°C for 5 seconds. This is one degree below the

melting point of the peroxiredoxin III product, and above the melting point for the primer dimers. Therefore this step is expected to melt most, if not all, primer dimers before determination of fluorescence. Upon completion of an experiment, melting peaks were examined to confirm the expected products were produced. Agarose gel electrophoresis was also used to examine the reaction products. A sample agarose gel is presented in appendix eight. An example of the amplification curves and melting peaks that were obtained during real time RT-PCR experiments can be found in appendix nine and ten respectively.

2.12.2 Determination of optimal primer concentrations

The optimal primer concentration should be determined before quantification of DNA samples. If primer concentration is too high primer dimers may become a serious problem. If primer concentration is too low, it may limit the PCR resulting in a shift in the C_T values for a sample. To determine the optimal primer concentration a series of primer concentrations from 0.5 μM to 4 μM were prepared, to give concentrations from 50 nM to 400 nM in the final reaction mixture. The concentration of the forward and reverse primers was identical in any reaction. Triplicate reactions of each primer concentration were run using a series of serial dilutions of a cDNA sample. C_T values and melt curves were examined and the lowest primer concentration which did not result in a shift in the C_T values was determined. The final products were examined using agarose gel electrophoresis to ensure a single product of the correct size was obtained.

2.12.4 Determination of primer efficiency

Ideally, a primer pair will give an efficiency of 2.0. That is, with each cycle the number of copies of the sequence of interest doubles. A number of factors, such as longer amplicons and impurities in the reaction mixture, can result in lower efficiencies. To enable correction for different primer efficiencies when determining relative expression levels, the average efficiency for each primer pair must be determined. A series of dilutions of cDNA were made and used in real time PCR reactions. The LightCycler™ 480 software (Roche) was used to produce a plot of C_T against log concentration. The primer efficiency was also calculated by the software using this plot. A series of ten standard curves were generated

over several days to give a total of 10 efficiency values. The average efficiency was then calculated.

2.12.5 Calculation of relative expression levels

The expression level of peroxiredoxin III after chemotherapy, relative to expression levels before chemotherapy were calculated using a method first described by Pfaffl (2001). These were normalized to an internal control, β-actin, to control for differences in RNA quality and total cDNA. The equation is given in section 3.6.

2.13 Statistical Analysis

A one-sample, two-sided t-test (α=0.05) was used to examine the statistical significance of any apparent differences between the observed mean fold change for each sample and a hypothetical mean of one, or no change. A sample calculation is given in appendix two.

2.14 Ethics Approval

This study (CEN/07/020003) was given ethical approval by the Central Regional Ethics Committee.

Chapter 3: Expression of peroxiredoxin III *in vivo*

3.1 Introduction

Recent unpublished work examining changes in gene expression in cells in culture suggested that peroxiredoxin III (prx III) may be up-regulated following exposure to doxorubicin. One of the cytotoxic functions of doxorubicin is to increase intracellular hydrogen peroxide (H_2O_2) levels. As prx III has been shown to remove H_2O_2 (Chang *et al.*, 2004), it has been suggested that prx III may play a role in the development of resistance to doxorubicin. Therefore a small clinical study was begun in an attempt to correlate expression of prx III *in vivo* with clinical outcome of chemotherapy with doxorubicin or epirubicin. As it is not possible to examine the response of tumour cells *in vivo*, white blood cells were chosen as an indicator of cellular responses to chemotherapy in this study. White blood cells are often used as markers for response to treatment as collection is not invasive, and many drugs reach target sites through the bloodstream, resulting in exposure of white blood cells to the drug (Lequerré *et al.*, 2006). It is important to note that this is a pilot study and the clinical outcome of chemotherapy for the patients involved will not be available for several years.

The aim of the work presented in this chapter was to examine the expression of prx III in cancer patients before, and three weeks after chemotherapy with epirubicin. Where possible, samples were to be obtained following three successive rounds of chemotherapy however as some patients did not tolerate chemotherapy well and time was limited, in most cases this was not possible. As little is currently known about the expression of peroxiredoxin III, these experiments were also performed in a number of control subjects at three week intervals.

The expression of prx III mRNA was examined using real time reverse-transcription PCR (RT-PCR). This technique utilizes a fluorescent dye, in this case SYBR Green, which binds non-specifically to double-stranded DNA, and a pair of primers designed to amplify a specific DNA sequence. Figure 3.1 outlines the principle of real time PCR. Real time PCR and real time RT-PCR are exactly the same; the RT simply indicates that the template used

in the reaction is cDNA rather than genomic DNA. The progress of the PCR is monitored in real time by the increase in fluorescence at the end of each cycle. Initially specific fluorescence due to replication of the DNA of interest can not be distinguished from background fluorescence levels. The "threshold cycle" (C_T), or the cycle where fluorescence from a PCR product can be distinguished from background fluorescence, is determined by the LightCycler software (Roche). During early cycles all the reaction components are fresh and in plentiful supply, leading to efficient replication. This is the exponential phase and is most useful for quantification purposes. As the reaction progresses, components become limiting and the rate of replication slows until eventually a plateau is reached and no further significant increase in fluorescence is seen. The more copies of the DNA of interest there are in the sample, the more rapidly fluorescence above background levels can be detected. Real time RT-PCR data can be used for absolute or relative quantification experiments. For the purposes of this study relative quantification was used. Changes in prx III were normalized to β-actin to control for variation in RNA quality and total cDNA quantity. β-actin was found to be a suitable loading control as microarray data showed that β-actin expression was unchanged following exposure to doxorubicin (Williams *et al.*, unpublished).

Changes in mRNA levels are not necessarily reflected in protein levels due to regulation of protein synthesis and degradation. Therefore SDS-PAGE followed by western blotting was used to examine prx III protein levels. Following electrophoresis (section 2.5), proteins are transferred to a PVDF membrane (section 2.6) and incubated with a primary antibody against the protein of interest. Excess primary antibody is then washed off and the membrane is incubated with a secondary antibody directed against the primary antibody. The secondary antibody is conjugated to horseradish peroxidase (HRP), which reacts with a proprietary reagent (Roche), to emit chemiluminescence. The binding of secondary antibody to the primary antibody can therefore be detected by exposing the membrane to X-ray film. Comparison of the protein of interest to a loading control such as β-actin can be used to control for differences in protein loading between two different samples.

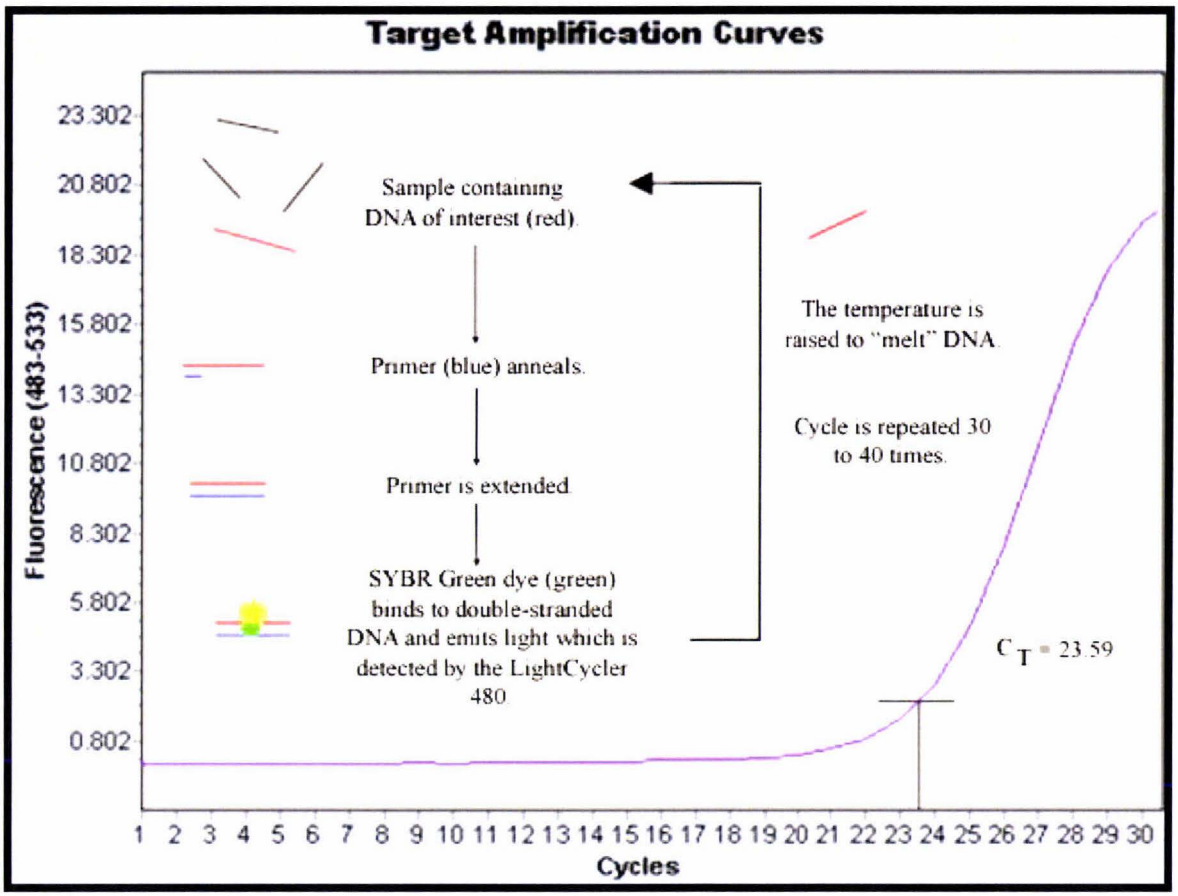

Figure 3.1 Outline of the principles of real time PCR.

Primers designed to the DNA sequence of interest anneal to DNA in the sample. The primers are then extended, as in normal PCR, to produce a double stranded piece of DNA. The SYBR Green dye binds to the double stranded product and emits light which is detected by the LightCycler 480. The "threshold cycle" (C_T), or the cycle where fluorescence from a PCR product can be distinguished from background fluorescence, is determined by the LightCycle software (Roche). During early cycles all the reaction components are fresh and in plentiful supply, leading to efficient replication. This is the exponential phase and is most useful for quantification purposes. As the reaction progresses, components become limiting and the rate of replication slows until eventually a plateau is reached and no further significant increase in fluorescence is seen.

3.2 Expression of peroxiredoxin III mRNA

Blood samples (8 mL where possible) were collected from patients immediately before, and three weeks after their first dose of chemotherapy. All patients received chemotherapy with epirubicin, however it should be noted that a cocktail of drugs is usually used. Therefore, it can not be ascertained with any certainty whether any changes in prx III expression are due solely to treatment with epirubicin. Patients also received varying doses of the chemotherapeutic cocktail, which was modified for each patient. The cocktail and dose received by each patient was not known at the time of writing.

Patient samples were collected in EDTA- or heparin-coated vacutainers, to prevent coagulation, and stored on ice. White blood cells were isolated as soon after collection as possible. Following isolation of white blood cells, RNA was extracted and 1 μg of RNA was used in first-strand cDNA synthesis reactions. Real time RT-PCR was performed using the program outlined in table 2.4. The primer sequences are given in figure 3.2. β-actin primers were designed by Kelly Senior (Massey University, Palmerston North) and produced an amplicon of 189 bp. Prx III primers were designed by Lehtonen *et al.* (2005) to give an amplicon of 352 bp. Both primers were designed to span an intron-exon boundary, to prevent amplification of genomic DNA. To confirm that the primers did not amplify genomic DNA, cDNA synthesis reactions were carried out minus reverse transcriptase. Real time RT-PCR experiments using the cDNA minus reverse transcriptase reaction products did not produce a product with either primer pair. This confirmed that the primers did not amplify genomic DNA.

β-actin forward primer	5' GGGAAATCGTGCGTGACAT 3'
β-actin reverse pimer	5' GAAGGAAGGCTGGAAGAGTG 3'
Prx III sense primer	5' CTTGGTGTATTTATCCAGGCAAGATGGC 3'
Prx III antisense primer	5' GGCCTGCTGCATGTGGAAGAACGA 3'

Figure 3.2 Primer sequences

β-actin primers were designed by Kelly Senior (Massey University, Palmerston North), to produce an amplicon of 189 base pairs (bp). Prx III primers were designed by Lehtonen *et al.* (2005) to produce an amplicon of 352 bp.

3.3 Specificity of prx III primers

Specificity of the prx III primers was determined by restriction enzyme digestion experiments and DNA sequencing of the PCR product. PCR was performed (section 2.11.1) to give a product of approximately 350 base pairs, as shown in lane four of figure 3.3. PCR with the β-actin primers also produced a product of the expected size (lane two). To confirm that this product was due to amplification of prx III, the product was isolated using the PureLink™ PCR Purification kit (Invitrogen) and digested using the restriction endonuclease *Sph*I. This was expected to produce two products, one of 109 bp and a second of 243 bp. The products of this digestion were examined using agarose gel electrophoresis. The results of the enzyme digest are shown in figure 3.4. Lane one contains 10 μL of a 1 kb plus DNA ladder, used to give an indication of the size of PCR and digestion products. Lane two contains 10 μL of the restriction enzyme digestion reaction. Two bands of the expected sizes are clearly visible in this lane. The digestion was only partially complete as there is still some visible undigested PCR product, which is the same size as the product in the undigested PCR sample loaded in lane three. A small amount of primer dimer is visible at the bottom of lane three. These results support the conclusion that the prx III primers are specific for prx III.

To further confirm that the PCR product was prx III, the purified PCR product was also sent to Lorraine Berry at the Allan Wilson Centre Genome Sequencing Service (Massey University, Palmerston North) to be sequenced. The sequence of the PCR product, aligned

with the mRNA sequence of prx III, NCBI accession number NM006793, is shown in figure 3.5. The sequences align, with only a few uncalled bases at each end of the PCR product sequence (top line) and a single mismatch within the sequence, which may be due to a polymorphism. A portion of the chromatogram obtained during DNA sequencing is presented in appendix twelve.

These experiments confirm that the prx III primers are specific for peroxiredoxin III.

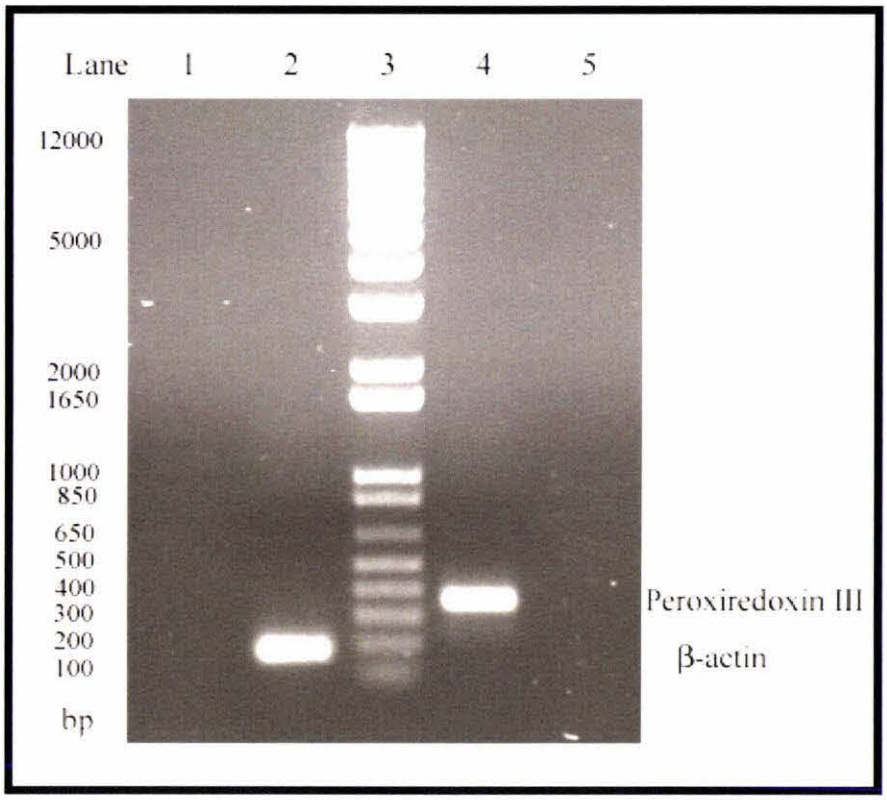

Figure 3.3 β-actin and peroxiredoxin III PCR products.

PCR was performed with β-actin (lane 2) or peroxiredoxin III (lane 4) primers and cDNA prepared from MCF7 as the template. Negative control reactions with water were also performed and are shown in lanes 1 (β-actin primers) and 5 (prx III primers). 10 µL (1/5) of each PCR reaction was separated on a 0.7% agarose gel in 1 x TAE buffer by electrophoresis at 100 V for approximately one hour. 10 µL of 1 kb plus ladder was loaded in lane 3. DNA was visualized by incorporation of ethidium bromide (0.5 µg/mL) into the gel and running buffer, and exposure to UV light. The sizes of the molecular size markers are shown on the left in base pairs (bp). PCR with β-actin primers produced a product of approximately 190 bp; while PCR with prx III primers produced a product of approximately 350 bp. Expected sizes were 189 bp and 352 bp respectively for β-actin and prx III.

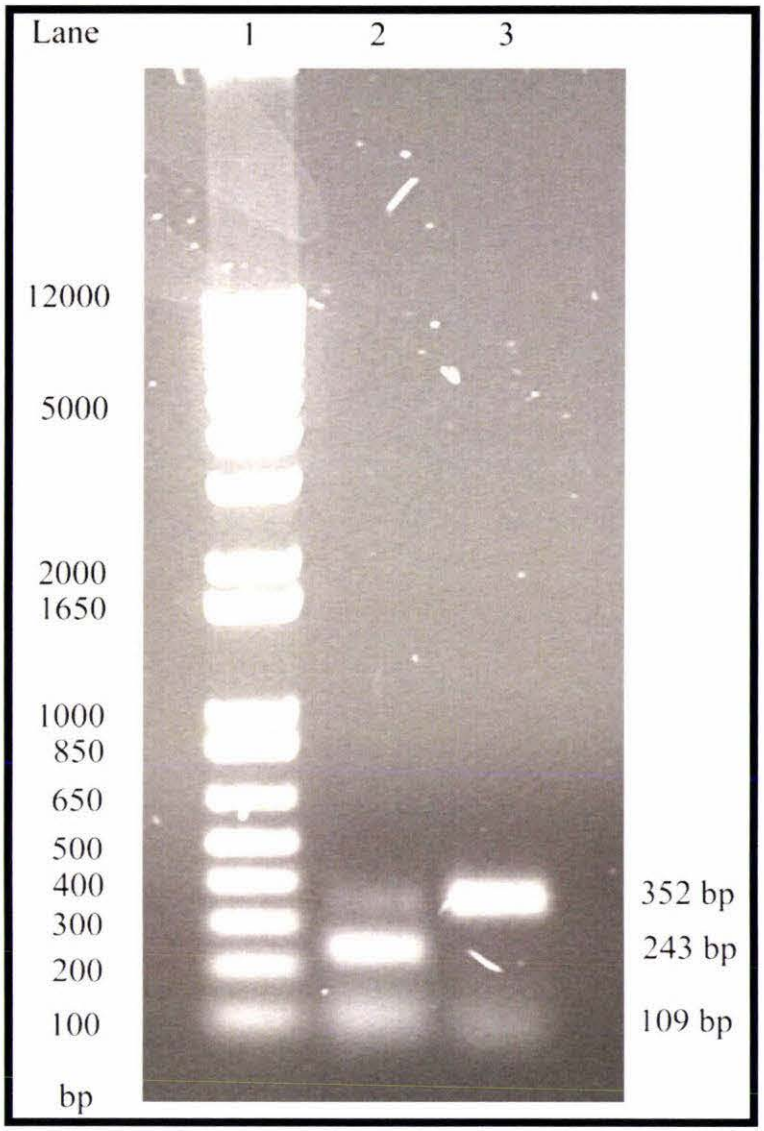

Figure 3.4 Digestion of the peroxiredoxin III PCR product with *Sph*I.

PCR was performed using prx III primers and MCF7 cDNA, and digested with the restriction enzyme *Sph*I. The digested PCR product and an undigested control sample were separated on a 0.7% agarose gel in 1 x TAE buffer by electrophoresis at 100 V for approximately one hour. DNA was visualized by incorporation of ethidium bromide into the gel and running buffer, and exposure to UV light. The sizes of the molecular markers are given on the left, in base pairs (bp). Lane one contains 10 µL of a 1 kb plus ladder. Lane two contains 10 µL of the digestion reaction. Lane three contains 10 µL undigested PCR product. Digestion of the PCR product with *Sph*I produced two products (lane two); one of 243 bp and the other of 109 bp. Digestion was incomplete with some product remaining undigested.

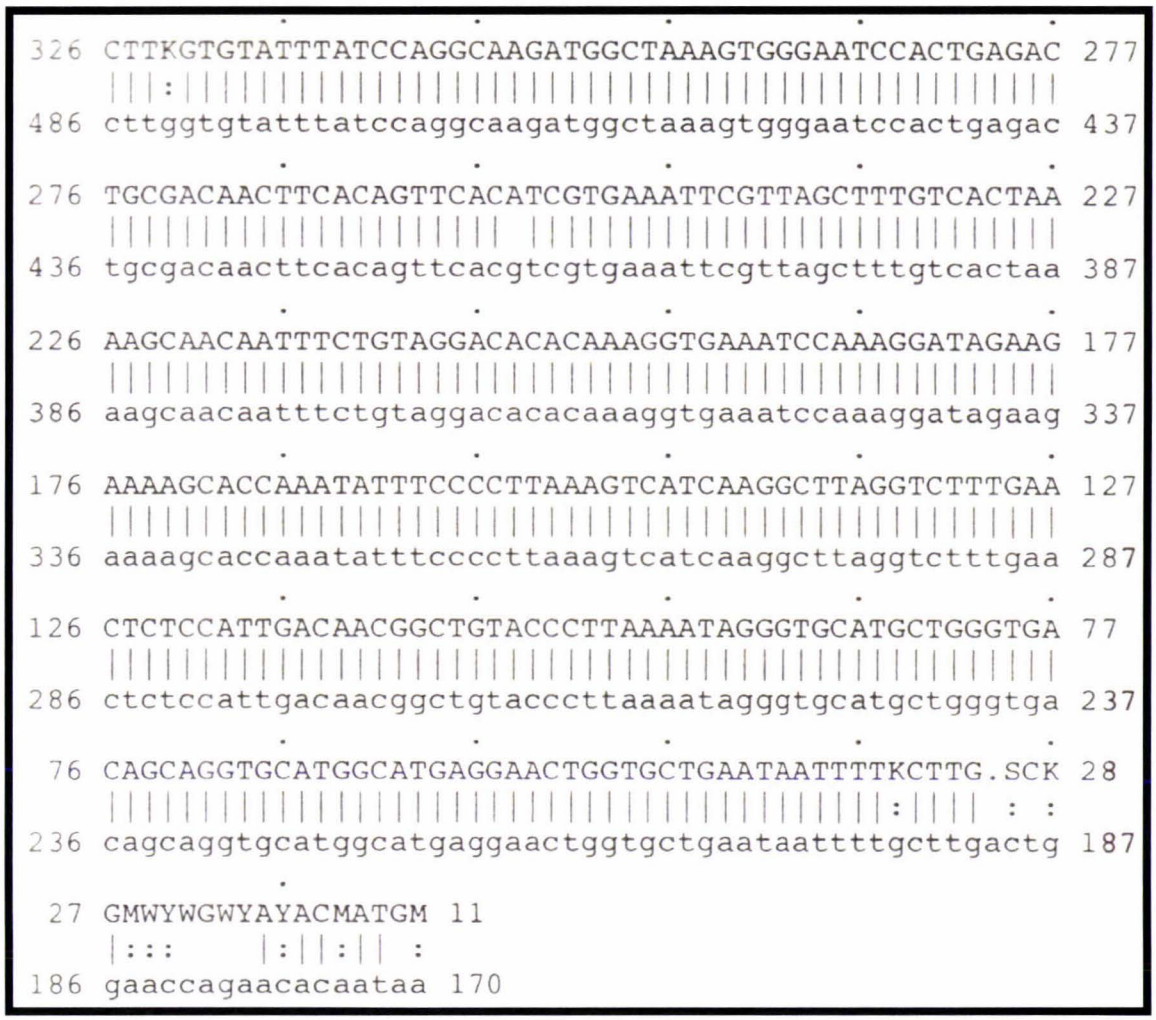

Figure 3.5 Alignment of PCR product sequence and prx III mRNA sequence

PCR was performed using cDNA prepared from MCF7 cells and prx III primers. The product was purified using the PureLink™ PCR Purification kit (Invitrogen) and sequenced by Ms Lorraine Berry at the Allan Wilson Centre Genome Sequencing Service (Massey University, Palmerston North)(top line). Prx III mRNA sequence (lower line) was obtained from the NCBI nucleotide database (accession number NM006793). Sequences were aligned using BestFit. A portion of the chromatogram obtained during DNA sequencing is presented in appendix twelve.

3.4 Determination of optimal primer concentrations

The optimal primer concentration was determined before real time RT-PCR was used for quantification experiments. Figure 3.6 shows the shift in amplification curves when primer concentration was too low. Two different dilutions, 1/10 and 1/100, of a cDNA sample were used. The purple (1/10) and brown (1/100) lines show amplification curves for reactions where the prx III primers are at a final concentration of 100 nM. The cyan and blue lines show the same samples amplified using primers at a final concentration of 50 nM. The cyan and blue lines are offset to the right, compared to the purple and brown lines. This is because the reduced amount of primer limited the PCR reaction, increasing the number of cycles required for amplification.

To determine the optimal primer concentrations, real time RT-PCR reactions were performed using final primer concentrations ranging from 50 nM to 400 nM for both the β-actin and prx III primers. The products were examined using a combination of melting curve analysis and agarose gel electrophoresis. Examples of melting peaks and agarose gel electrophoresis results are presented in appendix eight, nine and ten.

The optimal concentrations were found to be 200 nM for the β-actin primers and 100 nM for prx III. Although optimizing the prx III primer concentration greatly reduced primer dimer formation, the prx III primers were capable of dimer formation therefore an additional step was added to the cycle program as an extra precaution. Before fluorescence was detected at the end of each round of amplification, the temperature was raised to 85°C. This was expected to melt any prx III primer dimers, preventing their contribution to the fluorescence readings (Ball *et al.*, 2003).

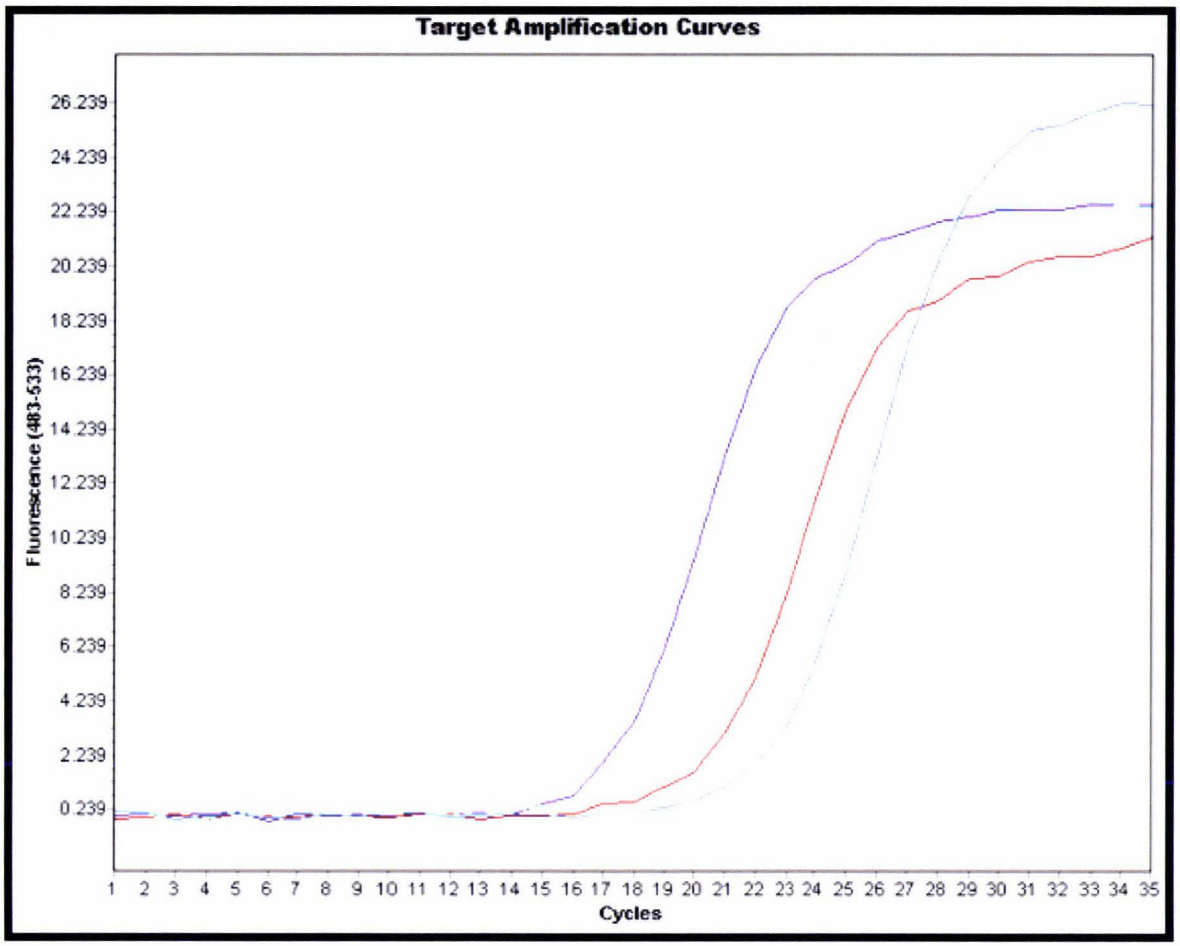

Figure 3.6 Low primer concentration results in a shift in amplification curves.

A sample of cDNA was diluted 1/10 and 1/100 in sterile water. Real time RT-PCR was performed on these two diluted samples with primers at a final concentration of 100 nM (purple and brown lines respectively) or 50 nM (cyan and blue lines respectively). The cyan and blue lines are shifted to the right, compared to the purple and brown lines. This is a result of limiting primer concentration, and shows that 50 nM is not suitable as a final concentration for prx III primers.

3.5 Determination of average primer efficiency

Relative quantification was performed using a method first described by Pfaffl (2001). This method requires determination of the average efficiency of each primer pair. To determine the average efficiency, a series of dilutions (1/5, 1/10, 1/50, 1/100, 1/500) of white blood cell first strand cDNA were created and used in real time RT-PCR experiments (section 2.12). A standard curve of log concentration versus fluorescence was produced and the efficiency was calculated by the LightCycler 480 software (Roche). The efficiencies determined from ten individual standard curves, generated over a number of days, were used to calculate the average efficiency. A sample of the data used to generate the standard curves is presented in appendix three. The average efficiencies of the β-actin and prx III primers, calculated from the efficiencies listed in table 3.1, were found to be 1.97 (±0.015) and 1.96 (±0.045) respectively. These are acceptable for use in quantification as the highest possible efficiency for PCR is 2.00.

Prx III efficiency	β-actin efficiency
2.03	1.969
1.971	1.986
1.937	1.991
1.927	1.961
1.940	1.942
2.032	1.991
1.959	1.973
1.968	1.962
1.900	1.967
1.909	1.976

Table 3.1 Efficiency values determined from ten individual standard curves.

A series of dilutions (1/5, 1/10, 1/50, 1/100, 1/500) of cDNA were generated and used in real time RT-PCR experiments to produce ten standard curves. These standard curves were used to calculate the efficiency of each primer pair. The averages of ten such efficiencies were used in subsequent relative quantification calculations. The average efficiency for the β-actin primers was 1.97 (±0.015), while the average efficiency for the prx III primers was 1.96 (±0.045). Appendix three shows a sample of the data used to calculate these efficiencies.

3.6 Fold change in prx III mRNA

The fold change in prx III mRNA was calculated using the formula shown below.

$$\frac{E_{\text{Prx III}}^{C_T \text{ before} - C_T \text{ After}}}{E_{\beta\text{-actin}}^{C_T \text{ before} - C_T \text{ After}}}$$

Where:

E is the efficiency of the indicated primer pair

C_T^{before} is the threshold cycle of the indicated gene for the sample taken before treatment.

C_T^{after} is the threshold cycle for the indicated gene for the sample taken after treatment.

This formula was first reported by Pfaffl (2001) as a method for calculating relative expression levels of a gene of interest. Normalisation to a house-keeping gene, such as β-actin, controls for differences in RNA quality and total cDNA quantity. Unlike other methods used for relative quantification, such at the $\Delta\Delta C_T$ method, this formula also allows for correction for differences in primer efficiency.

Each sample was analysed in triplicate with the average threshold cycle (C_T), as calculated by the LightCycler 480 software, being used to calculate the fold change. β-actin and prx III reactions for each sample to be compared were run at the same time. Where possible the average fold change was calculated from three separate experiments. The average fold changes for patient samples are shown in table 3.2, and changes for control samples are shown in table 3.3. All calculated fold changes and a sample calculation are given in appendix two. A sample of the data used to calculate the fold change values is presented in appendix six.

Two patients, patient two and patient three, showed a statistically significant increase in prx III mRNA three weeks following the first dose of chemotherapy treatment. One of these patients, patient three, also showed a further increase in prx III mRNA following the second

dose of chemotherapy. However, this patient also received treatment for a serious infection during the course of this study. It is unknown whether this would have influenced prx III expression as little is known about the expression and regulation of this gene. No other patients were followed beyond the first dose of treatment. One patient, patient five, showed a statistically significant decrease in prx III mRNA expression following chemotherapy. The remaining patients, patient one and patient four, showed no statistically significant changes in prx III mRNA following the first dose of chemotherapy.

Patient	Average fold change	Two-tailed p-value
One	0.731	0.1853
Two	2.22*	0.0084
Three	1.337*	0.0013
Three (Round 2)	2.33*	0.0012
Four	0.734	0.0916
Five	0.527*	0.002

Table 3.2 Prx III fold changes calculated for patients

Real time RT-PCR was performed using cDNA prepared from white blood cell samples collected immediately before and three weeks after chemotherapy. Where possible the results of three experiments were used to calculate the average fold change. * denotes a statistically significant difference from the hypothetical mean of 1.0, or no change, as determined by a one-sample, two-sided t-test ($p < 0.05$). Patients two and three showed statistically significant increases in prx III mRNA, while patient five showed a statistically significant decrease in prx III mRNA three weeks following the first dose of chemotherapy. Patient three showed a further increase in prx III mRNA three weeks following a second dose of chemotherapy. A sample of the data used to calculate these fold change values is presented in appendix six. All calculated fold changes used to determine average fold changes are presented in appendix two.

	Fold Δ between first and second sample		Fold Δ between second and third sample	
Control	**Average fold change**	**Two-tailed p-value**	**Average fold change**	**Two-tailed p-value**
One	1.03	0.4899	1.26	0.3143
Two	1.26	0.297	0.78*	0.0082
Three	1.24	0.4116	1.414	0.071
Four	1.363*	0.0255	1.10	0.6854

Table 3.3 Prx III fold changes calculated for all control samples

Real time RT-PCR was performed using cDNA prepared from white blood cell samples collected from control samples collected at three week intervals. Where possible the results of three experiments were used to calculate the average fold change. * denotes a statistically significant difference from the hypothetical mean of 1.0, or no change, as determined by a one-sample, two-sided t-test ($p < 0.05$). All calculated fold changes used to determine average fold changes are presented in appendix two.

One of the control subjects showed a small but statistically significant increase in prx III mRNA between the first and second sample, collected three weeks apart. However, no further increase was seen between the second and third sample, which were also collected three weeks apart. Another control subject showed no significant change in prx III mRNA between the first and second sample. However a small, but statistically significant change was seen between the second and third sample. These changes were also smaller than the changes seen in most of the patient samples.

The sample sizes in this study were too small to draw any conclusions; however the results suggest that prx III mRNA levels do not fluctuate greatly in the white blood cells of most healthy people. In contrast, some patients undergoing chemotherapy with epirubicin may show changes in prx III mRNA expression. SDS-PAGE followed by western blotting was

used in an attempt to determine whether these changes were translated into changes in prx III protein levels.

3.7 Expression of prx III protein

SDS-PAGE was performed using 20 μg (control samples) or 30 μg (patient samples) of total protein, and proteins were then transferred to a PVDF membrane (section 2.6). Prx III was detected using a mouse monoclonal anti-prx III (12B) antibody (Santa Cruz), at a dilution of 1/1000. β-actin was detected using a mouse monoclonal anti-β-actin (AC-74) antibody (Sigma) at a dilution of 1/2500. HRP-conjugated rabbit anti-mouse antibody (Sigma) was used at a dilution of 1/5000 to detect both primary antibodies.

A number of problems were encountered during the optimization of the SDS-PAGE and western blot experiments. Initially a polyclonal goat anti-prx III antibody (Santa Cruz) was used to detect prx III. Following several unsuccessful attempts to detect prx III, the antibody was tested on purified histidine-tagged prx III (Sapphire BioScience) and found not to detect prx III. Therefore, a new mouse monoclonal antibody to prx III (Santa Cruz) was ordered and tested on purified prx III. This was found to detect the purified protein. The method initially used to extract total protein also did not release prx III from mitochondria. As a result, prx III was collected with the cellular debris during centrifugation, and discarded. A number of different extraction methods were trialled before an appropriate method for the extraction of prx III was identified. A further problem was found with the membrane being used. A nylon membrane was initially used during the transfer of proteins for immunoblotting, however this was found not to hold protein well, as a second membrane placed behind the first during transfer was found to "capture" a reasonable amount of protein. Using PVDF for western blot experiments appears to rectify this problem.

Figure 3.7 shows western blot results for all available control samples and figure 3.8 shows western blots for all available patient samples. Initially relative quantification and normalization of prx III signals was to be attempted, however a number of problems prevented this.

As seen in figures 3.7 and 3.8 (lower panel), western blotting of β-actin resulted in a number of bands rather than a single clear band. A cluster of approximately seven bands was seen in most samples, however in longer exposures additional bands were also seen above these seven bands (figure 3.9). This may be due to non-specific binding of the antibody or degradation of the samples during white blood cell isolation or protein extraction. The regular appearance of the same seven bands, as well as the higher molecular weight bands would support non-specific binding of the antibody. Furthermore, there was no evidence to suggest that prx III was degraded, however degradation of the samples can not be ruled out. SDS-PAGE and western blotting of an MCF7 cell extract alongside a white blood cell extract showed a single band of the same electrophoretic mobility as the largest of the seven regular bands (appendix seven), therefore this band was expected to be β-actin. As one of the other bands showed a very similar electrophoretic mobility to β-actin, separation of these bands for quantification would not have been possible. As a result, quantification was not attempted.

β-actin was also much more abundant than prx III. Loading 20 μg or 30 μg of total protein gave clear bands for prx III after exposing the membrane to x-ray film for 3 minutes while β-actin gave indistinguishable bands after only five seconds. Loading only 10 μg total white blood cell protein was attempted, however the prx III signal often became too weak to be detected, even after longer exposures. Another loading control, α-tubulin, was also trialled. However, as shown in appendix five, the antibody gave a single clear band for MCF7 control extracts, but α-tubulin was not detected in white blood cell extracts. The reason for this remains unclear.

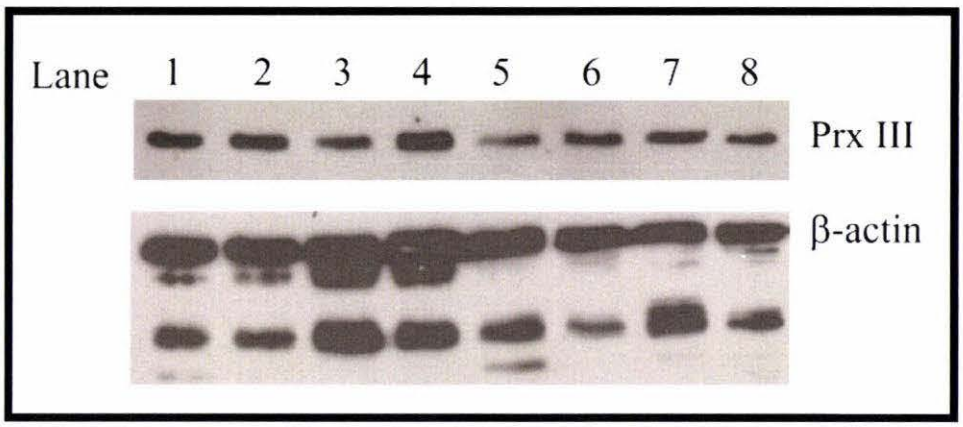

Figure 3.7 Western blot results for all control samples

One blood sample was taken from control subjects (odd numbered lanes) and a second was taken three weeks later (even numbered lanes). White blood cells were isolated and total protein as extracted. 20 µg of total protein was separated on a 10% SDS-PAGE gel and immunoblotted to detect prx III (upper panel). The membrane was stripped overnight in 0.1 M glycine, pH 3.0, to remove bound antibody, then blotted to detect β-actin (lower panel). Experiments using MCF7 extracts suggest the highest band in the lower panel is β-actin (appendix seven). The cause of the other bands seen in the lower panel remains undetermined.

Lane	Contents
1	20 µg control one, sample one
2	20 µg control one, sample two
3	20 µg control two, sample one
4	20 µg control two, sample two
5	20 µg control three, sample one
6	20 µg control three, sample two
7	20 µg control four, sample one
8	20 µg control four, sample two

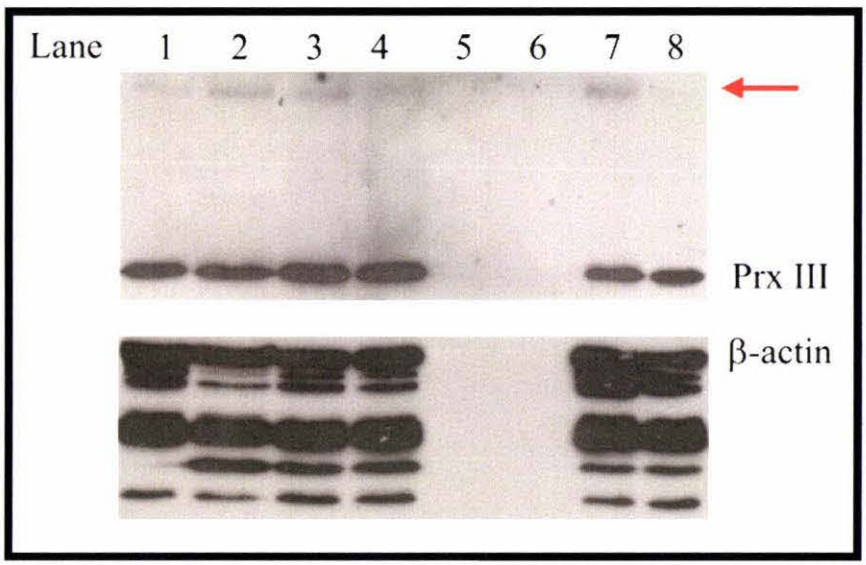

Figure 3.8 Western blot results for all patient samples

One blood sample was taken from patients immediately before chemotherapy (odd numbered lanes) and a second sample was taken three weeks following chemotherapy (even numbered lanes). White blood cells were isolated and total protein as extracted. 30 µg of total protein was separated on a 10% SDS-PAGE gel and immunoblotted to detect prx III (upper panel). The membrane was stripped overnight in 0.1 M glycine, pH 3.0, to remove bound antibody, then blotted to detect β-actin (lower panel). Experiments using MCF7 extracts suggest the highest band in the lower panel is β-actin. The cause of the other bands seen in the lower panel remains undetermined. Some prx III remained in dimer form (red arrow) despite boiling samples with treatment buffer containing β-mercaptoethanol for a minimum of five minutes.

Lane	Contents
1	30 µg patient one, sample one
2	30 µg patient one, sample two
3	30 µg patient two, sample one
4	30 µg patient one, sample two
5	Empty
6	Empty
7	30 µg patient three, sample one
8	30 µg patient three, sample two

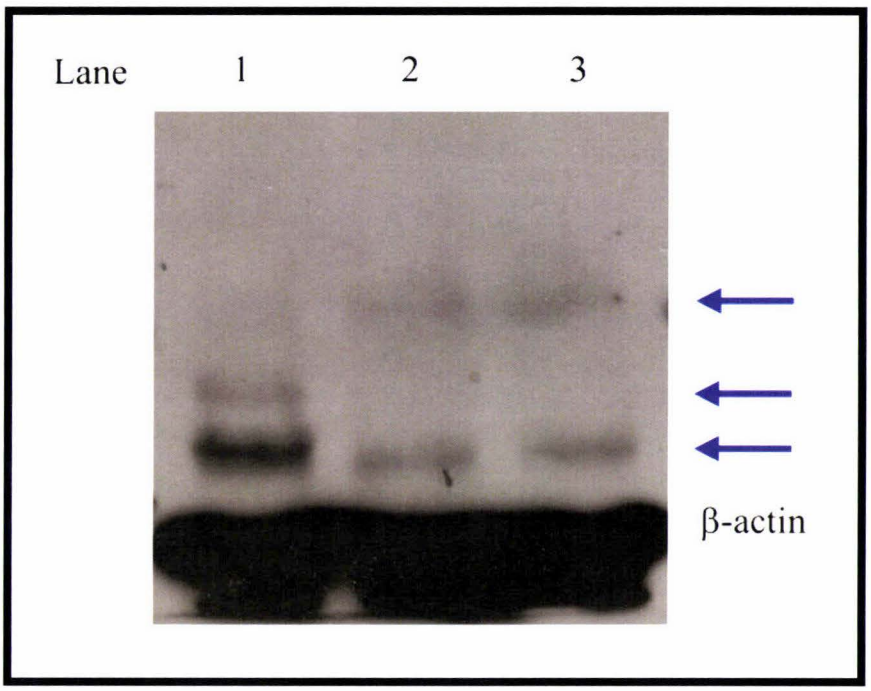

Figure 3.9 Longer exposures showed higher molecular weight bands were detected by the β–actin antibody

White blood cell extracts were separated by 10% SDS-PAGE at 120 V for approximately 90 minutes, transferred to PVDF membrane at 450 mA for 90 minutes and immunoblotted to detect β-actin. The membrane was exposed to x-ray film for two minutes. A number of higher molecular weight bands were detected (blue arrows).

Lane	Contents
1	40 µg white blood cell extract
2	30 µg white blood cell extract
3	20 µg white blood cell extract

A further problem was incomplete denaturation of prx III dimers. Despite boiling samples for a minimum of five minutes with treatment buffer containing β-mercaptoethanol, some prx III remained in dimer form. This was detected as a second band at approximately 55 kDa, as seen in figure 3.8 (red arrow). Quantification can not be carried out when there are two distinct bands for a protein.

Finally, normalization and quantification from immunoblots usually requires bands to be compared to be exposed to x-ray film at the same time. This is to ensure that differences in exposure time or chemiluminescence solution do not influence the results. As prx III is approximately 27 kDa in size, and β-actin is 42 kDa, cutting the membrane at 37 kDa was attempted. This would have allowed the upper half of the membrane to be used to detect β-actin, and the lower half to detect prx III at the same time. However, this was found to destroy the prx III signal. Therefore, the antibodies were stripped off the membrane between detection of prx III and β-actin. This, combined with multiple β-actin bands, means that quantification and normalization could not be performed.

As patient samples and time were limited, rectifying these problems was not possible during this study. Triplicates were not performed, to preserve remaining protein for future work, when these problems may be over-come. Unfortunately not all patient samples could be separated by SDS-PAGE and immunoblotted due to insufficient available sample.

A further method which can give an indication of protein loading is staining proteins in a polyacrylamide gel using Coomassie R-250 stain. Proteins can not be transferred to PVDF membrane for immunoblotting following staining therefore staining identical gels or loading duplicate samples on a gel and cutting the gel so that one sample can be transferred and the other is stained is required. An example of a Coomassie stained SDS-PAGE gel is given in appendix four. A 20 μg sample of the first (odd numbered lanes) and second (even numbered lanes) total protein extract, collected from control subjects three weeks apart, was separated on 10% SDS-PAGE. Overall, loading between the first and second sample of most control subjects appears to be similar. However, there appear to be some differences in the relative intensities of some of the bands between paired samples. For example, two

prominent bands seen in lane one are much less prominent in lane two. While every effort was made to ensure equal protein loading between lanes, some small differences were evident. This emphasizes the importance of using an internal control for protein loading for quantitative immunoblotting.

An additional problem, which reduced the time available to collect patient samples, was with the ethical approval for this study. Any changes to a study, including to patient consent forms or the information collected from patients must receive a new approval from the ethics committee. Following the initial ethical approval, it was determined that additional patient information should be collected for use in future analysis of the results. Therefore a second application to the ethics committee was required, which delayed the start of patient sample collection to late in 2007.

Due to all the problems outlined in this section, no conclusions can be drawn from the immunoblot results obtained in this study. The questions of whether the results obtained using real time RT-PCR are physiologically significant or reflected in protein levels remain unanswered at this point.

3.8 Chapter summary

Real time RT-PCR was used to examine prx III mRNA expression in the white blood cells of patients undergoing chemotherapy with epirubicin and control subjects. Specificity of the prx III primers was confirmed by restriction endonuclease digestion and DNA sequencing of the PCR product. Primer concentrations were optimized before real time RT-PCR was used to quantify prx III expression. To control for differences in RNA quality and total cDNA quantity, changes in prx III were normalized to β-actin.

White blood cells were collected from cancer patients immediately before and three weeks after chemotherapy, or from healthy controls at three week intervals. The results presented in this chapter suggest that some patients may show altered prx III mRNA expression three week following chemotherapy with epirubicin. In contrast, results obtained with control subject samples suggest that prx III mRNA levels may not normally fluctuate significantly.

However, sample sizes were too small to draw any conclusions about the expression of prx III mRNA.

As changes in mRNA are not necessarily reflected in protein levels, SDS-PAGE and western blotting experiments were carried out to examine prx III protein expression. However, due to a number of problems which could not be rectified in the time available, these results were inconclusive.

Chapter Four: Formation of complexes

4.1 Introduction

A number of studies have reported that the typical 2-cysteine peroxiredoxins, including prx III, are capable of forming higher molecular weight complexes. In particular, a decameric ring structure has been identified (Moon *et al.*, 2005; Cao *et al.*, 2007). The higher molecular weight structures have been shown to possess little peroxidase activity, and instead appear to act as molecular chaperones, preventing the unfolding and aggregation of a wide variety of proteins (Moon *et al.*, 2005). The signal to switch between the dimer and decamer structures remains unclear, however it has been suggested that oxidative stress may play a role in this switch. Cao *et al.* (2007) report that reduced prx III collects into higher molecular weight structures, while oxidized prx III is organized into dimeric structures, and was only found to form higher molecular weight structures at much higher protein concentrations (10 mg/ml). Such high protein concentrations may not be relevant *in vivo*. These results suggest that at times where there is less intracellular H_2O_2 and abundant prx III, prx III may take on a second role as a molecular chaperone. When H_2O_2 increases in response to various cellular signals, prx III activity returns to the main task of H_2O_2 removal.

The aim of the work presented in this chapter was to examine prx III higher molecular weight complex formation in MCF7 cells exposed to doxorubicin and in white blood cells of control subjects and patients undergoing chemotherapy with epirubicin. Native PAGE coupled with western blotting was used to examine complex formation. Unlike in SDS-PAGE, in native PAGE proteins are not denatured before being separated by polyacrylamide gel electrophoresis. Instead, proteins are separated on the basis of both size and charge. As a result complexes remain intact, and can be detected due to different mobilities in the polyacrylamide gel.

4.2 Detection of higher molecular weight complexes in MCF7 cells

MCF7 cells were exposed to 3 μM doxorubicin for 0 (control), 2 or 24 hours before total protein was extracted. This concentration of doxorubicin was chosen as the same

concentration was used in the study which identified prx III as possibly being up-regulated following exposure to doxorubicin. Higher doxorubicin concentrations also result in too much cell death. Protein extracts were separated on a 6% polyacrylamide gel, transferred to a PVDF membrane and immunoblotted to detect prx III. A mouse monoclonal anti-prx III (12B) antibody (Santa Cruz) diluted 1/1000 and a rabbit anti-mouse antibody conjugated to HRP (Sigma) diluted 1/5000, were used to detect prx III-containing complexes. These experiments were repeated four times. Figure 4.1 shows two representative immunoblot results. Higher mobility complexes were detected in all samples (blue arrows). Lower mobility complexes were detected in most MCF7 samples, in varying quantities. This suggests that cells usually contain some prx III in larger complexes however, as native PAGE separates proteins on the basis of both size and charge, it is not possible to estimate the sizes of the complexes detected this way. However, the higher mobility band is expected to be prx III dimer. The lower mobility band may be due to the decameric prx III structure, however other complexes of the various peroxiredoxins have also been reported and these can not be ruled out. There was no clear correlation between doxorubicin exposure and changes in the amount of higher molecular weight complex detected. Instead, these results suggest that prx III lower mobility complexes may normally fluctuate within cells.

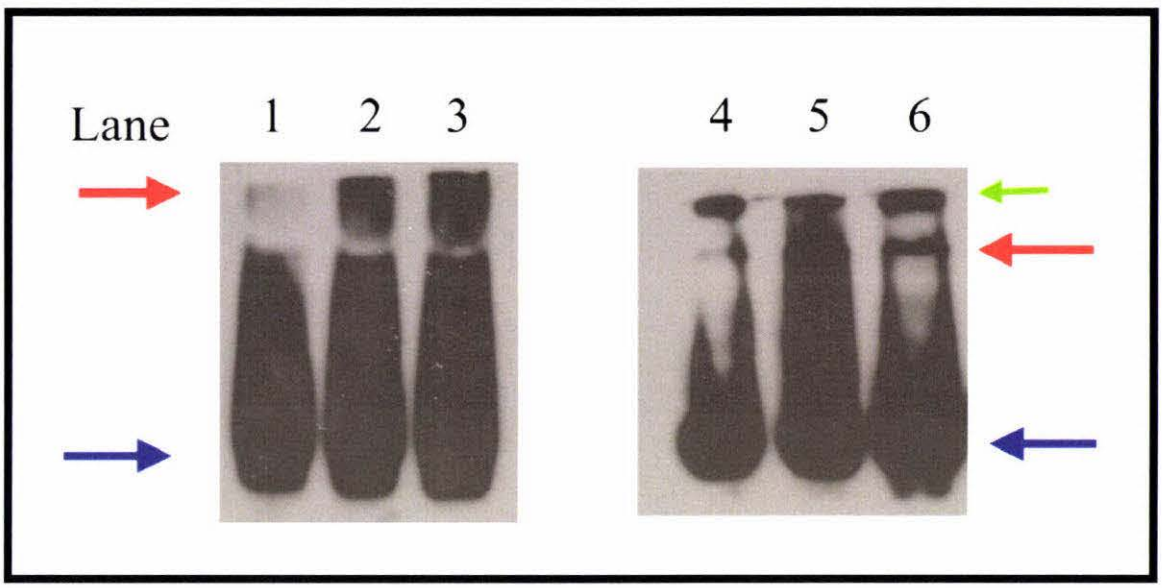

Figure 4.1 Native PAGE and western blotting of MCF7 extracts

Total protein extracts were prepared from control (unexposed) MCF7 cells (lane 1 and 4), and cells exposed to 3 μM doxorubicin for two hours (lane 2 and 5) or 24 hours (lane 3 and 6) on two different days. Samples were separated on 6% native polyacrylamide gels at 120 V for approximately 90 minutes, transferred to PVDF membrane at 450 mA for 90 minutes, and immunoblotted to detect prx III. Higher mobility complex (blue arrows) was detected in all samples and is expected to be prx III dimer. Lower mobility complex was also detected in most samples to varying degrees (red arrow). Some protein remained stuck in the stacking gel (green arrow). These experiments were repeated four times, and the results shown are representative of these experiments.

Lane	Contents
1	20 μg MCF7 total protein, unexposed
2	20 μg MCF7 total protein, 2 hour exposure
3	20 μg MCF7 total protein, 24 hour exposure
4	20 μg MCF7 total protein, unexposed
5	20 μg MCF7 total protein, 2 hour exposure
6	20 μg MCF7 total protein, 24 hour exposure

The variation in the amount of lower mobility complex detected in MCF7 extracts may also be due to differences in protein loading. As many common loading controls are known to form complexes with other proteins *in vivo*, it is not possible to directly control for differences in loading. One method for estimating whether protein loading was similar is to seperate identical sample volumes by SDS-PAGE and immunoblot with a loading control such as β-actin. However, this can only give a rough estimate of protein loading as differences in pipetting and transfer efficiency can not be controlled for.

4.3 Detection of higher molecular weight complexes in white blood cells

Native PAGE was also performed using patient and control samples extracted from white blood cells. Figure 4.2 shows immunoblot results for patient samples, and figure 4.3 shows immunoblot results for control samples. To give an indication of total protein loading, immunoblot results of similar SDS-PAGE experiments are also shown where possible (lower panels). All white blood cell extracts showed a higher mobility complex, predicted to be the dimer, and a much lower mobility complex. The amount of lower mobility complex appears to fluctuate between the first and second, or pre and post samples. However, as the loading control shows, loading was not entirely equal for some samples. These results are therefore difficult to interpret, particularly as the loading control could not be quantified. The results for a number of samples suggest that the apparent fluctuations in prx III higher molecular weight complex may not be solely due to differences in protein loading. For example, the SDS-PAGE results for control one (Figure 4.3 lanes 1 and 2, lower panel) suggest that sample loading may have been similar, perhaps with slightly more protein in lane one than lane two. However, the native PAGE results show an increase in lower mobility complex between sample one and sample two (figure 4.3 lanes 1 and 2, upper panel). The differences seen in lower mobility complex were reproducible. These results suggest that differences in protein loading may not be able to fully account for fluctuations in lower mobility complex formation in white blood cells. Instead, the amount of prx III lower mobility complex present in white blood cells may fluctuate, perhaps in response to oxidative or other stress. Patient samples also showed fluctuations in lower mobility complex formation, however with such a small number of samples and an absence of loading control data for some samples due to limited available protein, no correlation

between lower mobility complex formation and chemotherapy could be identified. A further consideration is that while doxorubicin and epirubicin function to increase intracellular H_2O_2, these drugs are often cleared rapidly from a patient's bloodstream (Ralph *et al.*, 2003). As a result, it is probable that no correlation will be seen between treatment and lower mobility complex formation in samples taken three weeks after treatment. Therefore, performing such experiments with samples taken in the period immediately following treatment, when epirubicin is still present in the bloodstream, may be more useful.

A small number of samples appeared to contain an additional prx III-containing complex, of a slightly lower electrophoretic mobility than the lowest molecular weight structure (green arrow, figure 4.2). This band was reproducible; however it was not possible to estimate the size of this intermediate complex from native PAGE experiments. Therefore, it is not possible to draw any conclusions about this complex.

These results suggest that the formation of prx III lower molecular weight complexes may fluctuate within cells. As it appears that the higher molecular weight complexes are formed from reduced prx III (Cao *et al.*, 2007), this would support the suggestion that lower mobility complexes are formed when there is more prx III than is required for the removal of H_2O_2. As H_2O_2 fluctuates, as part of signaling pathways, due increased electron transport chain leakage or in response to external stimuli, the amount of prx III required for H_2O_2 removal also fluctuates.

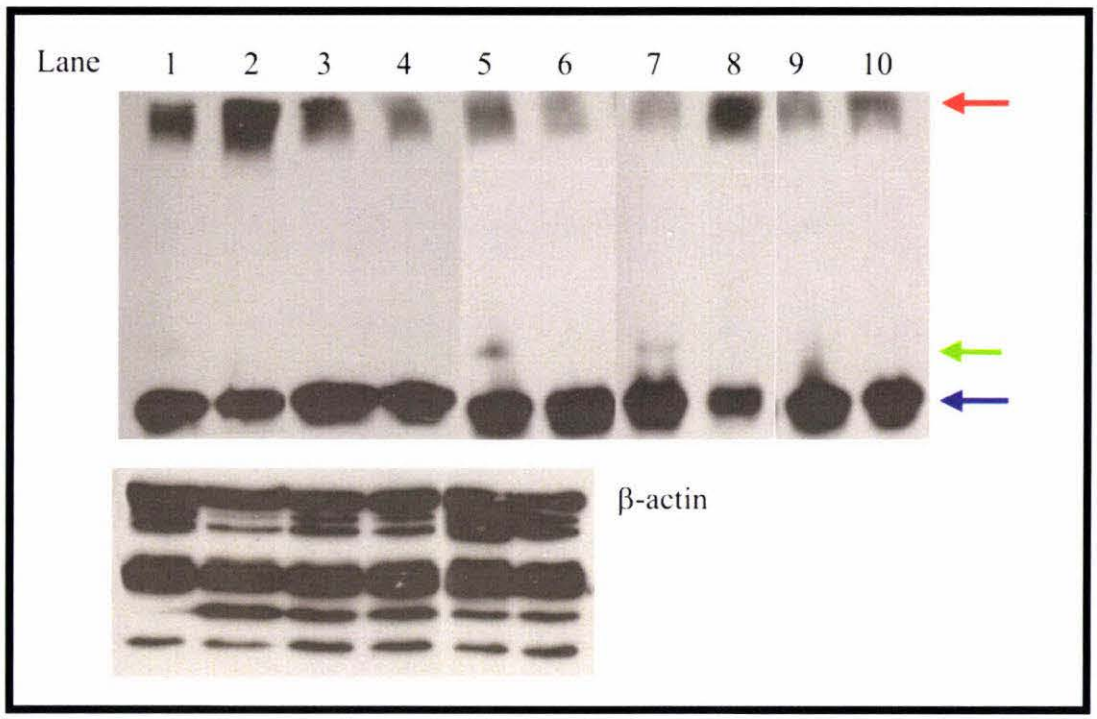

Figure 4.2 Representative western blot results for patient samples

Total protein extracts were prepared from white blood cells collected from patients immediately before chemotherapy (lanes 1, 3, 5, 7 and 9) and three weeks after (lanes 2, 4, 6, 8, 10) chemotherapy with epirubicin. Samples were separated on 6% native polyacrylamide gels at 120 V for approximately 90 minutes, transferred to PVDF membrane at 450 mA for 90 minutes, and immunoblotted to detect prx III (upper panel). Higher mobility complex (blue arrows) was detected in all samples and is expected to be prx III dimer. Lower mobility complex was also detected in all samples in varying amounts (red arrow). Some samples showed an additional complex (green arrow), which remains unidentified. 30 µg total protein was also separated by 10% SDS-PAGE and western blotted using the same conditions to detect β-actin (lower panel), where sufficient sample was available. These results are representative of duplicate, and in some cases triplicate, experiments.

Lane	Contents
1 & 2	20 µg total protein patient one
3 & 4	20 µg total protein patient two
5 & 6	20 µg total protein patient three
7 & 8	20 µg total protein patient four
9& 10	20 µg total protein patient five

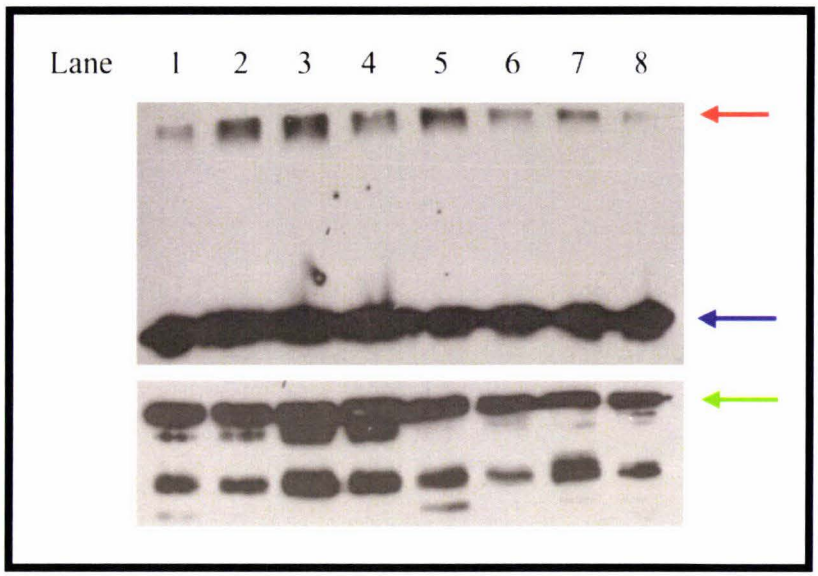

Figure 4.3 Representative western blot results for control samples

Total protein extracts were prepared from white blood cells collected from control subjects. Sample two (lanes 2, 4, 6, 8, 10) was taken three weeks after sample one (lanes 1, 3, 5, 7 and 9). Samples were separated on 6% native polyacrylamide gels at 120 V for approximately 90 minutes, transferred to PVDF membrane at 450 mA for 90 minutes, and immunoblotted to detect prx III (upper panel). Higher mobility complex (blue arrows) was detected in all samples and is expected to be prx III dimer. Lower mobility complex was also detected in all samples in varying amounts (red arrow). 20 µg total protein was also separated by 10% SDS-PAGE and western blotted using the same conditions to detect β-actin (green arrow, lower panel). Results presented here are representative of duplicate experiments.

Lane	Contents
1 & 2	20 µg total protein extract, control one
3 & 4	20 µg total protein extract, control one
5 & 6	20 µg total protein extract, control one
7 & 8	20 µg total protein extract, control one

4.4 Chapter summary

Native PAGE experiments coupled with western blotting were used to examine prx III lower mobility complex formation in MCF7 cells in culture in response to treatment with doxorubicin. The results suggest that cells contain at least some prx III in lower mobility complexes. The amount of lower mobility complex detected appeared to fluctuate between samples; however no correlation between lower mobility complex formation and doxorubicin exposure could be established. As loading differences could not be controlled for, it was not possible to determine if these fluctuations were due to differences in the amount of protein loaded, even though every effort was made to load equivalent amounts of protein.

The same experiments were repeated using control and patient white blood cells. Again, sample sizes were too small to draw conclusions, and controlling for differences in protein loading was difficult. However, in a number of cases there was a clear difference in the amount of lower mobility complex detected between the first and second sample of the same subject. These differences were reproducible, and did not always correlate with the results obtained for the loading control. This suggests that the amount of lower mobility complex may fluctuate in white blood cells, perhaps in response to changes in H_2O_2 concentration.

Chapter 5: Inactivation of peroxiredoxin III

5.1 Introduction

A number of studies have shown that prx III can be reversibly inactivated through over-oxidation of the active cysteine residue upon exposure to increasing amounts of H_2O_2. Over-oxidation prevents dimer formation, which in turn prevents reduction of hydrogen peroxide. The physiological significance of this remains to be elucidated, however it has been postulated that this may play a role in the detection of increasing H_2O_2 produced as part of a cellular death signal.

Over-oxidation of prx III results in a shift in the isoelectric point (pI) of the protein by 0.2 to 0.3 pH points. This can be detected as a more acidic, "satellite spot" in 2DE (Biteau *et al.*, 2003). To examine whether prx III was significantly over-oxidised in MCF7 cells following treatment with doxorubicin for two hours or 24 hours, two-dimensional electrophoresis (2DE) followed by immunoblotting to detect prx III was performed. As the name suggests, two-dimensional electrophoresis separates proteins in two dimensions. In the first step proteins are separated according to their pI. A protein extract is absorbed by an isoelectric focusing (IEF) strip, which contains an immobilized pH gradient. A current is passed through the strip, drawing proteins along the IEF strip until their pI is reached. At this point a protein has no net charge, preventing further movement through the IEF strip. If a protein does move from this point in the strip, it will again hold a net charge due to the change in pH, allowing the protein to move through the strip back to the point where it has no net charge. Following IEF, proteins are denatured using dithiothereitol, and cysteine residues are modified by iodoacetamide to prevent spontaneous formation of disulfide bonds. The IEF strip is then placed at the top of an SDS-PAGE gel and proteins are separated according to their relative molecular weights, as outlined in section 2.5. In this study a further step was included to enable specific detection of prx III. The proteins in the polyacryamide gel were transferred to a PVDF membrane and immunoblotted. An outline of these experiments is presented in figure 5.1.

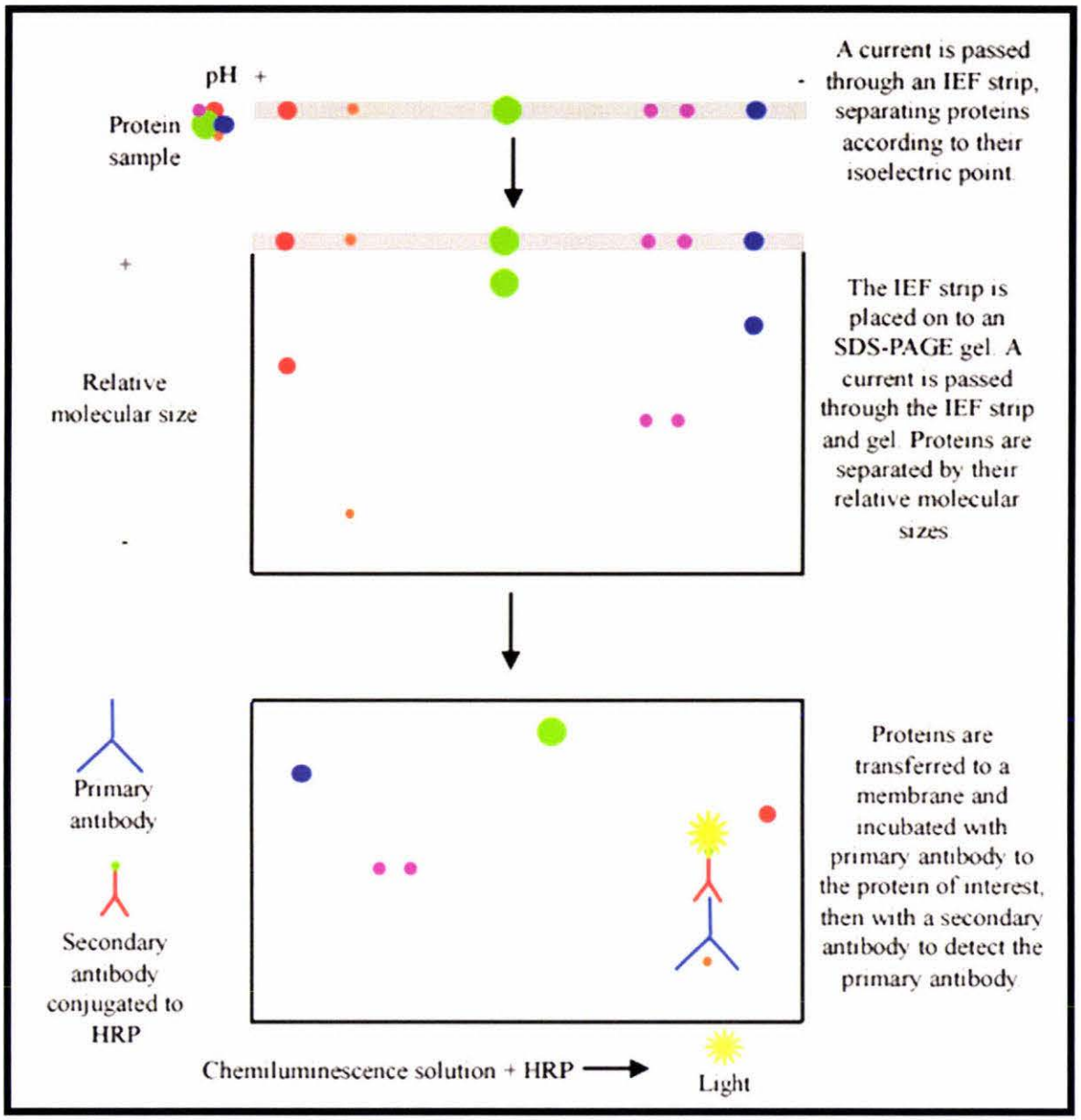

Figure 5.1 Outline of two-dimensional electrophoresis experiments

Proteins were separated according to their isoelectric point along an isoelectric focusing (IEF) strip. The IEF strip was then placed on top of an SDS-PAGE gel, and proteins were separated according to their relative molecular sizes. Proteins were then transferred to a PVDF membrane, and immunoblotted with primary antibody, followed by horseradish peroxidase (HRP) – conjugated secondary antibody. The membrane was incubated with chemiluminescence solution (Roche) and light emitted by HRP was detected by exposing the membrane to x-ray film in a dark room.

5.2 Oxidative stress and peroxiredoxin III over-oxidation

Before the 2DE and immunoblotting experiments outlined in section 5.1 could be used to examine prx III over-oxidation upon doxorubicin exposure, it was necessary to confirm that this method could detect over-oxidation of prx III. MCF7 cells, at a confluence of approximately 90%, were exposed to 100μM H_2O_2 for one hour. Total protein was then extracted, quantified and acetone precipitated before 300 μg of total protein was used for IEF on a seven cm pH four to seven IEF strip. The proteins were then separated in the second dimension on a 10% polyacryamide gel, transferred to PVDF membrane and immunoblotted to detect prx III. A mouse monoclonal anti-prx III (12B) antibody (Santa Cruz) diluted 1/1000 was used as the primary antibody. A horseradish peroxidase conjugated rabbit anti-mouse antibody (Sigma) diluted 1/5000 was used as the secondary antibody. Figure 5.2A shows the results obtained with a control extract from cells which were not exposed to 100 μM H_2O_2. Only a single spot is visible. This is expected to be active prx III, although peptide mass fingerprinting to confirm this was not performed. Figure 5.2B shows results obtained using a protein extract from cells exposed to 100 μM H_2O_2. A second, more acidic spot, of the same molecular weight as the first, is seen. This is expected to be over-oxidised prx III although peptide mass fingerprinting was not performed to confirm this. These experiments were performed in duplicate, and confirm that this method can be used to detect over-oxidised prx III.

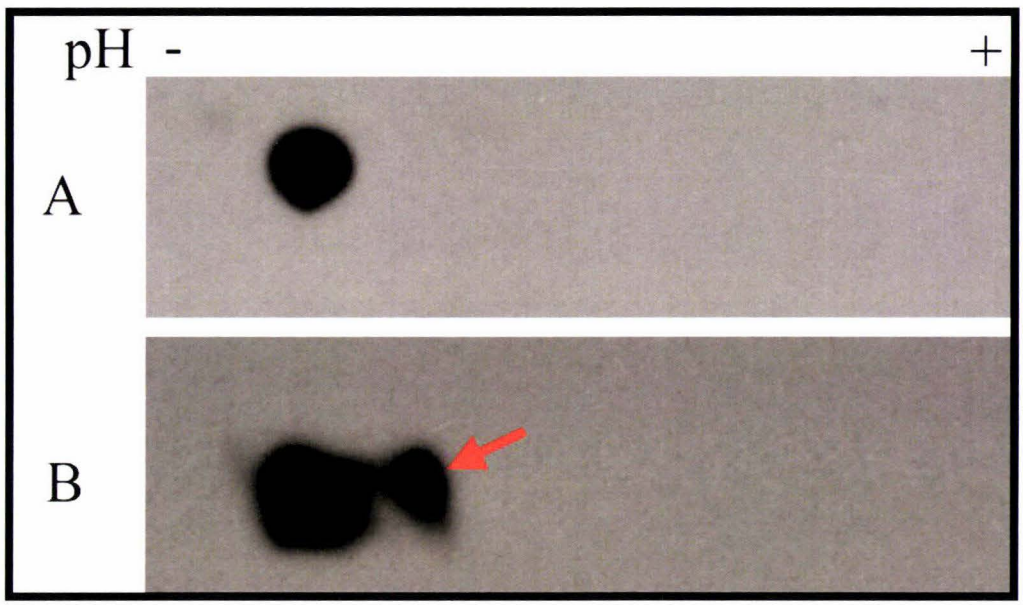

Figure 5.2 Over-oxidation of peroxiredoxin III

Total protein extracts from MCF7 control cells (A) or MCF7 cells exposed to 100 μM H_2O_2 for one hour were focused on a 7 cm pH 4 to 7 isoelectric focusing strip, separated on a 10% SDS-PAGE gel and immunoblotted to detect prx III. Membranes were exposed to X-ray film for one minute. Control extracts show only a single spot for prx III, expected to be active prx III. Extract from cells exposed to 100 μM H_2O_2 showed an additional satellite spot (red arrow), which is expected to be over-oxidised prx III. pH is indicated at the top. Therefore these experiments can detect over-oxidation of prx III.

5.3 Over-oxidation of peroxiredoxin III in response to doxorubicin exposure

2DE experiments performed as outlined in section 5.2 were also performed using total protein extracts from MCF7 cells exposed to 3 μM doxorubicin for two hours and 24 hours. Figure 5.3 shows representative immunoblots for these experiments. These experiments were performed in duplicate. Control extracts (figure 5.3A), extracts from cells exposed to doxorubicin for two hours (figure 5.3B) and extracts from cells exposed to doxorubicin for 24 hours (figure 5.3C) all showed only a single spot. This was expected to be active prx III as even exposure of cells to 100 μM H_2O_2 failed to eliminate all active prx III. These results suggest that exposure of MCF7 cells to 3 μM doxorubicin for two hours or 24 hours does not result in significant over-oxidation of prx III. However, the limit of detection for this method is not known, therefore some over-oxidation of prx III upon exposure to doxorubicin can not be ruled out. Some cell death was noticed in plates exposed to doxorubicin for 24 hours. If prx III is over-oxidised as part of a death signal, it would be expected that some over-oxidation might be detected in these samples. However, as degradation of proteins begins at the same time as cell death, it is possible that most prx III was degraded in these dead and dying cells and therefore could not be detected.

A number of studies have used cells in culture to examine responses to doxorubicin, and a wide range of doxorubicin concentrations have been used in these studies. It is not clear whether 3 μM doxorubicin accurately reflects concentrations seen in the bloodstream following chemotherapy. Therefore the results presented here may not be representative of events within white blood cells.

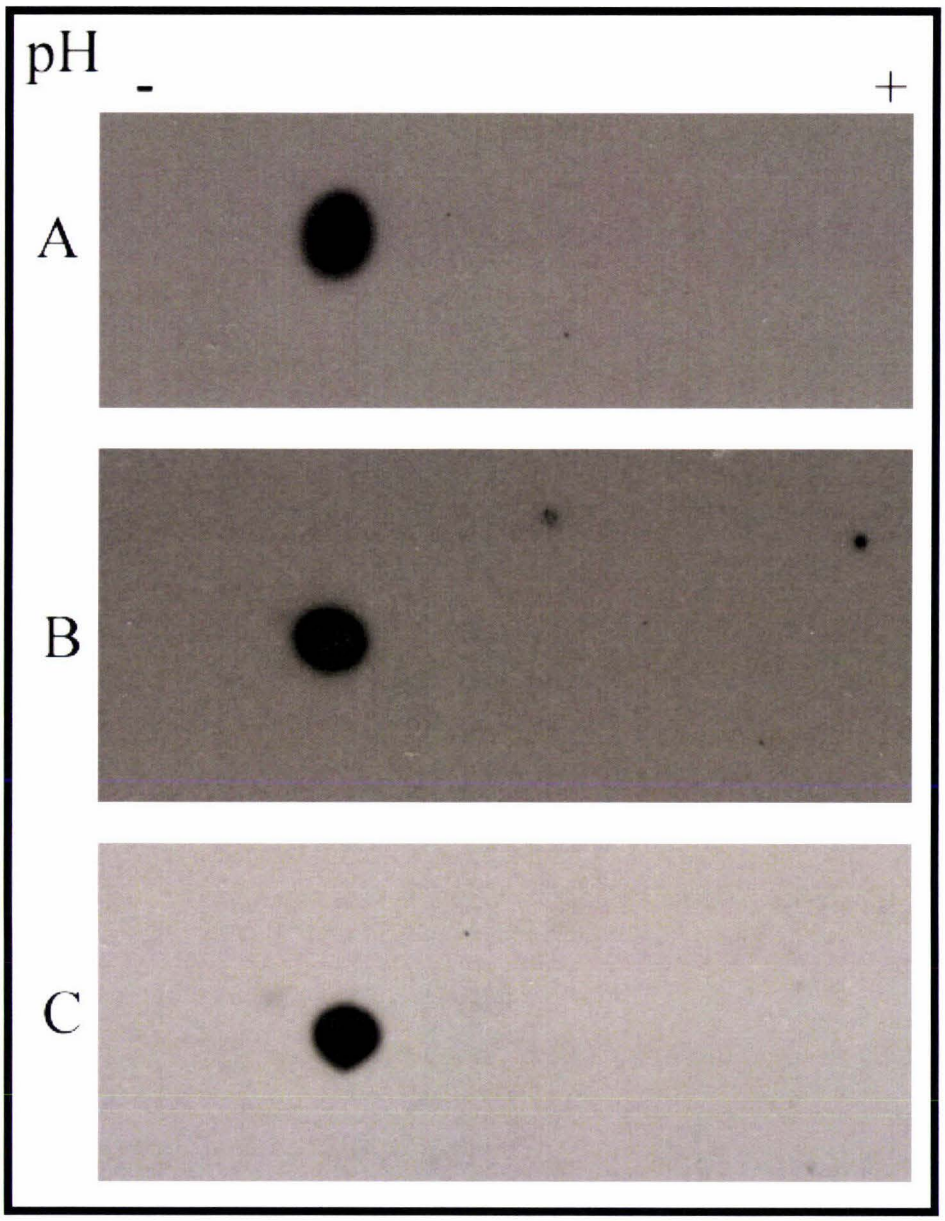

Figure 5.3 Exposure of MCF7 cells to doxorubicin did not result in prx III over-oxidation

300 μg total protein from control cells (A) and cells exposed to 3 μM doxorubicin for two hours (B) or 24 hours (C) was focused on a 7 cm pH 4 to 7 isoelectric focusing strip, separated on a 10% SDS-PAGE gel and immunoblotted to detect prx III. Membranes were exposed to X-ray film for one minute. All cell extracts show only a single spot for prx III, suggesting that prx III is not significantly over-oxidised upon exposure to 3 μM doxorubicin.

5.4 Chapter summary

Peroxiredoxin III has been shown to be over-oxidised in response to oxidative stress. This can be detected by the development of a second, more acidic spot in two dimensional electrophoresis (2DE) experiments. Exposure of cells to 100 μM H_2O_2 was confirmed to result in a second, more acidic spot, indicating that this method was suitable for detecting over-oxidation of prx III. Similar experiments performed with extracts from cells exposed to 3 μM doxorubicin for two hours or 24 hours did not show any detectable over-oxidation of prx III. However, the limits of detection for this method are unknown; therefore some undetectable over-oxidation of prx III can not be ruled out. Furthermore, it is unclear whether 3 μM doxorubicin accurately reflects the concentrations achieved in patient's bloodstreams following chemotherapy.

However, if the results presented here accurately reflect events occurring in white blood cells in patients undergoing chemotherapy with epirubicin, then it is likely that prx III is not significantly over-oxidised following chemotherapy. Therefore, the prx III present is likely to be capable of actively removing H_2O_2 produced as a result of epirubicin metabolism.

Chapter 6: Discussion and further work

6.1 Overview

Cancer is caused by a loss of control of cell division and differentiation, a process which is normally very carefully regulated. Treatment often involves a combination of surgery to remove the tumour, chemotherapy to target remaining cancer cells, and sometimes radiotherapy. While some success has been achieved with chemotherapy, many patients develop resistance to the drugs used in chemotherapy, reducing the efficacy of treatment. Therefore a great deal of research is being carried out to identify mechanisms of drug resistance in order to develop methods to over-come or avoid resistance.

A gene which was recently identified as being up-regulated in a number of different types of tumour (Yanagawa *et al.*, 1999; Chang *et al.*, 2001; Noh *et al.*, 2001; Kinnula *et al.*, 2002; Brixius *et al.*, 2007; Holley *et al.*, 2007) and also in cells in culture following exposure to the commonly used anti-cancer drug doxorubicin is peroxiredoxin III (Williams *et al.*, unpublished). Doxorubicin, or the almost identical drug epirubicin, is used to treat a variety of cancers. These two drugs induce cell death through a number of mechanisms, one of which is by increasing intracellular H_2O_2 levels (Tsang *et al.*, 2003). An up-regulation of prx III, which is involved in the removal of H_2O_2 (Chang *et al.*, 2004), may therefore play a role in the development of resistance to doxorubicin or epirubicin. However, before a role for prx III in the development of drug resistance can be further investigated, it is necessary to determine whether the changes seen in cells in culture are also seen in patients undergoing chemotherapy with doxorubicin or epirubicin.

The main aim of the work presented in this study was to examine prx III expression in patients undergoing chemotherapy with epirubicin. As little is currently known about *in vivo* prx III expression patterns, prx III expression was also examined in control subjects, using samples taken at the same time intervals as patient samples.

Prx III has been shown to form higher molecular weight complexes which exhibit minimal peroxidase activity and instead function as chaperones. Native PAGE was used to examine prx III complex formation, in cells in culture and in white blood cells.

Finally, prx III has been shown to be reversibly inactivated by over-oxidation of the active cysteine residue upon exposure to higher H_2O_2 concentrations. Two dimensional electrophoresis experiments were used to examine prx III over-oxidation in response to doxorubicin exposure.

6.2 Summary of results

Expression of prx III

Real time RT-PCR was used to examine prx III mRNA expression in patients undergoing chemotherapy with epirubicin and in control subjects (Chapter 3). While sample sizes were smaller than intended, and too small to draw any conclusions, the results suggest that prx III mRNA expression may change in some patients following chemotherapy with epirubicin. In contrast, the results obtained for control subjects suggest that prx III mRNA may not normally fluctuate significantly in white blood cells. The range of fold changes in prx III mRNA seen in patients is not unexpected as patients often respond differently to chemotherapy. Some patients respond very well, while others do not respond at all. Therefore it would be useful to examine whether there is any correlation between changes in prx III expression and patient survival one year and five years following chemotherapy.

The blood samples used in this study were taken three weeks following chemotherapy, which suggests that the changes seen in prx III mRNA may be more long-term, rather than a short term anti-oxidant response. This supports a possible role for prx III in drug resistance, as increased levels of prx III before subsequent doses of chemotherapy is expected to leave cells better prepared to deal with the increase in H_2O_2 caused by epirubicin.

To determine whether the changes seen in mRNA levels was reflected in protein levels, western blotting experiments were attempted to examine prx III protein levels (Chapter 3). Unfortunately a number of problems were encountered and these could not be resolved during the time available. Small alterations to the white blood cell isolation and protein extraction protocols, or a new loading control antibody could possibly resolve most of these problems.

Sample sizes were too small to draw any conclusions about the expression of prx III however, these results suggest that further investigation into prx III expression may be warranted.

Prx III complex formation

During the reduction of H_2O_2, the active cysteine residue of prx III is oxidized, producing an unstable cysteine-sulfenic acid intermediate which quickly forms a head-to-tail homodimer. Thioredoxin-2 then reduces the disulfide bond and active thioredoxin is restored by thioredoxin reductase-2 at the expense of one molecule of NADPH. A number of additional complexes containing prx III have been identified. In particular, prx III appears to form a decameric ring structure. Initially, the higher molecular weight complexes were thought to be formed from over-oxidised peroxiredoxins (Moon *et al.*, 2005). More recently, Cao *et al.* (2007) discovered that reduced prx III organizes spontaneously into these decameric structures. In contrast, oxidized prx III forms homodimers, and only organizes into decameric structures at high protein concentrations, which may not be seen *in vivo*. The physiological significance of these structures remains to be elucidated.

To examine whether exposure of MCF7 cells in culture to doxorubicin resulted in a shift from dimer formation to a higher molecular weight complex, or vice versa, native PAGE experiments were performed. The results showed a large amount of a lower higher mobility complex, expected to be prx III dimer, in all samples, and varying amounts of a lower mobility complex, possibly prx III decamer (Figure 4.1). It is not possible to determine the size of a complex using native PAGE as this technique separates proteins on the basis of

both size and charge, therefore it was not possible to confirm whether the lower mobility complexes were indeed the higher molecular weight decamer identified by Moon *et al.* (2005). No clear correlation was found between doxorubicin exposure and complex formation. However, it is unclear whether the doxorubicin concentration used in these experiments accurately reflects the concentrations achieved in a patient's bloodstream following chemotherapy. Furthermore, as no indication of protein loading was obtained for these experiments, it is possible that these apparent fluctuations were due to differences in protein loading.

Complex formation was also examined in white blood cell protein extracts. Western blot results from SDS-PAGE experiments using the same samples were used to give an approximate indication of protein loading in the native PAGE experiments. The results were difficult to interpret without being able to quantify the loading controls, however a number of samples showed fluctuations seen in lower mobility complex in white blood cells that may not be a result of differences in protein loading (Figures 4.2 & 4.3). Instead, it appears that the amount of lower mobility complex present in white blood cells may fluctuate naturally. As it appears that the lower mobility complexes may be formed from reduced prx III (Cao *et al.*, 2007), it is possible that the lower mobility complexes fluctuate in response to oxidative stress. Figure 6.1 presents a possible explanation for the fluctuations in lower mobility complex. When a cell is not growing rapidly or being exposed to increased levels of H_2O_2, only a small amount of prx III is required for H_2O_2 removal. Thioredoxin and thioredoxin reductase maintain a ready supply of prx III capable of H_2O_2 removal. Remaining prx III takes on the additional role of molecular chaperone, preventing unfolding and aggregation of a wide variety of proteins (Moon *et al.*, 2005). As H_2O_2 increases, for example as part of the growth signal, or due to breakdown of foreign molecules or inflammation and the immune response, more prx III is required for H_2O_2 removal. Some of the prx III higher molecular weight complexes dissociate to aid in removal. When it is no longer required for H_2O_2 removal, excess prx III returns to the role of molecular chaperone. This allows a rapid response to increase H_2O_2 levels as protein is already available within the cell. If further prx III protein is required for H_2O_2 removal, the

prx III protein in higher molecular weight complexes is already available to provide a "buffer" while new protein is synthesized.

Further examination of higher molecular weight complex formation in white blood cells is required to confirm that the amount of higher molecular weight complex does fluctuate, as only a few samples were available for this study and problems with the loading control prevented accurate analysis of results. However, if the changes in prx III mRNA are reflected in prx III protein levels, and protein not immediately required for H_2O_2 removal is maintained in the cell until required, this may have implications for patients undergoing chemotherapy with epirubicin. A higher amount of available prx III protein before subsequent doses of chemotherapy suggests cells may be able to cope with the amount of H_2O_2 produced during the metabolism of epirubicin. If cells are more tolerant of higher levels of H_2O_2, cell death is less likely to occur. Therefore, increased prx III expression may play a role in drug resistance to epirubicin.

Prx III inactivation

As reported by Biteau *et al.* (2003), prx III is reversibly over-oxidised at higher H_2O_2 levels, resulting in inactivation. It has been suggested that over-oxidation of the 2-cysteine peroxiredoxins plays a role in the detection of a death signal. H_2O_2 is produced in lower amounts as part of various signalling pathways; however H_2O_2 is also produced as part of a death signal. When H_2O_2 levels increase as part of a death signal this needs to be recognized by prx III, to prevent removal of the H_2O_2 and improper cell survival. Over-oxidation of prx III may serve as this "off switch," however this remains to be established.

To examine whether prx III is over-oxidised following exposure to doxorubicin, total protein extracts were subjected to two-dimensional electrophoresis (Chapter 5). An extract prepared from cells exposed to 100 μM H_2O_2 for one hour showed a second, more acidic satellite spot that was not seen in control extracts (Figure 5.2). This confirmed that the method was able to detect over-oxidised prx III. However, cell extracts exposed to 3 μM doxorubicin for two hours or 24 hours showed no over-oxidation of prx III (Figure 5.3). Some cell death was noticed in the plates of cells exposed to doxorubicin for 24 hours, therefore if over-oxidation plays a role in the detection of a death signal, it would be

expected that some over-oxidised prx III would be detected in these samples. However, it is possible that much of the protein in the dead cells had already been degraded and therefore could not be detected using this method.

It is unclear whether 3 μM doxorubicin accurately reflects the concentrations seen in a patient's bloodstream following chemotherapy. Repeating these experiments using white blood cell extracts taken from patients before and immediately after chemotherapy may be more useful.

Lower mobility complex was detected in all MCF7 extracts however there was no evidence for significant over-oxidation of prx III in these samples. This suggests that over-oxidation may not be responsible for the switch to lower mobility complex formation, and supports results presented by *Cao et al.* (2007) that reduced prx III organizes into decameric structures. Over-oxidised prx III may also form higher molecular weight structures, however these results suggest that most, if not all, lower mobility complex is formed by active prx III. These results also support the suggestion that lower mobility complex forms when there is abundant prx III which is not required for H_2O_2 removal.

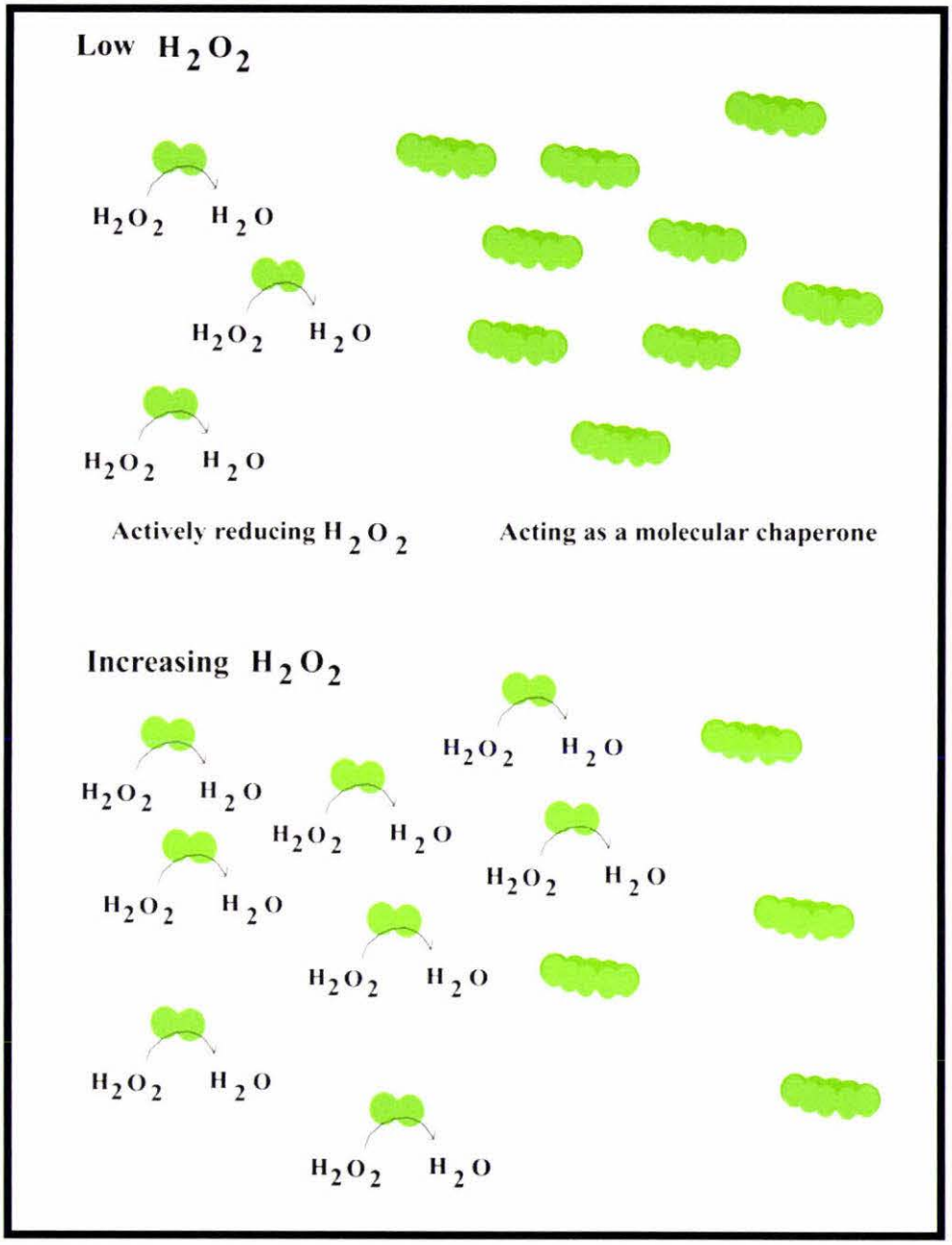

Figure 6.1 Overview of possible explanation of prx III complex formation

When a cell is not being exposed to increased levels of H_2O_2, only a small amount of prx III is required for H_2O_2 removal. Remaining prx III forms higher molecular weight complexes, taking on the additional role of molecular chaperone. As H_2O_2 increases, for example as part of the growth signal, or due to breakdown of foreign molecules or inflammation and the immune response, more prx III is required for H_2O_2 removal. Some of the prx III higher molecular weight complexes dissociate to aid in removal, until no longer required.

6.3 Future research

The results presented in this study suggest that further investigation of prx III expression in patients undergoing chemotherapy with epirubicin would be worthwhile. The SDS-PAGE and western blot experiments examining prx III protein expression were inconclusive. Therefore developing a more robust assay to examine proteins levels and control for protein loading is necessary for assessing prx III expression in response to chemotherapy. The problems encountered in this study may be resolved if a new antibody to β-actin, or another loading control such as glyceraldehyde 3-phosphate dehydrogenase is used. Denaturation of prx III dimers was another problem, which may be resolved by treating samples with β-mercapthoethanol or DTT overnight or modifying the treatment buffer.

Expanding this study to include more patients and follow patients through successive doses of chemotherapy as was initially intended, would allow conclusions to be drawn about prx III expression. Collection of more than 8 mL of blood from subjects would make further experiments easier as 8 mL was found to be insufficient for all the experiments that were to be carried out. It would be useful to repeat the native PAGE experiments presented in chapter four on additional white blood cells samples to confirm the fluctuations in lower mobility complex reported in this study. Furthermore, including additional control subjects in these experiments would also be useful to confirm the results presented here. To determine whether there is a correlation between changes in prx III expression through the course of chemotherapy and patient outcome, it would be necessary to follow up on patients one year and five years following chemotherapy. This was not possible during the course of this study. However, following up with patients will be important in assessing whether prx III plays are role in the development of drug resistance.

A further consideration in examining changes in expression is whether the protein present in cells is active. Peroxiredoxins have been shown to be inactivated by over-oxidation, and prx I has also been shown to be inactivated by phosphorylation (Chang *et al.*, 2002; Jang *et al.*, 2006). While Chang *et al.* (2002) were examining phosphorylation of prx I, the authors report that prx II also appeared to be phosphorylated by cdc2. As prx I and II are cytosolic proteins and prx III is a mitochondrial protein it is unlikely that prx III is phosphorylated by

cdc2 *in vivo* however phosphorylation by other kinases or regulation of activity through other modifications can not be ruled out. Therefore prx III activity in white blood cells should also be examined. Kim *et al.* (2005) present a method for testing 2-cys peroxiredoxin activity however prx III must first be isolated from a sample as the assay detects activity from all peroxiredoxins, not prx III specifically. A method for isolating prx III from white blood cells must be elucidated.

In chapter four, prx III complex formation in the white blood cells of patients undergoing chemotherapy with epirubicin was examined. No correlation between chemotherapy and variation in the amount of detected lower mobility complex was identified. However, as epirubicin is cleared rapidly from a patient's blood stream (Ralph *et al.*, 2003), collecting white blood cells immediately before and soon after chemotherapy may be more useful for these experiments.

To examine whether there is a correlation between increasing H_2O_2 concentration and lower mobility complex formation, performing native PAGE and western blotting experiments using total protein extracts prepared from cells exposed to increasing amounts of H_2O_2, for varying lengths of time, may be useful. The dye 2',7'-dichlorofluorescin diacetate (DCFH-DA) could be used to confirm increases in intracellular H_2O_2 (Carter *et al.*, 1994). DCFH-DA is a membrane permeable dye which is cleaved within cells and oxidized by H_2O_2 to produce the fluorescent product dichlorofluorescein (DCF), which remains trapped in cells. However, as noted previously, a putative antioxidant response element has been identified in the prx III promoter. If prx III expression is indeed increased in response to oxidative stress, this will complicate interpretation of the results and should be taken into consideration.

Furthermore, the function of the lower and higher mobility complexes needs to be confirmed. Molecular chaperone activity has been attributed to the higher molecular weight complexes formed by prx I and prx II, but have not yet been confirmed for prx III. Kim *et al.* (2005) present a method for examining peroxiredoxin peroxidase activity, while Moon *et al.* (2005) present methods for examining the molecular chaperone activity of

peroxiredoxin complexes. Therefore, following isolation of the higher and lower mobility complexes formed by prx III, it should be possible to examine the peroxidase and chaperone activities of these complexes.

Over-oxidation of prx III in MCF7 cells exposed to doxorubicin was examined in chapter five. The results suggest prx III is not significantly over-oxidised following doxorubicin exposure. However, as it was unclear whether 3 μM doxorubicin accurately reflects the concentrations achieved in a patient's bloodstream following chemotherapy, repeating these experiments using protein extracts from white blood cells collected from patients before and immediately after chemotherapy may yield more meaningful results. As white blood cells are often exposed to oxidative stress due to inflammation, the immune response and removal of foreign molecules, two-dimensional electrophoresis experiments using total protein extracts from control subjects would determine whether prx III is normally over-oxidised in white blood cells.

If prx III expression is found to be altered in patients undergoing chemotherapy with epirubicin, and these changes correlate with patient outcomes, examining the mechanisms of regulation of prx III expression may be useful in identifying new targets for preventing or limiting the development of drug resistance. Expression of mRNA is often regulated through the binding of transcription factors or other proteins to regulatory sequences with the promoter, and sometimes the introns, of a gene. Examining the binding of proteins to the prx III promoter sequence using electrophoretic mobility shift assays (EMSA) may be a useful start in identifying proteins which may play a role in the regulation of prx III mRNA transcription. Comparing the binding of proteins from control cell extracts with those of cells exposed to doxorubicin could provide some insight into the proteins involved in changes in prx III mRNA expression following doxorubicin exposure. A combination of peptide mass fingerprinting and antibody supershift assays could be used to identify proteins detected using EMSA. Searching available databases with the prx III promoter sequence may also provide some possible candidates for the regulation of prx III expression. Chromatin immunoprecipitation experiments using primers to small, over-lapping regions of the prx III promoter could be used to identify the regions of the promoter

which are bound by particular proteins identified using EMSA (Haggerty *et al.*, 2003). Once regions of the promoter bound by proteins are known, generating step-wise mutants and examining protein binding can be used to identify the minimum region required for protein binding.

The binding of proteins to a promoter sequence may positively or negatively regulate mRNA transcription, or may have no significant influence on expression. Luciferase reporter assays using constructs containing different regions of the prx III promoter could provide information on which regions of the promoter are important for positively or negatively regulating prx III mRNA transcription.

It has been suggested that prx III expression is not only regulated at the level of transcription, but also in protein synthesis or degradation. To examine whether prx III protein degradation rates are altered following exposure to doxorubicin, control cell extracts and extracts from cells exposed to doxorubicin could be prepared and used in western blot experiments examining prx III protein levels. Cyclohexamide could be used to block protein synthesis. Protein extracts prepared at intervals such as zero, two, five, 15 and 30 minutes following doxorubicin exposure could show whether there is a difference in the rates of prx III protein degradation.

The collective results for these experiments may yield novel insights into the factors regulating prx III expression and provide opportunities to develop more effective chemotherapy regimes.

6.4 Conclusion

Prx III mRNA expression appears to change in the white blood cells of some patients following chemotherapy with epirubicin. In some patients prx III mRNA was found to increase while other patients showed no change, or a decrease in prx III mRNA. In contrast, prx III mRNA does not appear to significantly fluctuate in white blood cells under normal circumstances. Due to unforeseen problems with western blotting experiments it was not possible to determine if the change in mRNA seen in patient samples was reflected in prx

III protein levels. Native PAGE results suggest that prx III may form higher molecular weight complexes in white blood cells, and that the amount of prx III found in higher molecular weight complexes may fluctuate. While the cause of such fluctuation remains unknown, it may be due to fluctuations in intracellular H_2O_2 levels. Prx III was not found to be significantly over-oxidised following exposure to 3μM doxorubicin for two hours or 24 hours. These results suggest that expanding this study to include additional patients and to follow patients further through treatment may be worthwhile. Determining whether these changes are reflected in prx III protein levels is also important. Finally, if prx III is found to be involved in the development of drug resistance, work to determine how prx III is regulated in response to doxorubicin or epirubicin will be important. Knowing the mechanisms involved in prx III may present further possible targets for preventing the development of drug resistance.

References

Allen, K. A., Williams, A. O., Isaacs, R. J., and Stowell, K. M. (2004). Down-regulation of human topoisomerase II-alpha correlates with altered expression of transcriptional regulators NF-YA and Sp1. Anti-Cancer Drugs *15*, 357-362.

Apel, K., and Hirt, H. (2004). Reactive oxygen species: Metabolism, oxidative stress, and signal transduction. Annual Review of Plant Biology *55*, 373-399.

Bae, J. Y., Ahn, S. J., Han, W., and Noh, D. Y. (2007). Peroxiredoxin I and II inhibit H_2O_2-induced cell death in MCF-7 cell lines. Journal of Cellular Biochemistry *101*, 1038-1045.

Bae, Y. S., Kang, S. W., Seo, M. S., Baines, I. C., Tekle, E., Chock, P. B., and Rhee, S. G. (1997). Epidermal growth factor (EGF)-induced generation of hydrogen peroxide - Role in EGF receptor-mediated tyrosine phosphorylation. Journal of Biological Chemistry *272*, 217-221.

Baker, A. F., Landowski, T., Dorr, R., Tate, W. R., Gard, J. M. C., Tavenner, B. E., Dragovich, T., Coon, A., and Powis, G. (2007). The antitumor agent imexon activates antioxidant gene expression: Evidence for an oxidative stress response. Clinical Cancer Research *13*, 3388-3394.

Ball, T. B., Plummer, F. A., and HayGlass, K. T. (2003). Improved mRNA quantitation in LightCycler RT-PCR. International Archives of Allergy and Immunology *130*, 82-86.

Biteau, B., Labarre, J., and Toledano, M. B. (2003). ATP-dependent reduction of cysteine-sulphinic acid by S-cerevisiae sulphiredoxin. Nature *425*, 980-984.

Blum, R. H., and Carter, S. K. (1974). Adriamycin - New Anticancer Drug with Significant Clinical Activity. Annals of Internal Medicine *80*, 249-259.

Bouck, N., Stellmach, V., and Hsu, S. C. (1996). How tumors become angiogenic, In Advances in Cancer Research, Vol 69, pp. 135-174.

Bradford, M. M. (1976). Rapid and Sensitive Method for Quantitation of Microgram Quantities of Protein Utilizing Principle of Protein-Dye Binding. Analytical Biochemistry *72*, 248-254.

Brixius, K., Schwinger, R. H. G., Hoyer, F., Napp, A., Renner, R., Bolck, B., Kumin, A., Fischer, U., Mehlhorn, U., Werner, S., and Bloch, W. (2007). Isoform-specific downregulation of peroxiredoxin in human failing myocardium. Life Sciences *81*, 823-831.

Budanov, A. V., Sablina, A. A., Feinstein, E., Koonin, E. V., and Chumakov, P. M. (2004). Regeneration of peroxiredoxins by p53-regulated sestrins, homologs of bacterial AhpD. Science *304*, 596-600.

Cao, Z., Bhella, D., and Lindsay, J. G. (2007). Reconstitution of the mitochondrial Prx II antioxidant defence pathway: General properties and factors affecting Prx II activity and oligomeric state. Journal of Molecular Biology *372*, 1022-1033.

Carter, W. O., Narayanan, P. K., and Robinson, J. P. (1994). Intracellular Hydrogen-Peroxide and Superoxide Anion Detection in Endothelial-Cells. Journal of Leukocyte Biology *55*, 253-258.

Chang, J. W., Jeon, H. B., Lee, J. H., Yoo, J. S., Chun, J. S., Kim, J. H., and Yoo, Y. J. (2001). Augmented expression of peroxiredoxin I in lung cancer. Biochemical and Biophysical Research Communications *289*, 507-512.

Chang, T. S., Cho, C. S., Park, S., Yu, S. Q., Kang, S. W., and Rhee, S. G. (2004). Peroxiredoxin III, a mitochondrion-specific peroxidase, regulates apoptotic signaling by mitochondria. Journal of Biological Chemistry *279*, 41975-41984.

Chang, T. S., Jeong, W., Choi, S. Y., Yu, S. Q., Kang, S. W., and Rhee, S. G. (2002). Regulation of peroxiredoxin I activity by Cdc2-mediated phosphorylation. Journal of Biological Chemistry *277*, 25370-25376.

Counter, C. M., Avilion, A. A., Lefeuvre, C. E., Stewart, N. G., Greider, C. W., Harley, C. B., and Bacchetti, S. (1992). Telomere Shortening Associated with Chromosome Instability Is Arrested in Immortal Cells Which Express Telomerase Activity. Embo Journal *11*, 1921-1929.

Deroo, B. J., Hewitt, S. C., Peddada, S. D., and Korach, K. S. (2004). Estradiol regulates the thioredoxin antioxidant system in the mouse uterus. Endocrinology *145*, 5485-5492.

Di Nicolantonio, F., Mercer, S. J., Knight, L. A., Gabriel, F. G., Whitehouse, P. A., Sharma, S., Fernando, A., Glaysher, S., Di Palma, S., Johnson, P., *et al.* (2005). Cancer cell adaptation to chemotherapy. Bmc Cancer *5*.

Faivre, E. J., and Lange, C. A. (2007). Progesterone receptors upregulate Wnt-1 to induce epidermal growth factor receptor transactivation and c-Src-dependent sustained activation of Erk1/2 mitogen-activated protein kinase in breast cancer cells. Molecular and Cellular Biology *27*, 466-480.

Gottesman, M. M. (2002). Mechanisms of cancer drug resistance. Annual Review of Medicine *53*, 615-627.

Haggerty, T. J., Zeller, K. I., Osthus, R. C., Wonsey, D. R., and Dang, C. V. (2003). A strategy for identifying transcription factor binding sites reveals two classes of genomic c-Myc target sites. Proceedings of the National Academy of Sciences of the United States of America *100*, 5313-5318.

Hanahan, D., and Weinberg, R. A. (2000). The hallmarks of cancer. Cell *100*, 57-70.

Harris, C. C. (1996). p53 tumor suppressor gene: From the basic research laboratory to the clinic - An abridged historical perspective. Carcinogenesis *17*, 1187-1198.

Hayflick, L. (1965). Limited in Vitro Lifetime of Human Diploid Cell Strains. Experimental Cell Research *37*, 614.

Holley, J. E., Newcombe, J., Winyard, P. G., and Gutowski, N. J. (2007). Peroxiredoxin V in multiple sclerosis lesions: predominant expression by astrocytes. Multiple Sclerosis *13*, 955-961.

Jang, H. H., Kim, S. Y., Park, S. K., Jeon, H. S., Lee, Y. M., Jung, J. H., Lee, S. Y., Chae, H. B., Jung, Y. J., Lee, K. O., *et al.* (2006). Phosphorylation and concomitant structural changes in human 2-Cys peroxiredoxin isotype I differentially regulate its peroxidase and molecular chaperone functions. Febs Letters *580*, 351-355.

Jeong, W., Park, S. J., Chang, T. S., Lee, D. Y., and Rhee, S. G. (2006). Molecular mechanism of the reduction of cysteine sulfinic acid of peroxiredoxin to cysteine by mammalian sulfiredoxin. Journal of Biological Chemistry *281*, 14400-14407.

Kang, S. W., Chae, H. Z., Seo, M. S., Kim, K. H., Baines, I. C., and Rhee, S. G. (1998). Mammalian peroxiredoxin isoforms can reduce hydrogen peroxide generated in response to growth factors and tumor necrosis factor-alpha. Journal of Biological Chemistry *273*, 6297-6302.

Kang, S. W., Rhee, S. G., Chang, T. S., Jeong, W., and Choi, M. H. (2005). 2-Cys peroxiredoxin function in intracellular signal transduction: therapeutic implications. Trends in Molecular Medicine *11*, 571-578.

Kim, J. A., Park, S., Kim, K., Rhee, S. G., and Kang, S. W. (2005). Activity assay of mammalian 2-cys peroxiredoxins using yeast thioredoxin reductase system. Analytical Biochemistry *338*, 216-223.

Kim, S. H., Fountoulakis, M., Cairns, N., and Lubec, G. (2001). Protein levels of human peroxiredoxin subtypes in brains of patients with Alzheimer's disease and Down Syndrome. Journal of Neural Transmission-Supplement, 223-235.

Kinnula, V. L., Lehtonen, S., Sormunen, R., Kaarteenaho-Wiik, R., Kang, S. W., Rhee, S. G., and Soini, Y. (2002). Overexpression of peroxiredoxins I, II, III, V, and VI in malignant mesothelioma. Journal of Pathology *196*, 316-323.

Knoops, B., Clippe, A., Bogard, C., Arsalane, K., Wattiez, R., Hermans, C., Duconseille, E., Falmagne, P., and Bernard, A. (1999). Cloning and characterization of AOEB166, a novel mammalian antioxidant enzyme of the peroxiredoxin family. Journal of Biological Chemistry *274*, 30451-30458.

Lee, W., Wells, T., and Kantorow, M. (2007). Localization and H_2O_2-specific induction of PRDX3 in the eye lens. Molecular Vision *13*, 1469-1474.

Lehtonen, S. T., Markkanen, P. M. H., Peltoniemi, M., Kang, S. W., and Kinnula, V. L. (2005). Variable overoxidation of peroxiredoxins in human lung cells in severe oxidative stress. American Journal of Physiology-Lung Cellular and Molecular Physiology *288*, L997-L1001.

Lequerré, T., Gauthier-Jauneau, A., Bansard, C., Derambure, C., Hiron, M., Vittecoq, O., Daveau, M., Mejjad, O., Daragon, A., Tron, F., Le Loët, X., and Salier, J. (2006). Gene profiling in white blood cells predicts infliximab responsiveness in rheumatoid arthritis. Arthritis Research and Therapy *8*, R105.

Li, L. Q., Shoji, W., Takano, H., Nishimura, N., Aoki, Y., Takahashi, R., Goto, S., Kaifu, T., Takai, T., and Obinata, M. (2007). Increased susceptibility of MER5 (peroxiredoxin III) knockout mice to LPS-induced oxidative stress. Biochemical and Biophysical Research Communications *355*, 715-721.

Liu, Y., Liu, H. L., Han, B. G., and Zhang, J. T. (2006). Identification of 14-3-3 sigma as a contributor to drug resistance in human breast cancer cells using functional proteomic analysis. Cancer Research *66*, 3248-3255.

Lothstein, L., Israel, M., and Sweatman, T. W. (2001). Anthracycline drug targeting: cytoplasmic versus nuclear - a fork in the road. Drug Resistance Updates *4*, 169-177.

Ministry of Health, N. Z. (2007). Cancer Control. [Online] Retrieved from: http://www.moh.govt.nz/cancercontrol (Retrieved 26 February 2008)

Moon, J. C., Hah, Y. S., Kim, W. Y., Jung, B. G., Jang, H. H., Lee, J. R., Kim, S. Y., Lee, Y. M., Jeon, M. G., Kim, C. W., *et al.* (2005). Oxidative stress-dependent structural and functional switching of a human 2-Cys peroxiredoxin Isotype II that enhances HeLa cell resistance to H_2O_2-induced cell death. Journal of Biological Chemistry *280*, 28775-28784.

Morandi, E., Zingaretti, C., Chiozzotto, D., Severini, C., Semeria, A., Horn, W., Vaccari, M., Serra, R., Silingardi, P., and Colacci, A. (2006). A cDNA-microarray analysis of camptothecin resistance in glioblastoma cell lines. Cancer Letters *231*, 74-86.

Noh, D. Y., Ahn, S. J., Lee, R. A., Kim, S. W., Park, I. A., and Chae, H. Z. (2001). Overexpression of peroxiredoxin in human breast cancer. Anticancer Research *21*, 2085-2090.

Nonn, L., Berggren, M., and Powis, G. (2003). Increased expression of mitochondrial peroxiredoxin-3 (thioredoxin peroxidase-2) protects cancer cells against hypoxia and drug-induced hydrogen peroxide-dependent apoptosis. Molecular Cancer Research *1*, 682-689.

Park, J. H., Kim, Y. S., Lee, H. L., Shim, J. Y., Lee, K. S., Oh, Y. J., Shin, S. S., Choi, Y. H., Park, K. J., Park, R. W., and Hwang, S. C. (2006). Expression of peroxiredoxin and thioredoxin in human lung cancer and paired normal lung. Respirology *11*, 269-275.

Pfaffl, M. W. (2001). A new mathematical model for relative quantification in real-time RT-PCR. Nucleic Acids Research *29*.

Rabilloud, T., Heller, M., Gasnier, F., Luche, S., Rey, C., Aebersold, R., Benahmed, M., Louisot, P., and Lunardi, J. (2002). Proteomics analysis of cellular response to oxidative stress - Evidence for in vivo overoxidation of peroxiredoxins at their active site. Journal of Biological Chemistry *277*, 19396-19401.

Ragu, S., Faye, G., Iraqui, I., Masurel-Heneman, A., Kolodner, R. D., and Huang, M. E. (2007). Oxygen metabolism and reactive oxygen species cause chromosomal rearrangements and cell death. Proceedings of the National Academy of Sciences of the United States of America *104*, 9747-9752.

Ralph, L. D., Thomson, A. H., Dobbs, N. A., and Twelves, C. (2003). A population model of epirubicin pharmacokinetics and application to dosage guidelines. Cancer Chemotherapy and Pharmacology *52*, 34-40.

Rangwala, S. M., Li, X. Y., Lindsley, L., Wang, X. M., Shaughnessy, S., Daniels, T. G., Szustakowski, J., Nirmala, N. R., Wu, Z. D., and Stevenson, S. C. (2007). Estrogen-related receptor alpha is essential for the expression of antioxidant protection genes and mitochondrial function. Biochemical and Biophysical Research Communications *357*, 231-236.

Rhee, S. G., Chang, T. S., Bae, Y. S., Lee, S. R., and Kang, S. W. (2003). Cellular regulation by hydrogen peroxide. Journal of the American Society of Nephrology *14*, S211-S215.

Salvatorelli, E., Guarnieri, S., Menna, P., Liberi, G., Calafiore, A. M., Mariggio, M. A., Mordente, A., Gianni, L., and Minotti, G. (2006). Defective one- or two-electron reduction of the anticancer anthracycline epirubicin in human heart - Relative importance of vesicular sequestration and impaired efficiency of electron addition. Journal of Biological Chemistry *281*, 10990-11001.

Sanchez-Font, M. F., Sebastia, J., Sanfeliu, C., Cristofol, R., Marfanya, G., and Gonzalez-Duarte, R. (2003). Peroxiredoxin 2 (PRDX2), an antioxidant enzyme, is under-expressed in Down syndrome fetal brains. Cellular and Molecular Life Sciences *60*, 1513-1523.

Sauna, Z. E., Kim, I. W., and Ambudkar, S. V. (2007). Genomics and the mechanism of P-glycoprotein (ABCB1). Journal of Bioenergetics and Biomembranes *39*, 481-487.

Seo, M. S., Kang, S. W., Kim, K., Baines, I. C., Lee, T. H., and Rhee, S. G. (2000). Identification of a new type of mammalian peroxiredoxin that forms an intramolecular disulfide as a reaction intermediate. Journal of Biological Chemistry *275*, 20346-20354.

Shay, J. W., and Bacchetti, S. (1997). A survey of telomerase activity in human cancer. European Journal of Cancer *33*, 787-791.

Sporn, M. B. (1996). The war on cancer. Lancet *347*, 1377-1381.

Sundaresan, M., Yu, Z. X., Ferrans, V. J., Irani, K., and Finkel, T. (1995). Requirement for Generation of H_2O_2 for Platelet-Derived Growth-Factor Signal-Transduction. Science *270*, 296-299.

Tsang, W. P., Chau, S. P. Y., Kong, S. K., Fung, K. P., and Kwok, T. T. (2003). Reactive oxygen species mediate doxorubicin induced p53-independent apoptosis. Life Sciences *73*, 2047-2058.

Williams, A. O., Isaacs, R. J., and Stowell, K. M. (Manuscript in preparation). Up-regulation of peroxiredoxin III in non-tumergenic and tumergenic breast cells in response to doxorubicin treatment. (Massey University, Palmerston North, New Zealand).

Wonsey, D. R., Zeller, K. I., and Dang, C. V. (2002). The c-Myc target gene PRDX3 is required for mitochondrial homeostasis and neoplastic transformation. Proceedings of the National Academy of Sciences of the United States of America *99*, 6649-6654.

Woo, H. A., Kang, S. W., Kim, H. K., Yang, K. S., Chae, H. Z., and Rhee, S. G. (2003). Reversible oxidation of the active site cysteine of peroxiredoxins to cysteine sulfinic acid - Immunoblot detection with antibodies specific for the hyperoxidized cysteine-containing sequence. Journal of Biological Chemistry *278*, 47361-47364.

Yanagawa, T., Ishikawa, T., Ishii, T., Tabuchi, K., Iwasa, S., Bannai, S., Omura, K., Suzuki, H., and Yoshida, H. (1999). Peroxiredoxin I expression in human thyroid tumors. Cancer Letters *145*, 127-132.

Yang, H. Y., Jeong, D. K., Kim, S. H., Chung, K. J., Cho, E. J., Yang, U., Lee, S. R., and Lee, T. H. (2007). The role of peroxiredoxin III on late stage of proerythrocyte differentiation. Biochemical and Biophysical Research Communications *359*, 1030-1036.

Appendix One: Bradford Protein Quantification Assay

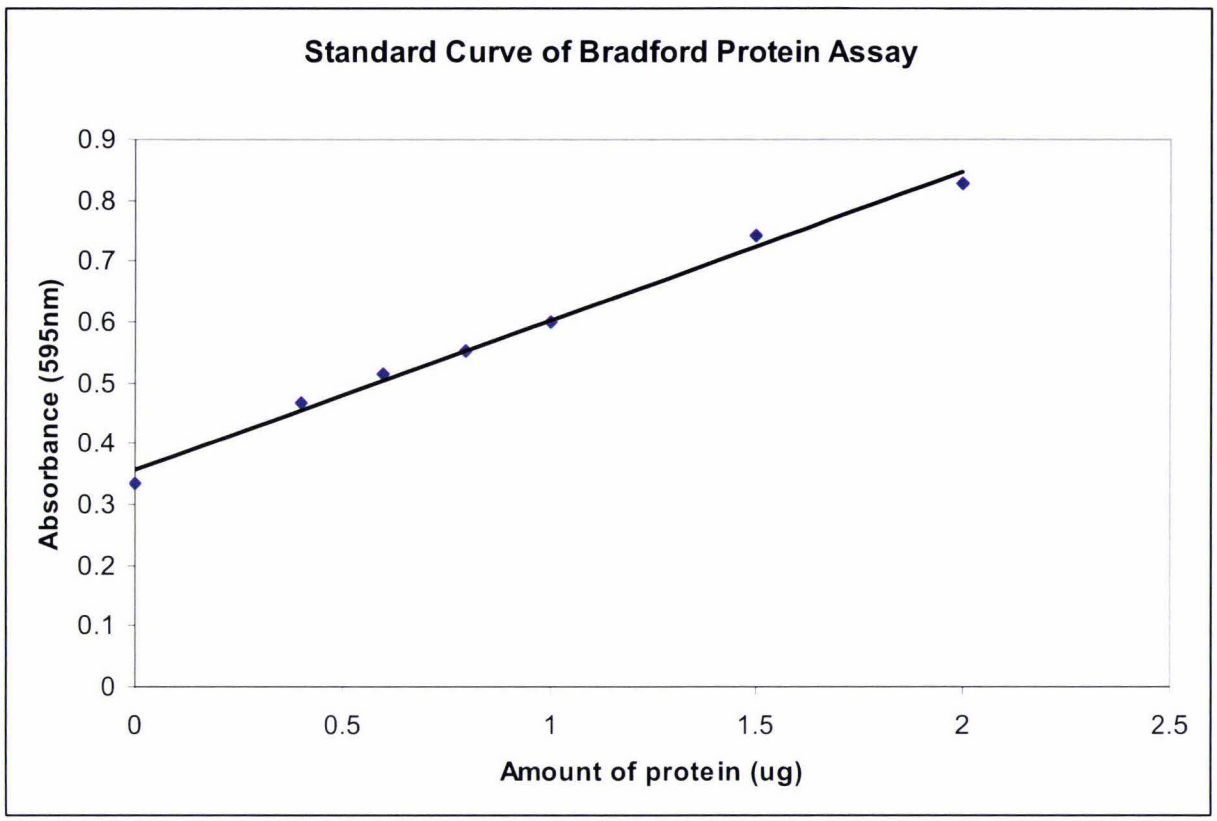

BSA Protein Standard (µg)	Absorbance at 595 nm (Average of triplicates)
0	0.335
0.4	0.467
0.6	0.516
0.8	0.552
1.0	0.600
1.5	0.742
2.0	0.828

White blood cell total protein extract (Diluted 1:10, 5 µL)	
Absorbance (595 nm)	**Amount of protein (µg) (from standard curve)**
0.685	1.3
0.672	1.25
0.687	1.31
Average	1.287
Original concentration	2.57 µg/µL

Appendix Two: One-sample, two-sided *t*-test

Patient	Fold change 1	Fold change 2	Fold change 3	Average fold change	Two-tailed p-value
One	0.57	1.0	0.624	0.731	0.1853
Two	**2.15**	**2.44**	**2.07**	**2.22***	**0.0084**
Three	1.33	1.32	1.36	1.337*	0.0013
Three (Round 2)	2.32	2.26	2.42	2.33*	0.0012
Four	0.77	0.863	0.57	0.734	0.0916
Five	0.533	0.53	-	0.5265*	0.002

Control	Fold change 1	Fold change 2	Fold change 3	Average fold change	Two-tailed p-value
One	1.0	1.09	0.99	1.03	0.4899
Two	1.525	1.37	0.897	1.26	0.297
Three	1.299	1.62	0.809	1.24	0.4116
Four	1.29	1.48	1.319	1.363*	0.0255
One (Round 2)	1.65	1.10	1.032	1.26	0.3143
Two (Round 2)	0.80	0.76	-	0.78*	0.0082
Three (Round 2)	1.47	1.19	1.582	1.414	0.071
Four (Round 2)	1.50	1.087	0.727	1.10	0.6854

Average fold change	$= \frac{\text{sum of fold changes}}{n}$	2.22
Standard deviation of values (s)	$= \sqrt{\frac{\sum(x_i - \text{mean})^2}{n-1}}$	0.194679223
Standard error (s.e)	$= s/\sqrt{n}$	0.112398102
***t*-statistic**	$= \frac{\text{Sample mean} - \text{hypothetical mean}}{\text{Standard error}}$	10.854
Two-tailed *p*-value	Determined using *t*-statistic	0.0084

Appendix Three: Sample of data used to generate standard curves

Data obtained using prx III primers

Standard	C_T	Efficiency (calculated by LightCycler 480 software)
2.00E-1	23.59	1.940
1.00E-1	24.64	
2.00E-2	26.87	
1.00E-2	28.26	
2.00E-3	30.64	

Standard curve generated by LightCycler 480 software

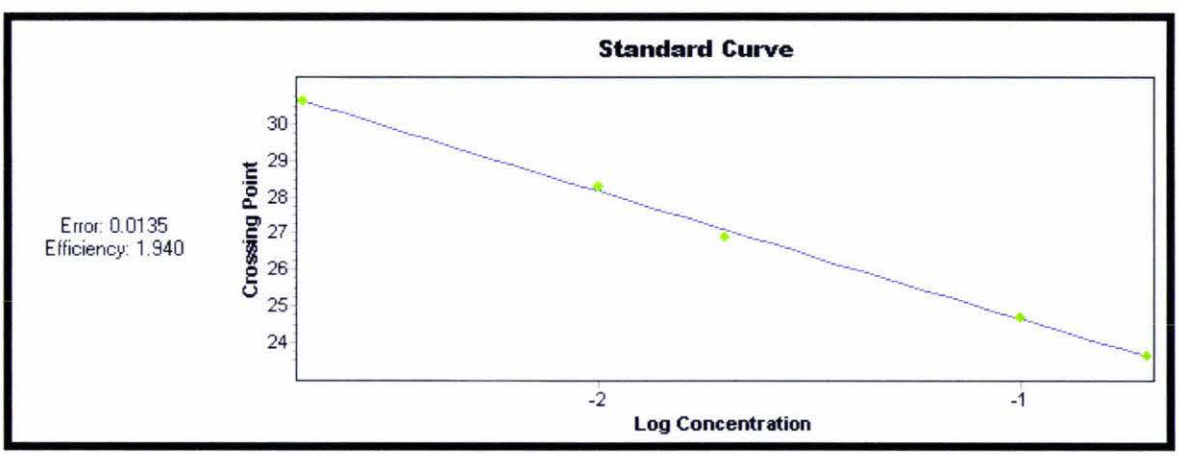

Appendix Four: Example of Coomassie-stained SDS-PAGE gel

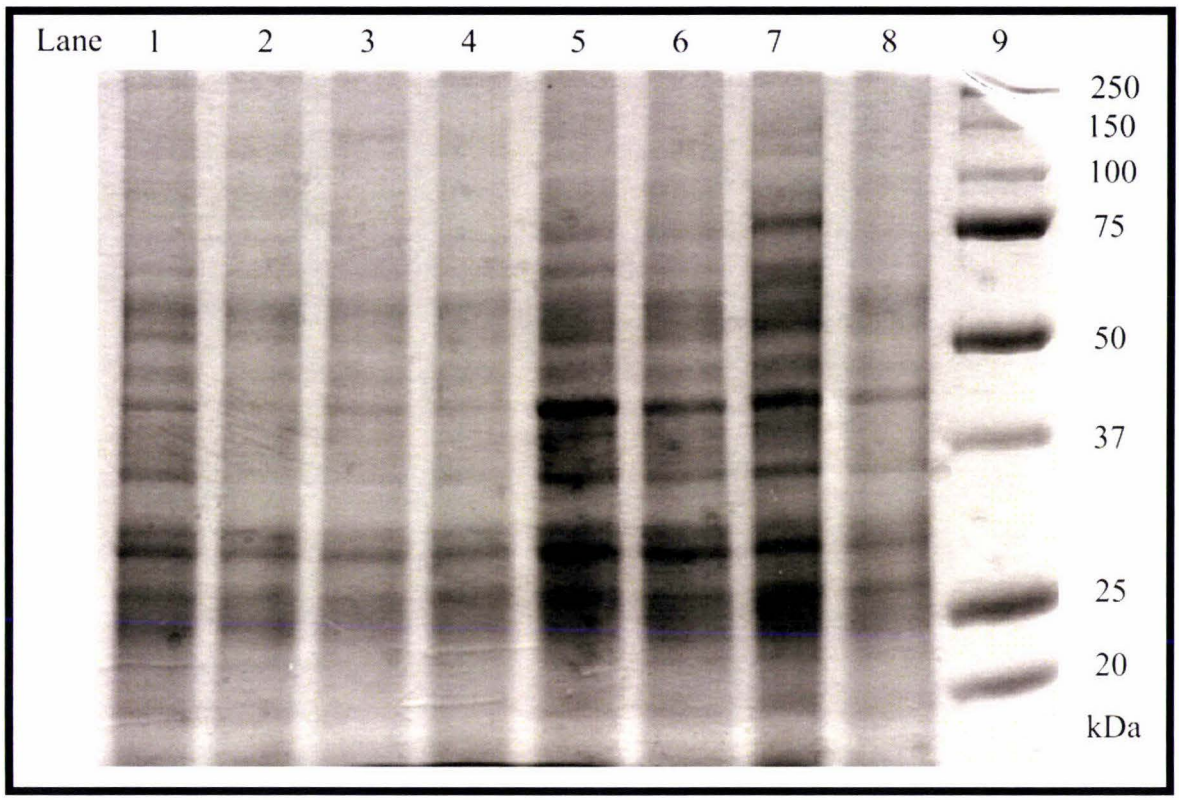

Total protein extracts (20 µg) from control subjects were separated by 10% SDS-PAGE for approximately 90 minutes at 120 V. The gel was then stained with Coomassie stain for 15 minutes with shaking, and de-stained overnight at room temperature, with shaking. The size of the markers is given on the right in kilodaltons (kDa).

Lane	Contents
1	Control 1, sample 1
2	Control 1, sample 2
3	Control 2, sample 1
4	Control 2, sample 2
5	Control 3, sample 1
6	Control 3, sample 2
7	Control 4, sample 1
8	Control 4, sample 2
9	Dual colour protein marker

Appendix Five: α-tubulin antibody

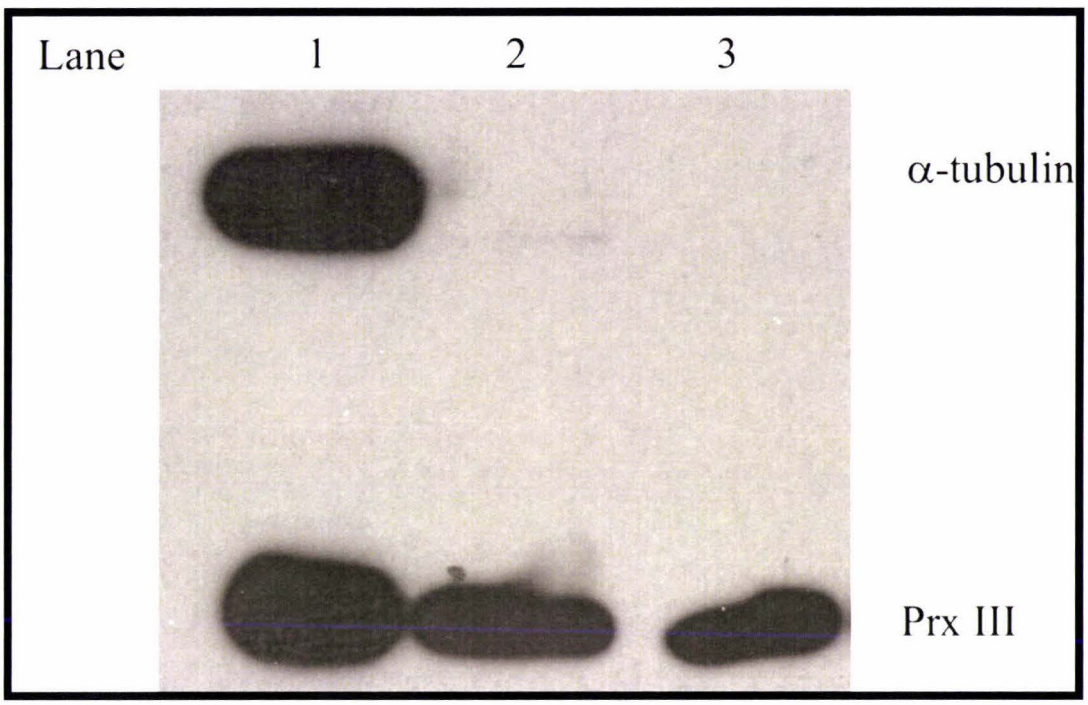

Protein was separated by 10% SDS-PAGE for approximately 90 minutes at 120 V, then transferred to PVDF membrane at 450 mA for 90 minutes. The membrane was cut at 50 kDa. The upper half of the membrane was incubated with a monoclonal mouse antibody to α-tubulin (DM 1A)(Sigma) . The lower half was incubated with a mouse monoclonal antibody to prx III (12B)(Santa Cruz). Both portions were then incubated with rabbit anti-mouse antibody, conjugated to horseradish peroxidase (HRP). Chemiluminescence solutions A and B were used to detect HRP. The membrane was exposed to X-ray film for one minute. Two separate white blood cell extracts were used. MCF7 cell extract was used as a positive control.

Lane	Contents
1	20 µg MCF7 total protein
2	20 µg white blood cell extract 1
3	20 µg white blood cell extract 2

Appendix Six: Sample of data used to calculate fold change

Sample	Gene	C_T	Average C_T	Fold Δ
Patient 1 Pre	Prx III	23.82	23.85	0.624
		23.79		
		23.93		
	β-actin	14.96	14.97	
		14.98		
		14.98		
Patient 1 Post	Prx III	25.52	25.22	
		25.02		
		25.13		
	β-actin	15.62	15.637	
		15.64		
		15.65		
Control 3 Sample 2	Prx III	24.77	24.84	1.582
		24.85		
		24.91		
	β-actin	17.16	17.137	
		17.09		
		17.26		
Control 3 Sample 3	Prx III	23.73	23.69	
		23.70		
		23.64		
	β-actin	16.68	16.67	
		16.67		
		16.66		

Appendix Seven: Identification of β-actin band

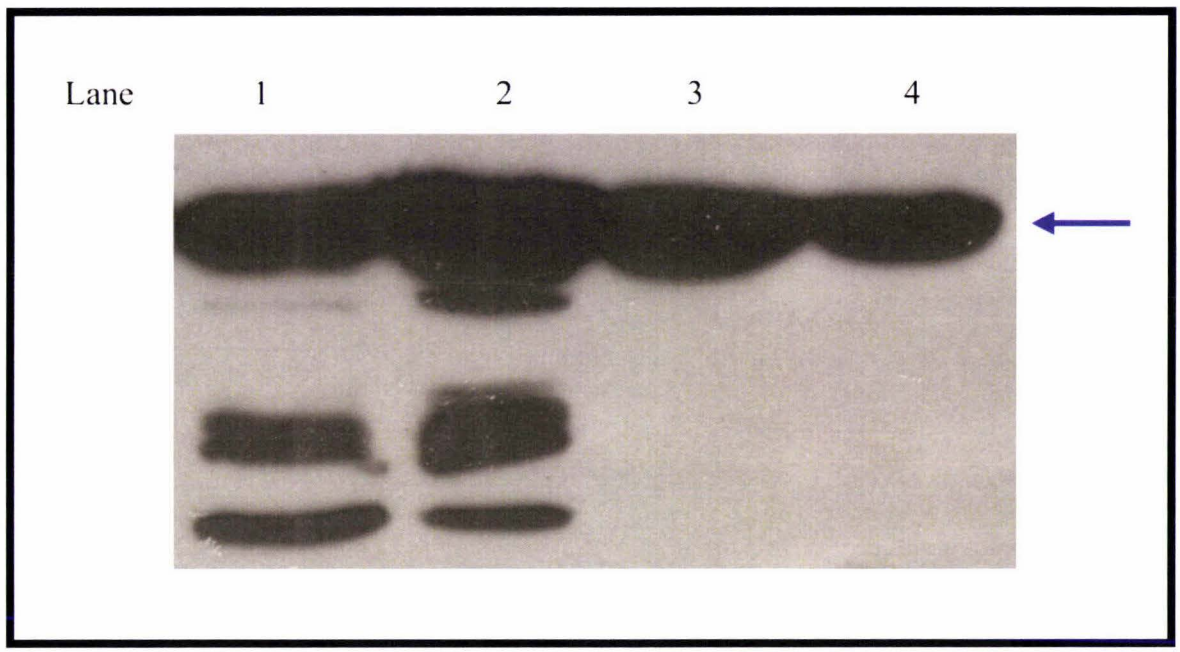

Total protein extracted from white blood cells or MCF7 cells was separated by 10% SDS-PAGE at 120 V for 90 minutes, transferred to PVDF for 90 minutes at 450 mA and immunoblotted to detect β-actin (blue arrow). The membrane was exposed to x-ray film for approximately 30 seconds.

Lane	Contents
1	20 µg white blood cell extract 1
2	20 µg white blood cell extract 2
3	Empty (over-flow from lane 4)
4	20 µg MCF7 cell extract

Appendix Eight: Example of agarose gel electrophoresis results obtained during real time RT-PCR optimisation

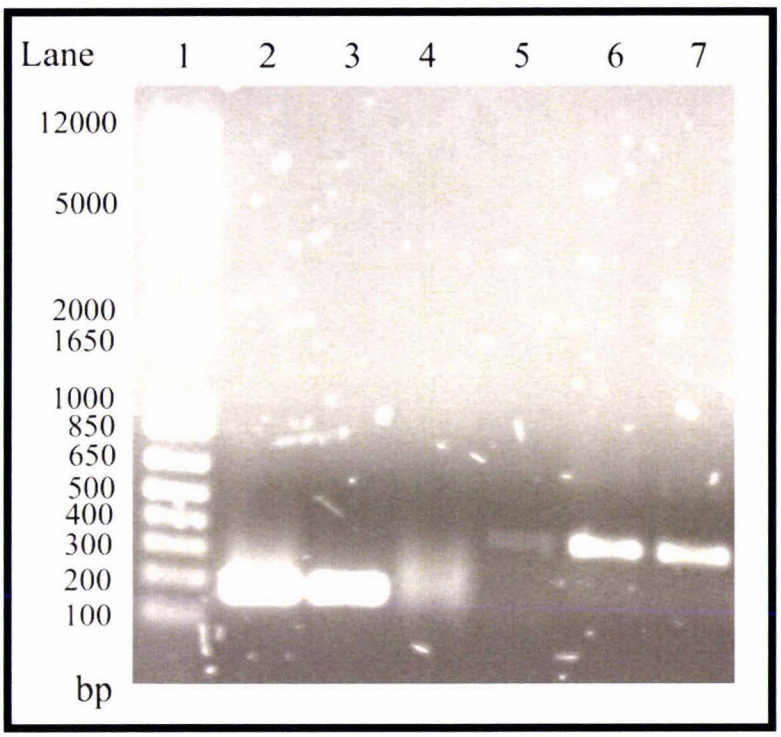

Real time RT-PCR experiments were performed with several different dilutions of white blood cell cDNA during optimization of the reactions. Aliquots (10 µL) of selected reactions were separated on a 0.7% agarose gel in 1 x TAE buffer at 100 V for approximately one hour, to examine the reaction products. DNA was visualized by incorporation of ethidium bromide into the gel and running buffer and exposure to UV light. The sizes of the molecular size standards are shown on the left in base pairs (bp).

Lane	Contents
1	10 µL 1 kb plus DNA ladder
2	10 µL β-actin primers + undiluted cDNA
3	10 µL β-actin primers + cDNA diluted 1/100
4	10 µL prx III primers + undiluted cDNA
5	10 µL prx III primers + cDNA diluted 1/10,000
6	10 µL prx III primers + cDNA diluted 1/100
7	10 µL prx III primers + cDNA diluted 1/100

Appendix Nine: Example amplification curves obtained during real time RT-PCR experiments

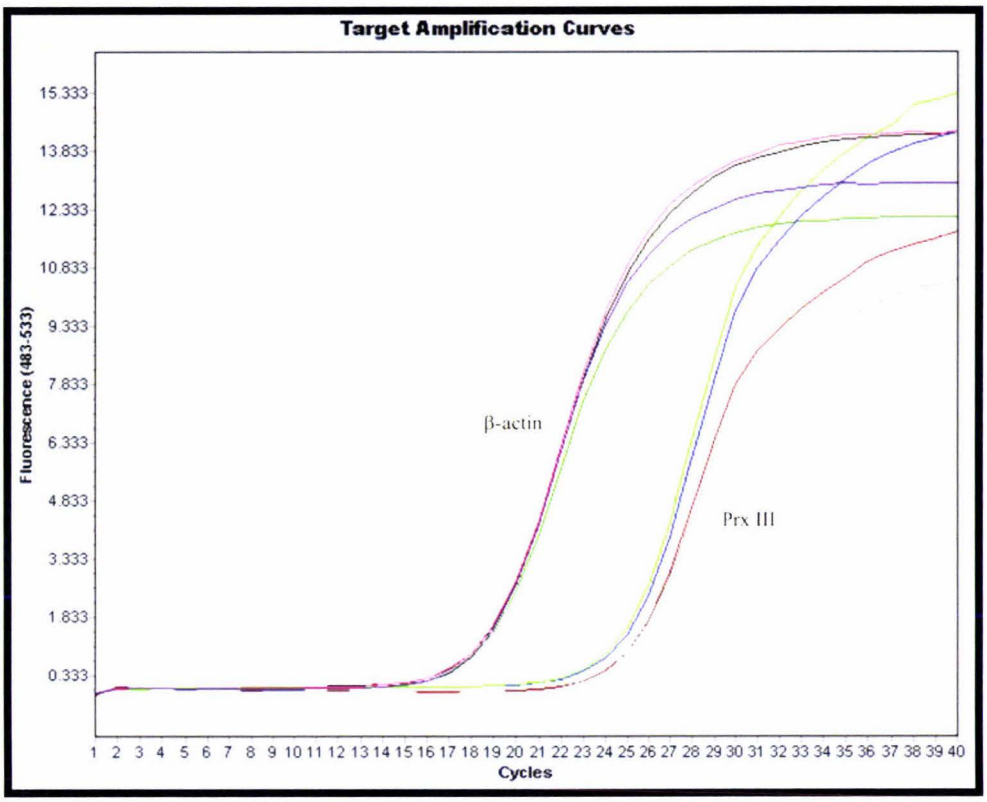

Real time RT-PCR was performed using first strand cDNA prepared from patient white blood cells and β-actin or prx III primers as indicated. Fluorescence was detected following every cycle of amplification. The amplification curves were created by the LightCycler 480 software using this fluorescence data. β-actin transcripts are more abundant than prx III transcripts therefore fluorescence increases more rapidly than for prx III. Samples shown are pre (β-actin: pink and black lines; prx III: red and grey lines) and post (β-actin: purple and dark green lines; prx III: blue and green lines) chemotherapy samples carried out in duplicate.

Appendix Ten: Example of results obtained during real time RT-PCR experiments

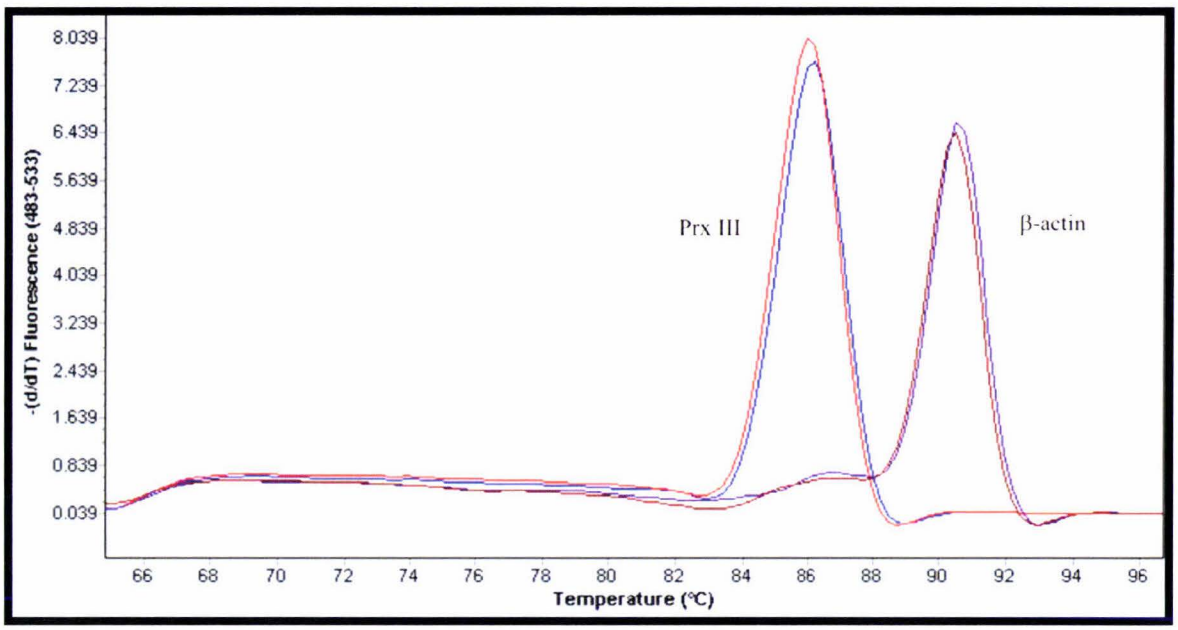

Real time RT-PCR was performed using first strand cDNA prepared from patient white blood cells and β-actin or prx III primers as indicated. Following real time RT-PCR, the temperature was raised and fluorescence was determined five times per degree Celsius. A melting peak profile was produced by the LightCycler 480 software using the fluorescence data. The prx III and β-actin primers produce products with different melting temperatures, as shown in the melting peaks.

Appendix Eleven: Coomassie stained 2DE gel to confirm successful isoelectric focusing

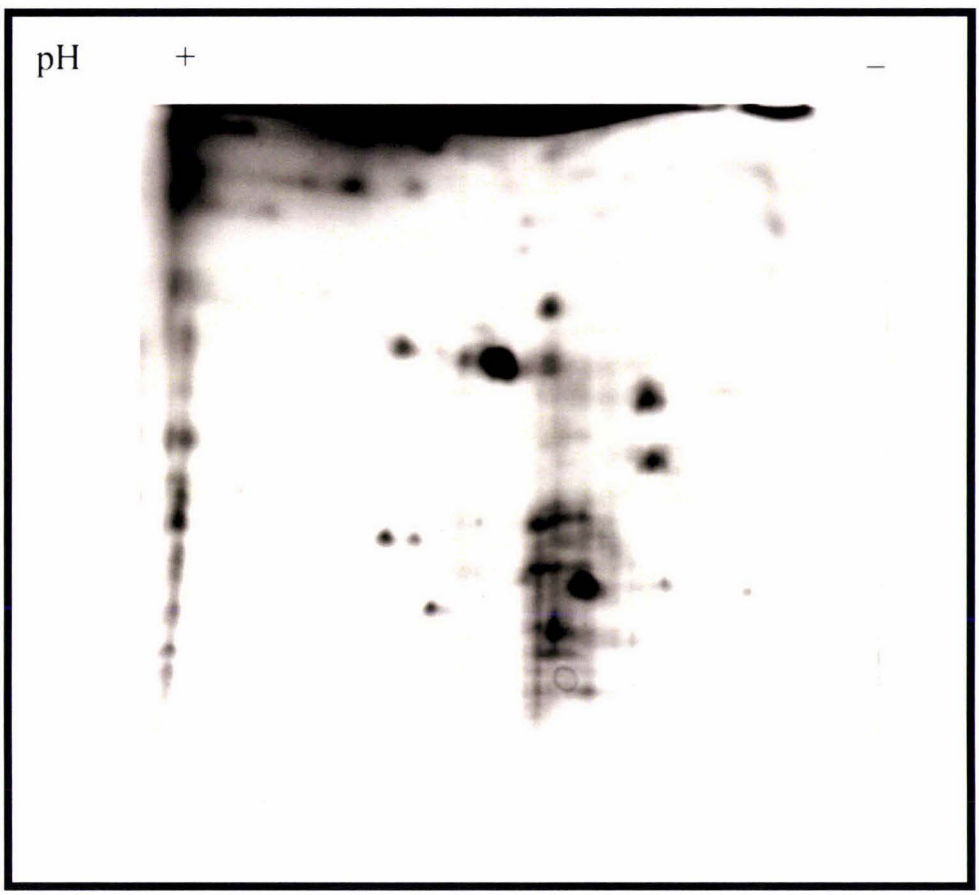

To confirm successful isoelectric focusing, 300 µg of MCF7 total protein was focused on a 7 cm isoelectric focusing strip as outlined section 2.7.2, then separated by 10% SDS-PAGE for 90 minutes at 120 V. The gel was stained with Coomassie stain for 15 minutes then de-stained for four hours. A number of protein spots are visible indicating successful isoelectric focusing. 2DE gels were not routinely stained as stained gels can not be immunoblotted, and sample was limited.

Appendix Twelve: Chromatogram from peroxiredoxin III DNA sequencing

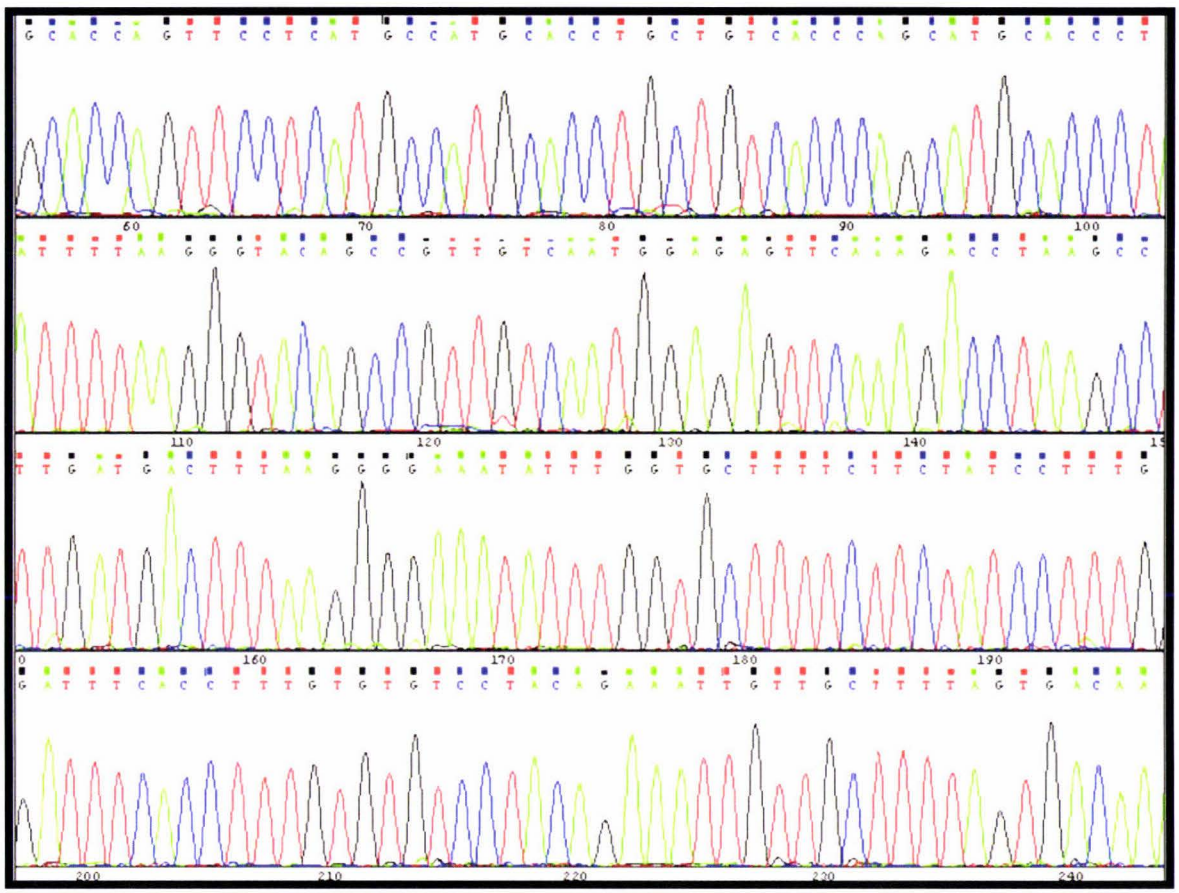

A portion of the chromatogram obtained during DNA sequencing of the prx III PCR product is shown to confirm the quality of the sequencing data.